Abstract

Byrd, Thesley A. Analysis of an Image-Based Fiber Length Measurement Device. (Under the direction of Dr. Jon Rust.)

Previous research by Yuksel Ikiz showed that the use digital imaging could provide more accurate and precise fiber length measurements when compared to current methods. This conclusion sparked the research by Stephen Stroupe, which resulted in the development of a system to deliver individualized cotton fibers to a digital camera for imaging. The system individualized fibers from sliver by utilizing a modified comber roll assembly. These fibers were deposited via a chute to an area between two electrodes, where one of the electrodes was charged with 12 kV. The voltage created an electrostatic field that captured the fibers and straightened them. Fibers would then bound between the plates until coming into contact with a non-conductive conveyor. Once in contact with the conveyor, the fibers remained and were passed over a backlighting source, which provided a silhouette of the fibers to a digital camera. The images were analyzed by using the algorithms that Ikiz had previously developed. Stroupe made some initial evaluations of the system's performance and concluded that further analysis would be necessary. It was the goal of this research to begin the analysis and to develop the system on the basis of increasing measurement precision and accuracy.

The specific objectives of this research were to improve image quality, evaluate sample selection, improve fiber presentation, determine measurement accuracy and precision, and compare our results to those of other fiber length measurement devices. These objectives were accomplished by using a variety of statistical, programmatic, and mechanical methods.

To improve image quality, a pulsing power supply was used in place of a continuous lighting system and was incorporated with a camera calibration routine. To keep the individualizer airflow from blowing long fibers through the electrodes, the comber roll was slowed, which necessitated the removal of the delivery chute. A belt slot was also milled into one electrode for concealing part of the belt to reduce fiber overlap. An additional experiment was conducted to determine the effect of sample size on the measurement repeatability, and to assess the system's ability to distinguish between two different fiber populations. Cut-length rayon fibers were used to assess measurement accuracy.

Through the above methods, the image quality was improved, with the contrast between fibers and the background more than doubling their original values. The number of fiber crossovers and entanglements was reduced by an estimated 9 percent with the removal the delivery chute. After cutting the belt slot, fiber overlapping was reduced to 1 mm on average. Although the fibers did not attach to the belt readily after the slot was milled, moving the system to a conditioned environment helped to increase the rate of fiber removal. After all changes, it was determined that our system showed improved accuracy when compared to other systems. However, the accuracy of the results was dependent upon the sample size and day on which the samples were run. The experiment also showed our system was in reasonable agreement with AFIS regarding the difference between the two fiber populations. The cut-length analysis showed our device's ability to measure individual cut-lengths fairly accurately, with a skew toward the lower tail because of the remaining overlap. Despite the existing issues with fiber overlap and broken skeletons, the system was improved through this research and shows promise of becoming a viable method for the measurement of cotton fiber length.

ANALYSIS OF AN IMAGE-BASED FIBER LENGTH MEASUREMENT DEVICE

by
THESLEY BYRD

A thesis submitted to the Graduate Faculty of
North Carolina State University
in partial fulfillment of the
requirements for the degree of
Master of Science

TEXTILE ENGINEERING

Raleigh

2003

APPROVED BY:

_____	_____
Dr. Jon Rust	Dr. Timothy Clapp
Head of Advisory Committee	

_____
Dr. Thomas Johnson

Biography

Thesley A. Byrd, Jr. was born in 1979 to Mr. Thesley A. Byrd Sr., and Shelia C. Byrd in Lee County, NC. He was raised in a quite country home where he lived with his parents and his only sibling, Jennifer Byrd. Baseball, basketball, and karate were his favorite pastimes while growing up. In addition to sports, Thesley was involved with his church and participated on a bible drill team where he was a six-year state winner. In high school, he was 1st vice president of the student council his senior year, received an award for perfect attendance in grades 1-12, and was a member of the 1996 Lee County Senior High School 4A State Champion baseball team. In 1997 he enrolled in North Carolina State University's first year college program and transferred to the Textile Engineering program in the College of Textiles the following year. He graduated Magna Cum Laude from there in the Fall of 2001. After graduation, Thesley enrolled in the Textile Engineering Master's program in the College of Textiles. He currently enjoys playing church softball and attending college sporting events.

Acknowledgements

I would first like to thank God for giving me the opportunity and ability to perform this research. In addition, I would like to thank North Carolina State University and the College of Textiles for its financial and material support. A special thank you goes to my advisor, Dr. Jon Rust, for giving me the opportunity to work under his direction and for his guidance throughout the past two years.

For his programming and technical assistance, I would like to thank Joe Brenzovich. I would also like to extend my appreciation to Mike Thompkins for his help in completing trials for the final data analysis. I would also like to thank Jan Pegram for allowing us to use space in the physical-testing laboratory. Finally, I would like to think my family and my girlfriend, Mary Scott, for their moral support throughout the graduate process.

Table of Contents

List of Figures

List of Tables

1. Introduction

In previous research, Stephen Stroupe developed a method whereby cotton fibers could be separated and individually delivered to a digital camera for measurement. The design of the system incorporated a fiber individualizer, a fiber straightening and transport method, and image processing algorithms that had been previously developed by Yuksel Ikiz. After the design and construction of the system was complete, Stroupe made an initial assessment of the system performance. He noted various regions in which the system could be improved and outlined possible areas for further research. It was this need for additional system analysis that served as an impetus for the research described herein.

After reviewing the system in its previous state, four primary objectives were identified. Those objectives were to advance image quality, improve fiber presentation to the camera, analyze the sample selection process, and perform gage R&R. A combination of programming, mechanical, and statistical methods was used to meet the objectives and evaluate possible solutions.

A new lighting technique and camera calibration routine were employed to reduce image noise and improve the contrast between the fibers and background. Various mechanical modifications were implemented in an effort to improve fiber individualization and reduce the amount of fiber overlap onto the conveyor. The sample selection process was evaluated by using a mixture of cut-length fibers and analysis of variance techniques. Cut-length fibers were also utilized to determine the measurement accuracy.

In addition to the above, several programming changes were made to include a purging procedure, separate fiber crossovers, detect entanglements, and connect broken u-

shaped fibers. A method for calibration of the resolution value was also developed to assure the measurement accuracy.

Once all of the system changes had been implemented, the accuracy of the data was greatly improved and a designed experiment was conducted to determine the effects of sample size and day on the measurements. The results of this designed experiment were then used to make comparisons to the data gotten from other measurement systems when testing the same sliver samples. When compared to the initial data that was taken prior to any modifications, the final statistics showed increased similarity to the results of HVI and AFIS, which are two of the primary devices that are currently used for fiber length determination.

2. Literature Review

2.1 Fiber Length Definitions

Fiber length is mostly determined by the variety of the cotton. However, a cotton plant's exposure to extreme temperatures, water stress, and nutrient deficiencies can reduce the length. Excessive cleaning and drying at the gin can also cause fiber length reduction through increased mechanical damage, which is already prevalent. Fiber length has effects on yarn strength, yarn evenness, and on the efficiency of the yarn spinning process. In addition, the fineness of a yarn that is produced is affected by fiber length [9]. The following sections review the various parameters that are used to define the length and length distribution of a cotton sample.

2.1.1 Mean Length

The mean length is the average length of all the fibers in the test specimen based on the mass-length data, as defined by ASTM Standards [1]. The number-length data may also be used to report the mean length of a cotton sample. The mean length by weight tends to hide the short fibers in the sample, while the mean length by number tends to emphasize them. With the assumption that fiber length and linear density are statistically independent, the mean length by weight is always greater than the mean length by number [12].

2.1.2 Upper Half Mean Length

The upper half mean length (UHML) of a fiber sample is the mean length by number, of the longer one half of the fibers by weight, as defined by ASTM Standards [1]. It is generally the length parameter that is used to define the fiber length of a given sample. The following table gives classifications of the UHML.

Table 2.1: Length Classification [10]

Category	UHM (in.)
Short	Below 0.99
Medium	0.99 to 1.10
Long	1.11 to 1.26
Extra Long	Above 1.26

2.1.3 Upper Quartile Length

The upper quartile length (UQL) of a fiber sample is the length that is exceeded by 25% of the fibers by weight in the test specimen, as defined by ASTM Standards [1]. The UQL may also be reported on a number basis. Cui and Calamari report that the number and weight measurements of the UQL may give opposite rank [12].

2.1.4 Short Fiber Content

The short fiber content (SFC) is the percentage of fibers (by number or by weight) in a test specimen that is shorter than 12.5 mm (0.5 in.) in length, as defined by ASTM Standards [1]. Short fiber content is important because short fibers cannot wrap around one another; therefore, they increase the weight and bulkiness of yarns while making no contribution to yarn strength. There is currently no official USDA measurement of SFC.

2.1.5 Span Length

The span length of a fiber sample is the distance spanned by a specified percentage of the fibers in a sample, taking the amount reading at the starting point of the scanning as 100%, as defined by ASTM Standards [1]. For example, the 2.5% span length is the length exceeded by only 2.5% of the fibers by number. Table 2.3 shows the classifications of the 2.5% span length.

Table 2.2: Classifications of the 2.5% Span Length [17]

Category	2.5% Span Length (mm)
Short-B	Less than 20
Short-A	20.5 to 24.5
Medium	25.0 to 29.0
Long	29.5 to 32.5
Extra Long	More than 33

2.1.6 Uniformity Index

The uniformity index of a fiber sample is the ratio between the mean length and the upper half mean length, expressed as a percentage of the upper half mean length, as defined by ASTM Standards [1]. If all of the fibers in a sample were the same length, then the uniformity index would be 100 percent. However, due to natural variation, the uniformity index will always be less than 100 percent. The uniformity has relations to the short fiber content, where a low uniformity index is likely to have a higher percentage of short fibers [9]. Table 2.2 may be used as a guide for the interpretation of length uniformity.

Table 2.3: Guide for Uniformity Index Interpretation [9]

Degree of Uniformity	**Uniformity Index**
Very High	Above 85
High	83 – 85
Intermediate	80 – 82
Low	77 – 79
Very Low	Below 77

2.1.7 Uniformity Ratio

The uniformity ratio is the ratio between two span lengths, expressed as a percentage of the longer length, as defined by ASTM Standards [1]. It is usually calculated and reported

as the ratio of the 50% span length to the 2.5% span length, and multiplied times 100 to get a percentage. The following table shows the classification of the uniformity ratio.

Table 2.4: Uniformity Ratio Classification [17]

Category	Uniformity Ratio Percentage
Poor	Less than 42%
Fair	42-43%
Average	44-45%
Good	46-47%
Very Good	More than 47%

2.2 Fiber Length Measurement Systems

Many methods have been developed for length measurement of a fiber sample. In this section an individual fiber test, standard array method, two forms of High Volume Instrumentation (HVI), and the Advanced Fiber Information System (AFIS) are reviewed.

2.2.1 Oiled-Plate Method

This is an individual-fiber method that is used to measure the length distribution of cotton and short man-made staple fibers [24]. The measurement of individual fibers makes this method the most accurate of any other in existence. It has a very labor-intensive procedure, however, and requires a skilled operator to obtain accurate results. One hour is generally required for the measurement of 300 fibers when using this technique. Therefore, it would take approximately 2.5 hours to complete the measurement of a single cotton sample using this procedure [24].

In this method, a sheet of glass is smeared with liquid paraffin, and some fibers are placed on the far-left corner of the glass sheet. Then, the fibers are drawn out one at a time by the tips of the little fingers of each hand of the operator. The fibers are straightened and smoothed out over a centimeter scale that has been etched on the underside of the glass sheet.

The paraffin serves to prevent the fibers from being blown away and to assist in keeping the fibers flat and straight for measurement. The length of each individual fiber is noted and is entered into the length groups of a frequency table [24]. From the individual fiber measurements, the various length statistics can then be calculated.

Although the oiled-plate method provides the most reliable results when performed in the approved manner, the measurement of individual fibers by an operator is very tedious and time consuming. Therefore, more efficient methods with less measurement accuracy are generally preferred.

2.2.2 Array Method

The array method, with the one exception of measuring many individual fibers, is known as the most accurate method of determining the fiber length statistics of a sample. It is commonly used to estimate the bias of other fiber measurement systems [2]. This method is very time consuming, however, and also requires the services of a very skilled operator to obtain accurate and precise results. It takes approximately 2 to 3 hours to perform a test on a single sample using this method [5].

The procedure for this method requires that 75 mg of fibers be sorted into common length groups. These sorted fibers are placed on a velvet board in 0.125-inch intervals. Once the sample has been sorted into its length categories, the fibers are then weighed, starting with the longest length group. The mean length, upper quartile length, and other length measurements are calculated from this weight data [2].

The most common error in fiber length measurement for this method is due to operator error in combing and sorting the fibers into the arrays. The operators have to be

well trained and must display repeatability that is within the ASTM standard values to be qualified for use of the array method [2].

Cui and Calamari have concluded that both weight and number data are important when examining the length distribution of a fiber sample [12]. Another issue with the array method is its reporting of length statistics by weight values only. Therefore, it is difficult to compare the results from the array method with other methods that report length statistics by number [28].

2.2.3 HVI-Spinlab

HVI-Spinlab is one of the high volume instruments used for fiber length measurement and the determination of other fiber length parameters. The system is also equipped to measure micronaire, color, trash, strength, and elongation [3]. Every bale of cotton in the United States is measured by this official USDA method

The system functions by passing a combed sample of fibers, which are assumed to be caught at random along their lengths, under a detection device. The resulting fiber beard is scanned from base to tip, and the amount of light passing through the beard is used to measure, indirectly, the number of fibers that extend to various distances. This information is recorded and used, along with equations and other constant parameters, to measure the fiber length statistics of the sample [3].

For the HVI-Spinlab system, samples are taken at random from a cotton bale or some other form of cotton fiber. The ASTM procedure requires that at least two fiber samples be prepared for testing. The samples are prepared by placing the cotton into fibrosamplers. A curved plate inside of the sampler guides the fibers through small perforations. The

protruding fibers are then moved over the surface of a combing device, which forms the fiber beard. The beard is then ready to be processed by the HVI-Spinlab system [3].

There are many sources of measurement error in the HVI-Spinlab system. One assumption of the Spinlab measurements states that a fiber is caught in the comb in proportion to its length, as compared to the total length of all fibers in the sample. This assumption results in the need for equations to indirectly calculate the length distribution [3]. Secondly, the detection device does not scan the entire lengths of the fibers. As supported by the assumption that fibers are caught at random along their lengths, an unknown length of fiber is hidden from the light scanning device by the clamp. The uncertainty of this parameter leads to obvious errors in the determination of the sample length distribution.

Further inaccuracies in the HVI statistics occur because of the use of length biased samples, in which fibers are removed from the population in direct proportion to their length. This means that the proportion of shorter fibers is less and the proportion of longer fibers is more in the sample than in the population. The use of such length-biased samples has a great influence on the reported SFC measurement [31].

The SFC, as measured by HVI-Spinlab, is also affected by the scanning mechanism. The sensing device begins a scan at approximately 0.15 to 0.20 inches away from the true baseline of the sample. Therefore, many of the short fibers in the sample are ignored by the system. Even fibers that are 0.40 inches long will be ignored by a scan if half of its length is hidden in the clamp. Hence, HVI has been deemed ineffective in the measurement of short fiber content [3]. Even with the use of an improved calibration routine there is large variability in HVI measurements of SFC between cottons with similar length and length uniformity values [14].

2.2.4 HVI-MCI

The HVI-MCI measurement system, which was derived from an earlier pneumatic fiber length measurement device developed by brown [7], is similar to the Spinlab system in that fibers are placed into fibrosamplers, combed outward, and passed under a sensor for an indirect measurement of fiber length. The system utilizes air pressure and an orifice to measure the pressure drop across the orifice as the fiber specimen is passed through. By assuming that the fibers are uniform in cross-section, the pressure drop is a measure of the number of fibers in the path of the airflow. Therefore, as the fibers are passed through the orifice, the pressure drop profile gives a measure of the number of fibers present at a given length in the sample.

The HVI-MCI system has many of the same error sources that are associated with the HVI-Spinlab measurement device in regards to the unmeasured holding length and the start of the scan. As with the Spinlab, the MCI system begins its scan approximately 0.20 inches away from the baseline. Combining this scan with the average 0.11 length holding length, 0.31 inches of a fiber is unmeasured on an average [22]. In addition, the MCI system also makes use of length biased samples, the consequences of which have been previously discussed.

2.2.5 AFIS

The Advanced Fiber Information system (AFIS) was designed to rapidly measure the dimensions of individual cotton fibers by utilizing an Electro-optical sensor [4, 6]. The output of the system includes the measurement of the mean length, upper half mean length, short fiber content, upper quartile length, span length, and various other length parameters [6].

The AFIS separates individual fibers from the sample by using pinned and perforated cylinders along with stationary carding flats as in Figure 2.1. The sample is inserted via the feed roll and feed plate mechanisms. As the fibers are inserted into the system they come into contact with the rotating pinned and perforated cylinder. The rotation of the pins allows the fibers to be pulled individually from the sample. Perforations in the pinned cylinder provide a means for forced air to remove any trash or dust from the system. A second pinned cylinder rotates in the opposite direction of the first, and each individual fiber is transferred from the pins of the first cylinder to the pins of the second. Once the fibers have been transferred, they are combed further by a carding flat and are subsequently removed from the surface of the cylinder and aerodynamically directed toward an Electro-optical sensor [6].

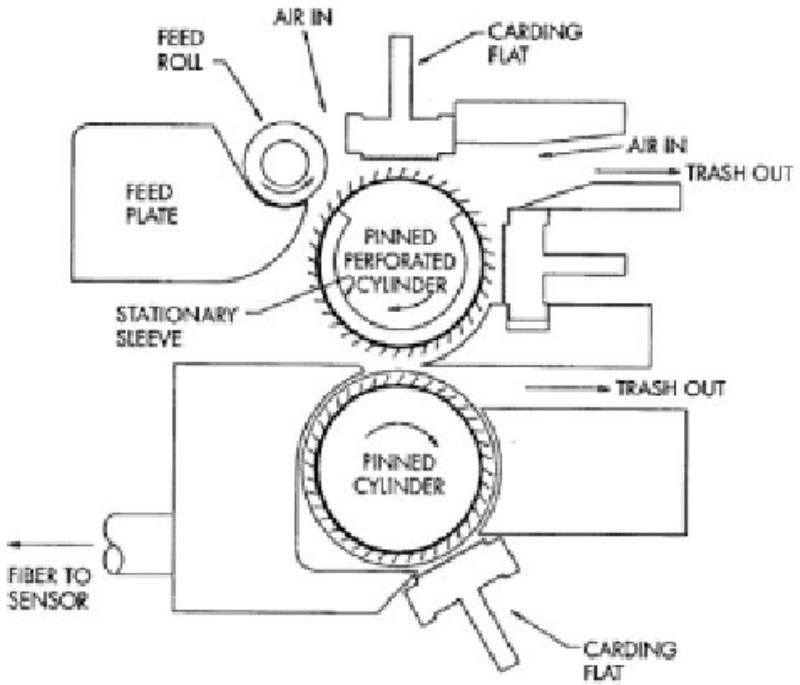

Figure 2.1: AFIS Individualizer Component [4]

Figure 2.2 is an illustration of the optical sensor component of the AFIS measurement system.

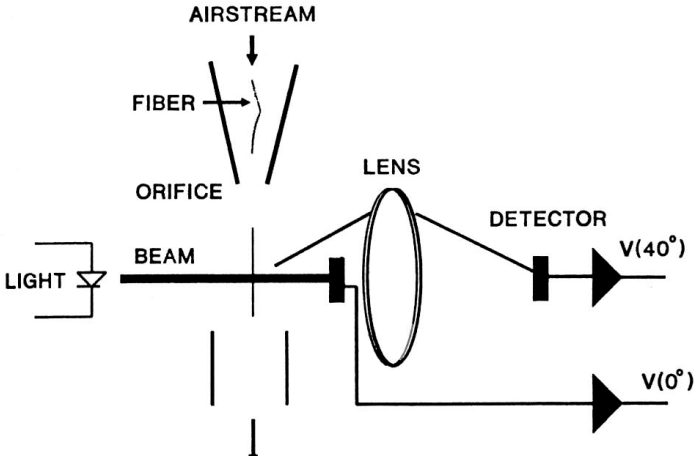

Figure 2.2: AFIS Electro-Optical Sensor [4]

As the individual fibers are carried aerodynamically to the sensor, they pass through a beam of light. A portion of the light is scattered and the amount of light directed at the detector is reduced, while the amount of light at a scattering angle is increased. This change in the amount of blocked or scattered light is reported as a voltage signal, and a waveform of the fiber passage is produced as in Figure 2.3 [6].

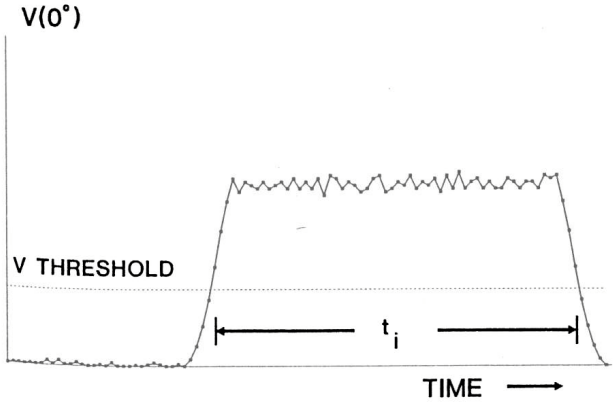

Figure 2.3: Produced Voltage Waveform [6]

If the individual fibers are assumed to be moving at a constant speed, then the length of the fiber can be calculated as the speed (s) multiplied by the time (t_i) that the fiber was in the path of the light beam. However, an experiment that was conducted with known fiber lengths inserted into the system, led to the rejection of the assumption of constant fiber speed [6]. To compensate for the errors caused by this assumption, an additional detector was placed downstream in the system. The detector consists of two sensors that had a known distance apart that were used to calculate the individual fiber speeds from the light scattering, thus, giving a more accurate measure of fiber length [6].

After implementing the speed detection device, the correlation coefficients on the mean length and short fiber content between AFIS and array method were found to be 0.99 and 0.91 respectively [6]. Therefore, as indicated by Stroupe, AFIS is comparable to the array method and should be included in the evaluation of any new fiber length measurement system [28].

Bragg and Shofner stated two main advantages of the AFIS system over other systems. The first advantage noted was that AFIS gives direct length measurements, as opposed to HVI, which has measurements that are based on length biased samples and requires equations to indirectly calculate the parameters. Also, other measurement systems calculate the weight-based parameters by assuming constant fiber fineness. By measuring both fiber length and diameter, Bragg and Shofner note the AFIS system is capable of calculating directly the numerical and weight based results without the assumption [6], although AFIS commercial software does make use of it [11].

A Study by Cui and Calamari used the diameter calculations of the AFIS system to recalculate the short fiber content by weight of fiber samples without the constant fiber

fineness assumption. They found that the average difference between the calculated values ranged from -0.4 to 0.4%, with an average difference of -0.03%. Therefore, it was concluded that the inclusion of the fiber diameter has only a minor influence on the calculated values of short fiber content by weight for AFIS system [11].

There are several issues with AFIS that lead to error in the measurement of fiber lengths. The most notable is the breakage of fibers in the fiber individualizer component of the system. Bragg and Shofner report that the UHM is reduced by about 1-2 mm and the SFC was increased by approximately 7% when comparing AFIS with hand sorting methods [6]. This error can be even greater for poorly oriented samples [26].

Another issue with the AFIS measurement system deals with the orientation of the individual fibers in the air stream as they pass through the light beam of the sensor. If a fiber is not straight and is folded over onto itself, the AFIS will measure the fiber to be shorter than its actual length. Conversely, if two fibers are touching one another as they pass through the sensor, the length will be reported as a single long fiber instead of two shorter fiber segments.

2.3 Prior Work in Image Processing for Fiber Length Measurement

In prior research, Yuksel Ikiz used image processing to measure fiber length [15, 16]. The success realized through his work was the impetus for the research that was performed by Stephen Stroupe [28], whose work is the motivation for the current project. The primary objective of Ikiz's work was to show that image processing could be an alternative method to existing fiber length measurement techniques [15]. The method that he used was to acquire a digital image of a fiber, identify the pixels of the image in which the fiber resides, and use those pixels to compute the fiber length. Accuracy, precision, and time were the three main

parameters that Ikiz used to evaluate the performance of various measurement techniques [15].

2.3.1 Experimental Procedure

In order to determine the conditions for which optimum measurement performance occurred, Ikiz identified five important factors. These factors were sample preparation, lighting, resolution, preprocessing, and processing. The different levels of each of these factors were employed for the measurement of cut-length polyester fibers of 1.5 inches with an approximate sample size of 30 fibers. In each of the measured samples, the calculated fiber length and the computer processing time were recorded. Cut-length polyester fibers were used because cotton fibers are highly variable in length and are not easily measured by hand. Therefore, polyester fibers provided a known length for which the precision and accuracy of the various measurement conditions could be compared. All of the image acquisition for the research was made with a CCD camera with 256 gray levels and 238x192 pixel resolution. In addition, all measurement algorithms used for image analysis and length computation were written by Ikiz himself. In order to make length comparisons to the results from these algorithms, samples of the polyester fibers were also measured on the Spinlab-HVI, AFIS, and by hand [15].

The first step of the measurement process was to prepare the polyester samples for measurement by sandwiching the fibers between two transparent slides [15]. Preparing the fibers in this manner assured that the fibers were held in the camera's plane of view and kept in focus. The polyester fibers were either placed individually between the slides or placed with two fibers crossing over [15]. Hence, individual polyester fibers and crossed over fibers made up the two levels of the experimental factor named sample preparation.

Two experimental levels of lighting, were the use of backlighting and frontlighting techniques [15]. In backlighting, fibers blocked the light that was shining from below and cast shadows in the image that appeared darker than the background and represented the area of the fibers. A beam splitter was used to create the backlighting. Front lighting, created by two 75 W halogen light sources, allowed fibers to reflect the light from their surface and create bright areas in the darker background [15].

Changing the distance between the camera and sample controlled resolution. Moving the camera closer to the sample resulted in higher resolutions. The four resolution levels used in the experiment were 37, 57, 106, and 185-micron. To obtain the 37 and 57-micron resolution values, the camera had to be moved so close to the sample that an entire fiber could not fit into one image. Consequently, multiple small images had to be combined together into a larger image for measurement purposes [15]. This method was deemed impractical with regard to time and complexity [28].

A preprocessing technique was necessary to scan the image and distinguish between the background and the fibers. Ikiz examined two types of preprocessing techniques for their effectiveness. The first method considered was global thresholding, whereby each pixel was checked for a lower or higher gray value than the threshold value, and was turned either black (representing background) or white (representing fiber) based on that comparison. However, due to uneven lighting and excessive noise, this method was not adopted for the experiment. Instead, local thresholding was applied. The two levels that were selected for this preprocessing technique were the 4-neighborhood and 8-neighborhood local thresholding applications. The 4-neighborhood thresholding application compared a reference pixel with its four side neighbors against the threshold criterion, and the 8-neighborhood application

compared the reference pixel with all of its 8 neighbors. In each case, if the difference between any of the neighbors and the reference pixel exceeded the threshold value, then the reference pixel was assumed to be a fiber and assigned a white pixel. Otherwise, the reference pixel was assigned black [15].

Once a sample had been prepared and the image preprocessed by one of the local thresholding applications, the next step was to obtain the lengths of the fibers. This task was accomplished by using the outlining, thinning, adding, and crossover algorithms. Outlining was used to locate the perimeter pixels of a fiber. Once the entire perimeter of a fiber had been outlined, the resulting count of even (N, S, E, W) and odd (diagonal) numbered connections were used to calculate the fiber length. The even connections were assigned a value of 1 unit spacing and the odd a value of 1.41 times the unit spacing. The final fiber length was calculated by summing the unit spacing, multiplying by the spatial resolution of the pixels, and dividing by two [15].

Thinning was another length determination algorithm that was used. Thinning was used to erode a pixel block that represented a fiber down to one-pixel in width. In this case, the length could be determined by simply counting the even and odd connections in the line segments making up the fiber [15].

Broken skeletons, which occurred when portions of a fiber were broken into segments due to insufficient contrast, caused inaccuracies in the length data. In order to make the connection between broken segments, the adding algorithm was created. Connections were made by adding an additional row of white pixels around the perimeter of the original image. This process was repeated several times and then the reverse process was applied an equal number of times. If any connections were made between the fiber segments, those

connections were retained during the reversal process. The adding of pixels was termed the dilation procedure and the reverse process was termed erosion [15].

An additional algorithm was used to evaluate the length of fibers that were crossed over one another. After thinning the fibers down to one pixel in width, any fiber that had more than two white pixel neighbors represented an intersection point of a fiber crossover. These intersection points were used to separate the crossover into individual fiber lengths by connecting the intersection point to the appropriate fiber end. If a neighborhood of white pixels had exactly four fiber ends, then it was known that two fibers were present in the block and the separation procedure was used. However, if only three ends were identified and the shortest segment was greater than 5 pixels long, then the entire fiber was eliminated. Otherwise, one fiber length was recorded. Any white pixel block that had more than 5 ends present was also eliminated from the image [15].

2.3.2 Results and Conclusions

After completing the experimental runs, Ikiz analyzed the results and concluded that the front lighting technique was superior to the backlighting technique in regard to processing time. However, the reflection of light from dust and other small particles on the mounting surface created very noisy images. This noise caused the program to identify false fibers, which greatly reduced the accuracy and precision of this method. Therefore, it was concluded that the best accuracy and precision could be obtained with backlighting. In addition to reducing noise generation, backlighting also allowed for higher resolution images, which further improved measurement precision. The 4-neighborhood preprocessing technique had a faster processing time than the 8-neighborhood technique. However, even for the lowest threshold values, the 4-neighborhood technique produced numerous broken

skeletons. Therefore, the 8-neighborhood preprocessing technique was concluded to be the technique of choice.

Precision was significantly improved when thinning was used. However, this improvement came at the expense of processing time. Without any fiber crossovers, the outlining technique was concluded to be the fastest algorithm, and was also within the desired precision range of 0.50 mm. When crossovers were present, thinning was chosen as the technique to use. The adding algorithm, when used with backlighting, also served to improve the precision. However, as noted previously, the use of additional algorithms for precision improvement significantly increased the processing time. Ikiz selected 57-micron resolution-backlighiting-8N-thinning-adding as the desired method of analysis with fiber crossovers. Without fiber crossovers, the desired method was chosen to be 106-micron resolution-frontlighting-8N-outlinning. The added processing time of the thinning and adding algorithms led to the conclusion that a commercialized system should present samples that are virtually free of crossovers [15].

Each of the image processing algorithms, with the exception of one, reported the fiber lengths as being greater than the given cut length of the polyester. Ikiz listed random noise, lighting conditions, and digitization as three reasons for this bias toward longer length measurements. Due to the excessive noise in the images, it was inevitable that some of the noise pixels would be connected to fiber pixel blocks. The addition of these noise pixels to the fiber length caused an upward bias in the measurement results. Uneven lighting hindered the amount of contrast between the background and fibers. This created fibers whose width spanned more than two pixels, which lead to further increase in the length results for outlined fibers. It was known that digital measurements record lengths larger than the actual length,

especially when the pixel size is small relative to the curvature. Dorst and Smeulders presented a formula to correct for digitization error in the case where curvature is present. Cotton fibers are not perfectly straight because of inherent crimp; therefore, Ikiz incorporated this equation into his computing to obtain more accurate results [15].

The fiber length distributions of Spinlab-HVI, AFIS, and hand measurements are shown in Figure 2.4 along with length distributions of two different experimental setups using Ikiz's algorithm. The graph shows that the use of Dorst and Smeulders equation produced more accurate results. Also, the experimental setup of backlighting-37 micron resolution-8N-thinning provided the best accuracy and precision of all the other measurement methods. Only AFIS produced a curve whose precision was comparable to that of this particular experimental treatment. However, under the assumption that the cut length of 38.1 mm is accurate, the AFIS length measurements produced very inaccurate results [15].

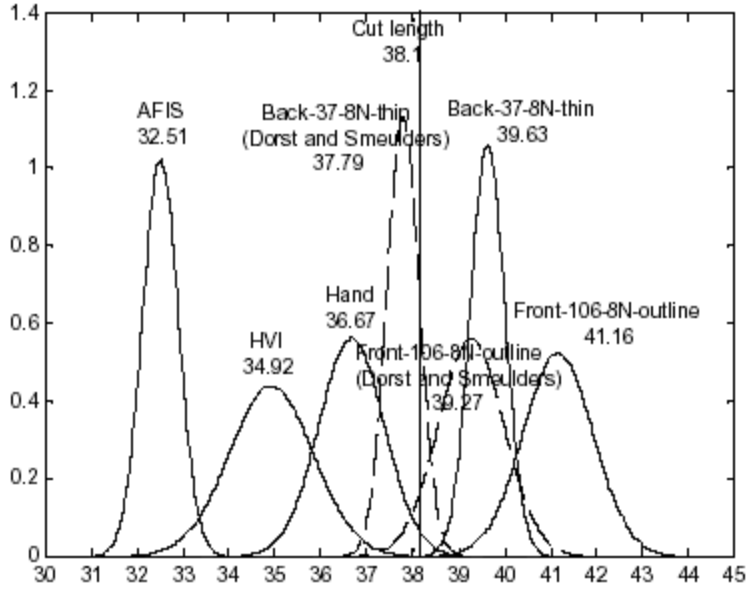

Figure 2.4: Ikiz's Accuracy and Precision Results [15, 16]

The results of Ikiz's work have shown that digital imaging can be used to obtain accurate and precise measurements of fiber length. In fact, the results have also shown that these methods can provide an increase in both accuracy and precision over current methods. Ikiz stated that the next step toward implementation of such a system was to devise a means by which fibers could be delivered, individually, to a digital capturing device [15]. Rust and Stroupe [28] have developed a mechanical means of such fiber delivery.

2.4 Prior Work in Fiber Delivery and Control

In research subsequent to Ikiz's work, Stephen Stroupe, along with the assistance of his advisor, Dr. Jon Rust, developed a mechanical system whereby cotton fibers could be individualized, straightened and delivered to a digital camera for measurement [28]. This system is the subject of the current research project. The primary objective of Stroupe's work was to individualize and straighten cotton fibers from a sliver sample, and provide a method for unbiased delivery of those fibers to the digital imaging device. In addition, it was Stroupe's objective to provide digital images that were compatible with the analysis software that was previously developed by Ikiz [15].

2.4.1 Prototype Design

In the first step of the prototype design, Stroupe identified five components that would be necessary in order to complete the stated objectives. These components were a fiber individualizer, a fiber transport chute, a fiber controller, lighting, and an imaging device that could interface with the software. These components were developed using a combination of existing technology and a 3D Computer Aided Drawing system known as IronCAD [28].

The fiber individualization component of the system was created by modifying a comber roll assembly, which is used in rotor spinning machines to individualize fibers from sliver prior to twist insertion [28]. Figure 2.5 is a detailed view of the assembly's and its components.

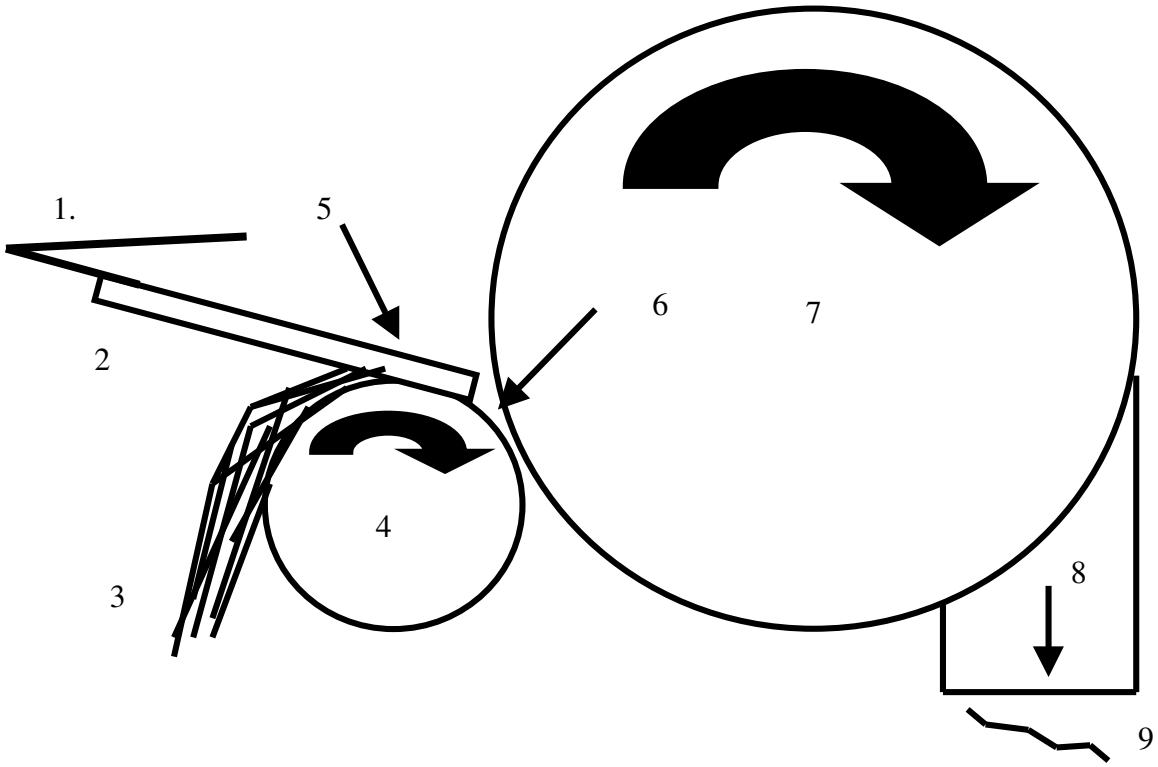

1. Spring Mechanism
2. Feed Plate
3. Fiber Sample in Sliver Form
4. Feed Roll
5. Feed Plate/Feed Roll Contact Point
6. Fiber Grasping Region
7. Comber Roll
8. Fiber Outlet
9. Airborne Individualized Fiber

Figure 2.5: Fiber Individualizer [28]

In the system shown in Figure 2.4, each of the components work together to obtain fiber individualization. The spring mechanism (1) exerts a force on the feed plate (2), which then creates a force at the feed plate/feed roll contact point (5). At this contact point (5), the sliver (3) is inserted and held in place by a frictional force. The feed roll (4) rotates in order to feed the sliver (3) through the contact point (5). As the sliver (3) is inserted, it comes into contact with the comber roll (7), which rotates at a high rotational velocity and contains pins that grasp the fibers at the fiber grasping region (6). Pins were used in lieu of teeth to prevent fiber breakage. As the pins grasp the fibers, they are removed from the sliver (3) individually. As the comber roll (7) rotates, the individualized fibers follow the rotation and are prevented from leaving the surface by an enclosure. After a number of degrees of rotation by the comber roll (7), the individualized fibers are released through the fiber outlet (8) with the assistance of air currents and centrifugal forces. This process results in airborne individualized fibers (9) [28].

A number of modifications were made to the comber roll assembly to ensure functionality. First, a DC motor was placed into contact with the extended axle of the comber roll to create a friction drive component for comber roll rotation. In addition, the feed roll was modified to be driven by a stepper motor, which was connected to the feed roll through a belt and pulley system. A square wave signal generator controlled the stepper motor. The gear ratio between the stepper motor and the feed roll was designed to be 2:1.4, which allowed the feed roll rotation to be controlled very precisely [28].

Stroupe investigated many different delivery chutes and chute arrangements to determine the best conditions for fiber delivery to the controller. After investigating anti-static tubing, plastic tubing, metal tubing, and tubeless delivery methods, he concluded that a

4-inch long metal tube was the preferred design. In addition, the tube was grounded to prevent the build-up of static charge inside the tube, which could affect the behavior of the fibers in the controller [28].

The function of the fiber controller was to gain control of each airborne and individualized fiber, and deliver each fiber in a manner that could be utilized by the imaging system. This function was accomplished through the use of mechanical and electrostatic methods [28]. The fiber controller was designed and constructed as seen in figure 2.6.

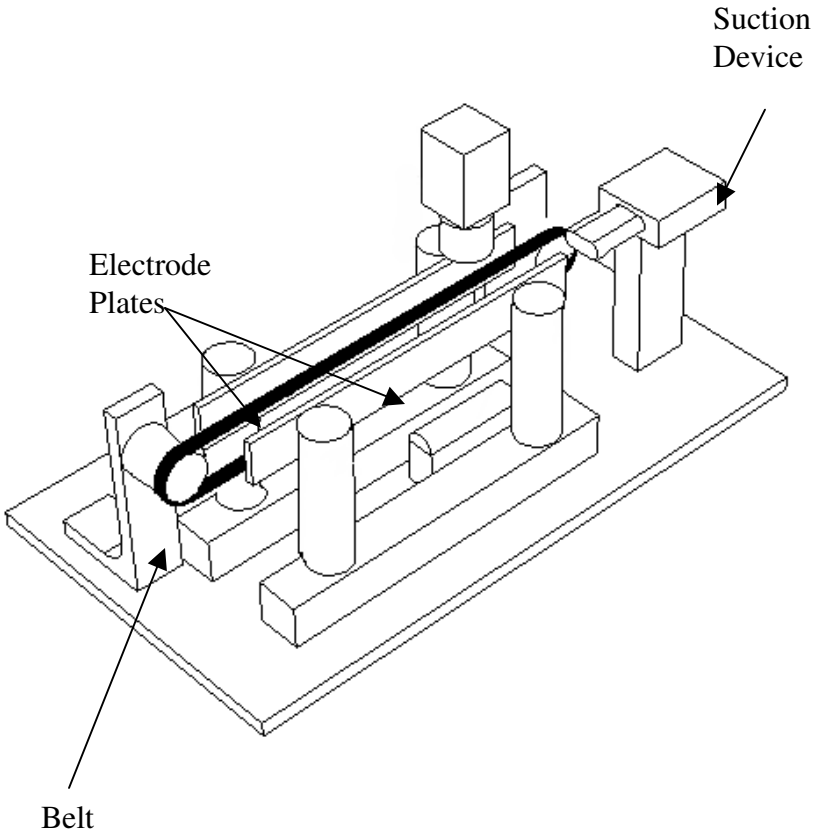

2.6: Overview of Fiber Controller [28]

As seen, the major components of the controller were the metal electrode plates, belt/conveyor, and the suction device. The system was set up such that the plate opposing

the belt was connected to a high voltage source of positive 12,000-volts DC [28]. The second electrode plate was connected to ground and obtained an induced negative charge. This arrangement created a strong electrostatic field in the region between the plates. The purpose of the electrostatic field was to gain control of airborne fibers and straighten them. The electrode plate support structure was constructed of nonconductive materials to prevent the loss of static charge [28].

Upon entering the electrostatic field, the fibers acquired a charge and were immediately attracted to the oppositely charged electrode plate. After coming into contact with the electrode, the charge characteristics changed and the fiber moved toward the opposing plate. This motion of fibers bounding between the plates continued until they approached the vicinity of the belt [28]

Through the use of pulleys and a DC motor, an opaque nonconductive conveyor was set up to traverse in the region between the plates. Upon coming into contact with the belt, one end of the fiber adhered to it, while the other end was extended outward into the open space. The fiber was reported to maintain this fixed position relative to the belt. As the belt moved, it conveyed fibers to the imaging device. The thickness of the belt was selected to be no more than the camera's depth of view, to prevent the fibers from being out of focus. The belt was aligned with the vertical center of the plates and was adjusted to be in contact with, or in close proximity to, the grounded electrode. The electrode spacing was set to provide a distance great enough between the negative electrode plate and the belt edge for the longest fiber to be fully straightened, without coming into contact with the opposing plate [28].

Initially, the electrode plates were constructed with rectangular cross-sections. However, with this plate configuration, there was no impetus for the fibers to move into the

vicinity of the conveyor [28]. Therefore, it was necessary to create an area of increased electrostatic field strength near the belt. This was accomplished by reconstructing one of the plates to have the cross-section seen in figure 2.7.

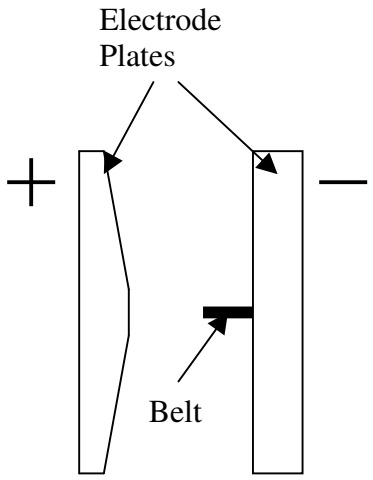

Figure 2.7: Modified Electrode Plate Cross-Section [28]

The electrostatic field strength varies with the voltage divided by the distance between the electrodes. Without changing the voltage level, the electrostatic field strength was increased near the belt by decreasing the distance between the electrodes at that area, using this tapered plate design. Observations made with this design in place revealed that the fibers moved to the belt much more readily [28].

After the installation of the modified electrode plate, a suction device was added to remove the fibers from the belt. The movement of the belt and fibers out of the space between the electrode plates caused them to lose their charge characteristics. It was, therefore, relatively simple to remove the fibers from the conveyor with a concentrated area of suction. The addition of this device assured that no fiber was carried through the measurement zone twice [28].

After eliminating fluorescent light as a viable backlighting source, Stroupe performed research in the area of LED illumination. An exhaustive search led to the acquisition of the LDL-TP series of high luminosity backlighting developed by CCS, Inc. The lighting provided optimum background uniformity through the use of a diffusion plate cover for the LED array. The power supply of the LED provided luminosity adjustment with a 256 gray-level control [28].

Image acquisition was performed by using a Pulnix TM-1020-15 CCD digital camera that was interfaced with the computer using an EDT frame grabber board. The Pulnix camera provided progressive scanning with 15 frames per second and an 8-bit and a 256 gray scale level output. The camera also had a built-in electronic shutter with nine available shutter speeds, ranging from 1/16 of a second to 1/16,000 of a second. The camera, along with a magnifying lens, was mounted directly above the backlighting source with only a portion of the conveyor visible in the bottom of the image [28].

2.4.2 Results and Discussion

Once the various components of the prototype had been designed and constructed, they were integrated into the system and Stroupe began his initial evaluations of performance. Fiber delivery to the conveyor and image quality were the primary areas of focus for these evaluations [28].

In his assessment of fiber delivery to the belt, Stroupe listed voltage level, electrode plate spacing, comber roll speed, feed roll speed, and belt speed as the parameters of interest. From observational studies, Stroupe established that the highest voltage level (+12,000 VDC) and the fastest comber roll speed (6,000-rpm) provided the best fiber delivery results. In addition, it was established that the closest electrode plate spacing that would allow for the

straightening of the longest fiber (1.4 in), was the best setting for the electrode plate spacing parameter. Therefore, the only factors remaining to be varied were the feed roll speed and belt speeds [28].

Stroupe set four levels for the feed roll speed (.22, .44, .66, .88 Hz) and three levels for the belt speed (3.53, 4.56, 5.58 in/s) and incremented the levels with various combinations. He made visual observations of the fiber individualization and fiber spacing on the belt for the different combinations. It was concluded that a feed roll setting of 0.44 Hz and a belt speed of 4.56 in/s provided the best fiber spacing and individualization results [28].

The next step of the evaluation was to determine the settings for superior fiber image quality. Stroupe identified belt speed, camera shutter speed, lens aperture, LED illumination level, and fiber-to-lens distance as important factors in determining the image quality. The belt speed and the fiber-to-lens distance had already been established and, therefore, were not varied in this analysis. Three shutter speeds were used in practice (1/500, 1/1000, 1/2000s) and the LED illumination level and camera aperture were adjusted for each shutter speed to provide the similar background gray-scale values in the range of 170–180 [28].

For each shutter speed setting, seven images were acquired and judged for quality on the basis of fiber diameter and the contrast level [28]. The fiber diameter results are shown in Table 2.5.

Table 2.5: Fiber Pixel Diameter at Different Locations and Shutter Speeds [28]

Pixel Location	1/500 Shutter Speed	1/1000 Shutter Speed	1/2000 Shutter Speed
200	16	7	6
300	12	7	4
400	14	8	5
500	15	8	5
Ave. Diameter	14.25	7.5	5

The apparent fiber diameters, in pixels, were counted at different locations on the fiber from the top of the image for three shutter speed settings. The 1/500 sec. shutter speed produced a very wide fiber, which can lead to decreased contrast and measurement precision. The fiber diameters are significantly reduced for the 1/1000 sec. and the 1/2000 sec. shutter speed settings, with the 1/2000 sec. providing the smallest diameter.

The contrast-level was then determined by observing the same images. This level was decided by examining a 9-pixel block on both the left and right side of the fibers at each of the pixel locations used for the diameter determination. After obtaining this 9-pixel block, the greatest gray-level difference between any two pixels in the block was defined as the contrast level [28]. The results from these calculations are seen in Table 2.6.

Table 2.6: Contrast Values between Fiber and Background [28]

	1/500 Shutter Speed	1/1000 Shutter Speed	1/2000 Shutter Speed
200 Left	10	14	16
200 Right	9	17	11
300 Left	7	13	14
300 Right	3	16	14
400 Left	10	19	15
400 Right	10	24	13
500 Left	9	18	18
500 Right	9	18	14
Ave. Contrast	8.375	17.375	14.375

These results indicate that the 1/1000-sec. shutter speed produced the highest contrast level between the background and the fibers, making this shutter speed the desirable setting. Although the previous results showed that the 1/2000-sec. shutter speed produced the smallest diameter fiber, it did not produce the highest contrast because the aperture had to be opened to adjust for the illumination. This adjustment caused a reduction in the crispness of the fiber image, which resulted in the lower contrast level. In addition, it should be noted that the individual contrast values are fairly consistent for the 1/1000-sec. and the 1/2000-sec. shutter speeds, which indicates that there was consistent contrast along the length of the fibers [28].

2.4.3 Conclusions

Stroupe concluded that the designed system provided a means by which fibers could be individualized, straightened, and delivered to a digital camera for measurement of their lengths. In his recommendations for further research Stroupe identified the following: [28]

- Modification of Yuksel Ikiz's code to function with the system
- Obtain processed images for visual inspection of code's functionality
- Isolation of the camera from machine vibrations
- Replacement of the woven belt to eliminate fiber protrusions
- Ensure fiber image quality
- Compare measurement results to other measurement system's results
- Test for accuracy and precision of the results

2.5 Moisture Regain and Conductivity of Cotton Fibers

The nature of cotton fibers allows them to absorb moisture from air. Morton and Hearle noted that the level of moisture absorbed into the fibers is one of the most important

factors in determining the electrical properties of cotton, as well as other fibers [24]. The moisture regain (R) is most commonly used to represent the amount of moisture in cotton and is defined as the ratio of the mass of absorbed water to the mass of dry fiber, multiplied times 100%. As the relative humidity of the environment increases, the moisture regain of cotton also increases. Figure 2.8 shows this relation between regain and relative humidity for various textile fibers.

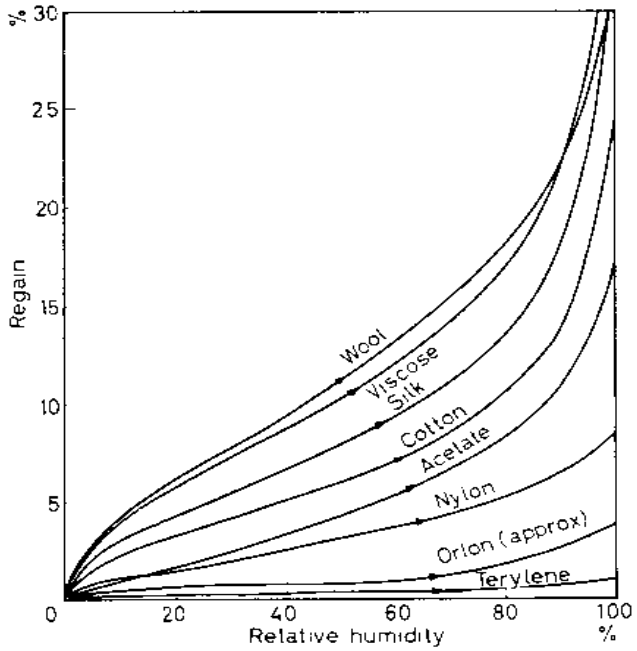

Figure 2.8: Regain vs. Humidity for Cotton [24]

It can be seen that the regain of cotton increases from approximately 4 percent at 20% relative humidity to about 8.5 percent for standard laboratory conditions of 68% relative humidity. There are only small differences in these numbers for cottons of different origins [Morton].

Moisture is one of the most important factors in determining the electrical resistance of textile fibers. In fact, it has been found that fibers conditioned at 10 and 90% R.H. show a

million-fold difference in their resistivity values [24]. The graph in Figure 2.9 shows a plot of log resistance versus relative humidity for various fibers.

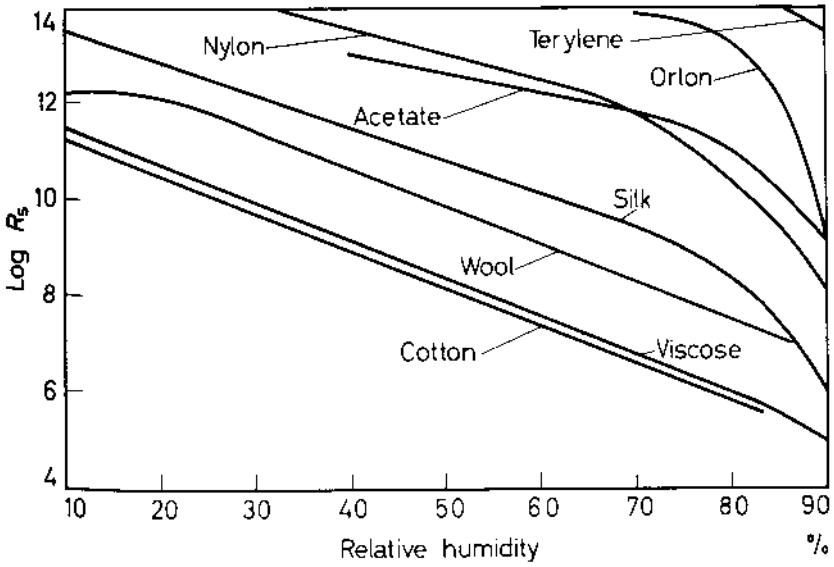

Figure 2.9: Log Resistance vs. Humidity for Various Fibers [24]

At 10% R.H., cotton has a resistance of approximately 10^{11} ohm-meters. This resistance value decreases to about 10^{7} ohm-meters at 68% relative humidity. It should also be noted here, that the log resistance values for cotton and viscose rayon at various relative humidity values are similar.

2.6 Flock Motion in Electrostatic Fields

Flocking is a process whereby monofilament fibers (flock) of 0.25 – 5.00 mm in length are applied directly to the surface of a substrate that has been coated with an adhesive. Nylon, rayon, and polyester are the monofilament fibers that are typically used for the process. Electrostatic flocking is one of the more common methods of applying flock to a material. The behavior of fibers in the electrostatic flocking process is very similar to the

fiber behavior observed in the system that was developed by Rust and Stroupe. An example of an electrostatic flocking system is given in Figure 2.10.

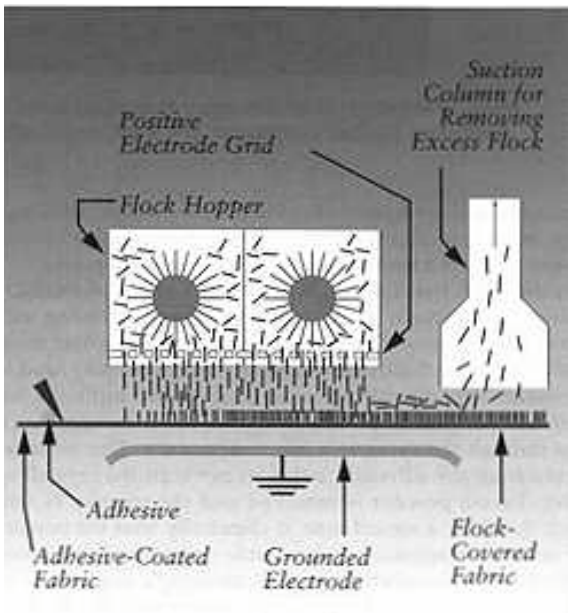

Figure 2.10: Electrostatic Flocking System [29]

In the electrostatic system, a potential difference is created between two conducting electrodes. One of the electrodes is connected to a high voltage direct current source, while the opposing electrode is grounded. The charged electrode is contained inside of a hopper and the substrate is passed over the grounded electrode. When the voltage is applied, the flock fiber takes on a charge at one of its poles and is driven at a high velocity from the hopper through a metal screen and then to the substrate. The dipole characteristic of the flock fibers allows them to align vertically with the electrostatic field. They move back and forth between the charged electrode and the fabric in this manner until becoming embedded into the adhesive. Any fibers that do not adhere to the material are removed via a suction column [29].

Kim and Lewis conducted a study in order to understand the motion of flock in an electrostatic field during the flocking process. They conducted three experiments that established the basic parameters involved in the process. These experiments helped them to better understand the effects of relative humidity and moisture on the motion of flock particles [19].

The first experiment by Kim and Lewis was to study the effect of relative humidity on the flock motion. For this experiment, they used a SPG 1000 Flock Motion Tester, which is used to evaluate the motion of the fibers as they are influenced by the electrostatic field. Nylon flock fibers were placed on a metal platform that served as one of the electrodes to form the electrostatic field. A 40 kV direct current voltage was applied to the electrode for 30 seconds and the fibers were dispersed in the electrostatic field away from the metal platform. Samples of flock fibers were conditioned at a specified relative humidity of 0, 47, 60, and 87%. The samples were then tested and the fiber flock activity was determined by the grams of fiber disrupted by the electrostatic field per second of exposure to the electrical field (mg/s). From this experiment, Kim and Lewis concluded that the fiber activity increased as the moisture content (%RH of the conditioning) increased. They proposed that this outcome was possibly a result of the influence of moisture on the conductivity and on the induced surface charges of the fibers [19].

Kim and Lewis also studied the effects of moisture on mechanical siftability. Siftability is a term used to describe the ability of flock fibers to be sifted through a metal wire screen. An RPG 1000 Siftability Tester was used for evaluation in the conduction of this experiment. The tester consisted of a metal screen-walled cylindrical chamber that could be rotated. Nylon fiber samples, of 20 grams each, were conditioned at 0, 47, 60, and 87

percent relative humidity and were placed inside of the chamber. The weight of fibers that had been sifted through the wire screen after 60 revolutions determined the siftability. The results showed that the siftability of flock fibers decreased as the relative humidity of the samples increased. Kim and Lewis stated that the likely cause of this result was an increase in contact adhesion between the fibers at increasing moisture levels [19].

A third experiment by Kim and Lewis studied the effect of moisture on the conductivity of the flock material. They used a MAHLO Texo-Meter to test the conductivity of 20-gram fiber samples that had been conditioned at 0, 47, 60, and 87 percent relative humidity [19]. A graph of these results is shown in Figure 2.11.

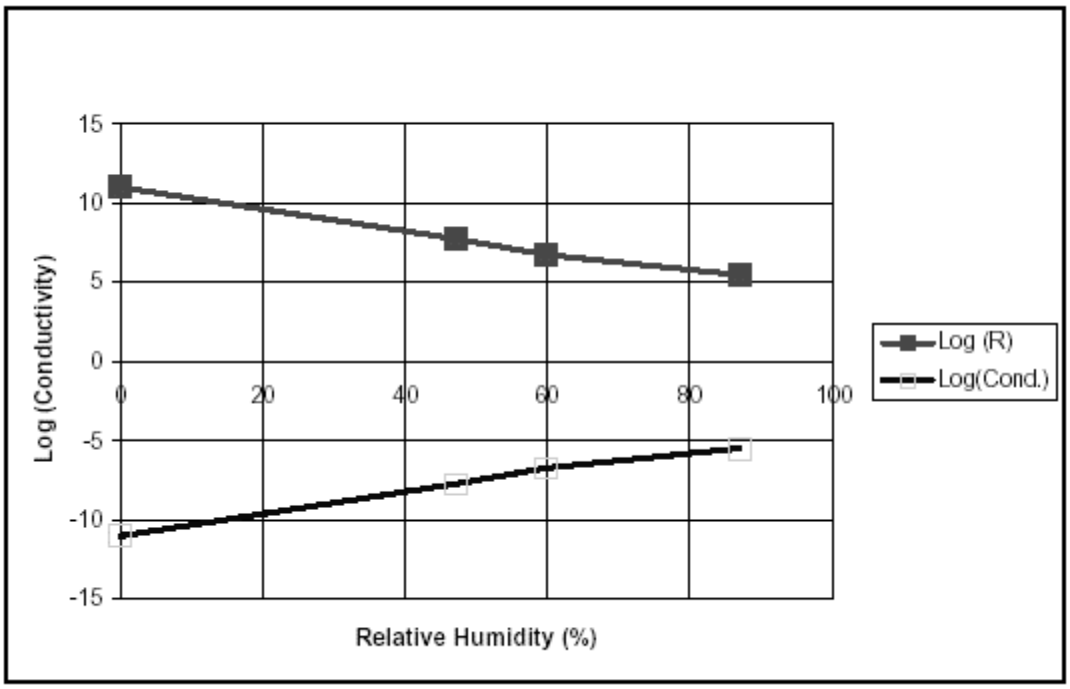

Figure 2.11: Rayon Conductivity vs. %R.H. [19]

It can be seen from the figure that the nylon sample conditioned at the low relative humidity showed very little conductivity, with values similar to that of nonconductors. Kim

and Lewis stated that the contact charging of flock particles is not possible for this range of conductivity. However, an increase in the moisture content of the fibers in the samples with higher humidity conditioning showed substantial increases in conductivity. They concluded that the sample conditioned at 87% relative humidity, although it would have improved electrical properties over the others, allowed excessive fiber-to-fiber adhesion. Therefore, as a compromise, they selected a range of 50% to 70% relative humidity conditioning for optimum performance of the electrostatic flocking using the nylon fibers. It was thought that this range would provide the best fiber behavior with the least amount of fiber clumping [19].

An additional study by Kim and Lewis looked further into the motion of flock particles in an electrostatic field. They used the experimental setup shown in Figure 2.12 to investigate the effect of fiber length and linear density on flock motion. In addition, the effects of electric potential and relative humidity on flock motion were examined [20].

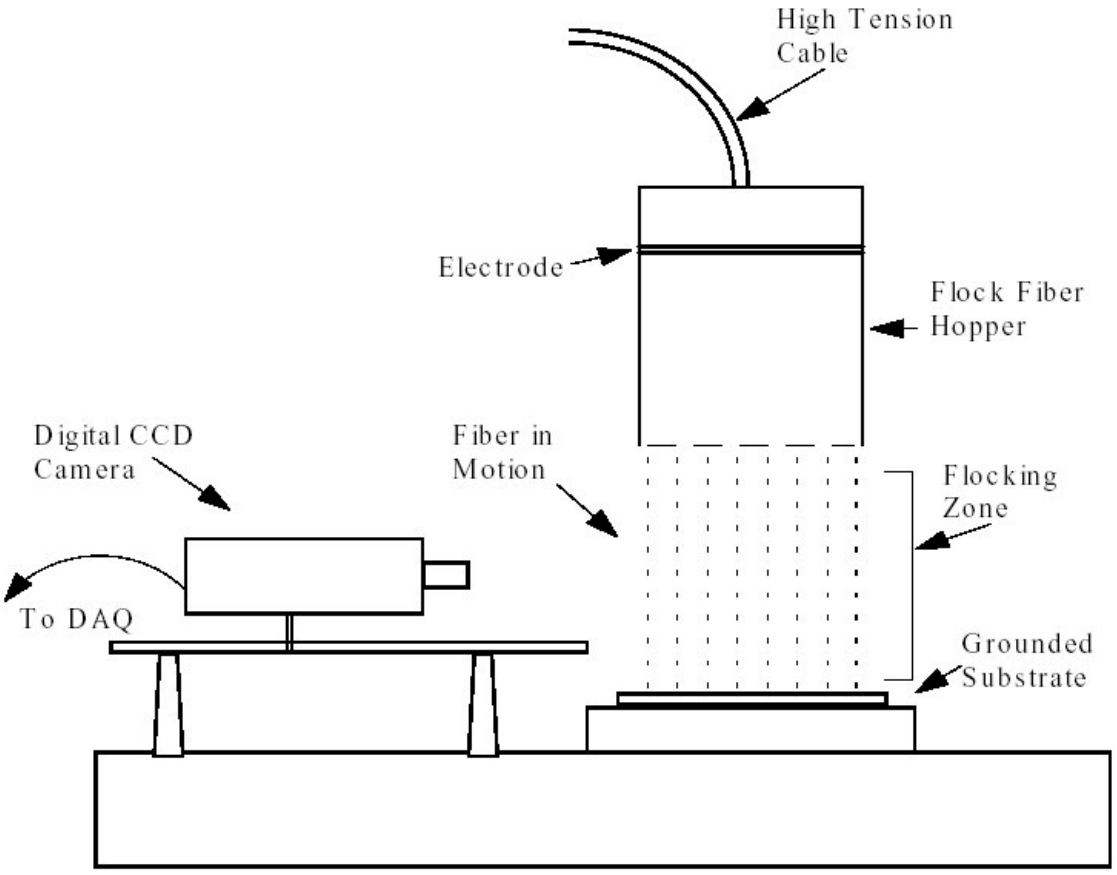

Figure 2.12: Experimental Setup [20]

In Figure 2.12, the digital CCD camera was mounted and set up to view the region between the flock hopper and the grounded substrate. This allowed the researchers to view and trace the motion of the fibers as they were accelerated by the force of the electrostatic field. The digital camera was connected to a computing device, which was used to analyze the displacements of the fibers over time. [20].

They were able to measure the flock displacements for 800 microseconds by using the CCD camera and accompanying image analysis software. From this information, they were able to obtain velocity profiles on the flock fibers. In the first experiment, it was found that fibers with higher surface areas attained higher velocities on average. Two types of

nylon fibers (1.5 d / 1.25 mm, 3 den / 2.5 mm) were used in the experiment and the relative humidity (40%) and voltage level (40 kV) were kept constant. The 3 denier / 2.5 mm flock had an average velocity that was two times that of the 1.5 d / 1.25 mm flock because of a higher net charge, which is the major driving force in an electrostatic field [20].

In the second experiment the voltage level was set to 40 kV and 70 kV, while the fiber geometry (3 den / 2.5 mm) and relative humidity (60%) were kept constant. It was concluded that the average velocities of the flock at the two potentials were similar; however, the variability in the velocities was much greater for the 70 kV potential [20].

To test the effect of moisture, two levels (40%, 60%) of relative humidity were selected for study, while the geometry (1.5 den / 0.05") and the potential (40 kV) were kept constant. The results showed similar distributions and statistics for both samples. Kim and Lewis indicated that this was an expected result because the fibers were being charged by corona discharge in this experiment, and not by direct charging. They note that corona discharging is not critically dependent upon the surface conductivity of the fibers, which is controlled by relative humidity. In direct fiber charging; however, the surface conductivity is very important to the effectiveness of charge transfer. Therefore, the relative humidity has a significant effect for direct charging of the flock material [20].

3. Research Approach

3.1 Work Objectives

Before starting the principle project work, several objectives were established.

- Improve image quality
- Improve fiber individualization
- Improve accuracy and reliability of fiber measurement
- Determination of biased fiber selection
- Development of system calibration method
- Determine Accuracy and Repeatability of Measurements

3.2 Research Methods

Research was initially begun in meetings with Dr. Jon Rust and Stephen Stroupe to discuss the fiber measurement system that had been developed as part of Stephen's research for his Master's thesis. These meetings consisted of discussions regarding the system's functionality and the previous image analysis research performed by Yuksel Ikiz. Further work with Stephen consisted of completing the system setup to prepare for data collection and system analysis.

After the system setup was complete, the first trail runs were conducted and observations of the performance were made. After review of the initial data, it became apparent that there were multiple opportunities for improvement in several key areas of the device. These areas were identified and potential methods for their improvement were examined.

Initially, the primary focus was on improving the quality of images that were produced by the combination of the digital camera, frame grabber, and computer logic. Due to a lack of sharp contrast between fibers and the background, many of the images contained broken skeletons. A pulsing power supply for the LED array, along with a camera calibration method, was incorporated in an effort to reduce or eliminate the occurrence of broken skeletons and excessive noise. The image quality was also degraded by tiny fibers that protruded from the surface of the woven polyester conveyor belt. An examination into nonconductive belting materials absent of fiber reinforcement was made in order to find a replacement for the polyester conveyor.

Once the image quality had been improved, a calibration device was necessary in order to obtain a resolution value that the programming logic must use to accurately measure fiber lengths. A glass slide and a fine-tip opaque pen were used to produce the calibration device. This device utilized the same backlighting and thresholding procedures used for fiber detection.

Additionally, fiber samples were collected at two locations of the fiber delivery and measurement process to establish whether a biased selection of fibers occurs in the system. These fiber samples were tested via HVI and the results were subject to hypothesis testing. By using an Analysis of Variance (ANOVA), it was possible to conclude whether fibers were being sampled selectively, and modifications were made accordingly.

Improvement in the individualization of fibers on the belt was also important in obtaining fast, accurate, and reliable fiber length results. A $2^{\wedge 4-1}$ Fractional Factorial Experiment, with one replication, was conducted and analyzed to determine the settings that would provide the greatest percentage of individualized fibers to the camera for

measurement. Mechanical and programming methods were also utilized to improve individualization and crossover separation.

Another issue relating to fiber presentation was the overlapping of fibers onto the conveyor. This overlapping effect allowed portions of fibers to be hidden from the camera's view. Initial investigation into this area consisted of research in electrostatics and the charging of materials in electrostatic fields. Based on this and other research, multiple mechanical and material modifications were investigated as potential solutions to overlapping. After completing all of the changes, sample data was again collected and compared to the initial results. Subsequent experiments were also conducted to determine the accuracy and repeatability of the system's measurements, as well as its ability to distinguish between two different fiber populations. The data from these experiments were then used to make comparisons with HVI and AFIS results.

4. Experimental

4.1 Image Quality

Initially, the setup and configuration of the system was completed and sample fiber images were obtained. It became immediately apparent that there was a need for improved contrast between the fibers and background of the images, and great significance was placed on the improvement of image quality. Without sufficient contrast for the entire lengths, many fibers were broken into, and analyzed as multiple fiber segments instead of one continuous fiber. In addition to contrast, noise levels in the images and the detection of false fibers were areas in need of improvement.

4.1.1 Depth of Focus

In order to obtain sufficient contrast between the fibers and the background, it is important for the camera to have an adequate depth of focus. It is necessary to have a depth great enough to ensure that focus is not affected by any out-of-plane movement of the fibers, which is caused by fiber crimp and fiber location on the belt. However, the depth of focus does have a limiting value. It is undesirable to obtain a focus depth so large, that fibers on the plates above or below the conveyor can be viewed by the camera and measured. Allowing the camera to focus on these fibers provides an additional source of measurement error, which is attributable to a portion of the fiber length being blocked from the camera's view by the belt. In addition, focusing on these areas allows for multiple measurements of any motionless fibers that may be present.

A greater depth of focus can be obtained by closing the camera's aperture. However, closing the aperture further from its initial setting reduces the amount of light entering the camera and hinders the systems ability to provide contrast. By observing the spectral response curve of the Pulnix TM1020-15 CCD progressive scan camera [30] in Figure 4.1, it is seen that the camera has the greatest sensitivity at approximately 535 nm wavelength light, which is in the wavelength range of green light. The possibility of acquiring a green LED light source to improve the camera's sensitivity to the light was examined. This option was determined to be infeasible at the time.

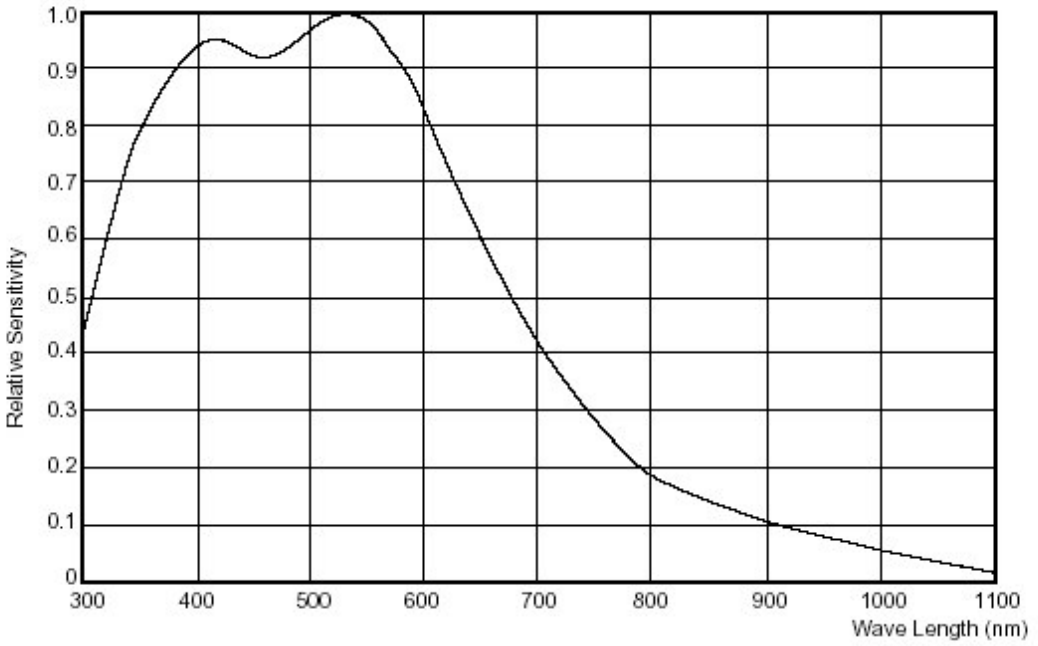

Figure 4.1: TM1020-15 Spectral Response curve [30]

The alternative option was to obtain a pulsing power supply for the existing red LED light source, which provides up to three times greater light intensity. This increase in intensity would allow for further a decrease in the camera's aperture, an increased depth of focus, and improved fiber contrast.

4.1.2 Shutter Speed

Another determining factor in the image quality is the camera shutter speed. Without an adequate shutter setting, the fiber images become blurred, causing a loss of sharp contrast with the background. Therefore, it is necessary to have a shutter speed that is fast enough to provide crisp images with fiber widths of only a few pixels. Such an image would allow for the highest possible contrast between the fibers and the background and improved precision.

When increasing the shutter speed, less light is allowed to enter the camera and the aforementioned depth of focus once again becomes an issue. By employing a CCS Inc.

PTU-2012 pulsing power supply, which provides pulse width settings from 10 to 990 µs and has a trigger cycle of 1 ms, the image quality could be improved without significantly changing the shutter speed from its original setting of 1/1000 sec.

Using the pulsing power supply for this purpose required that the light pulse and the shutter speed be timed in a manner such that there is only one light pulse per shutter opening. By allowing two pulses to occur during a single shutter opening, a fiber is lighted twice and two side-by-side cloned fibers appear in the image. Hence, it is imperative that the shutter speed be slightly faster than the trigger cycle to prevent double light pulses during an opening. The shutter speed was increased by 65µs from 1/1000 sec. by employing the down trigger in Mode D of the Pulnix camera, which changes the shutter speed by one horizontal line scan time (65µs). The timing diagram for the setup is shown in Figure 4.2.

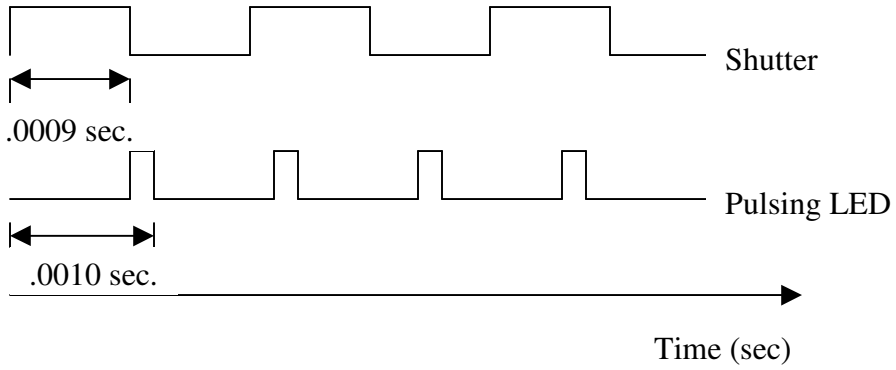

Figure 4.2: Timing Diagram

From Figure 4.2 it can be seen that an opening of the shutter does not receive a pulse of light from the LED at all times. Therefore, some of the captured images have very low background pixel averages, and the contrast between the fibers and the background is lost when this occurs. By devising a system to trigger a pulse of the light during the opening of the shutter, this issue can be resolved. However, as a quick solution, the program was altered

to halt image analysis on images with a pixel background average less than 150. This change disallows the analysis of some fiber images, but also prevents the analysis of images known to contain numerous broken skeletons.

4.1.3 Background Uniformity

The background uniformity is also critical for ensuring that high quality fiber images are obtained. The threshold value for distinguishing between the background and a fiber is often set in the range of 8 to 15 gray-levels. Therefore, any gray-level differences between pixel-block neighbors this great or greater in the background is marked as a white pixel, which is representative of a fiber. Initially, the background contained such excessive inconsistencies that white pixels dotted a majority of the image, creating unacceptable noise levels and making the detection of fibers extremely difficult. Often, the noise pixels would exist in such large groups that they were outlined and measured as false fibers. In addition, these pixel dots would frequently combine with the white pixels of true fibers, which caused length to be added to those fiber measurements.

The lack of background uniformity necessitated the development of a calibration routine for the CCD camera that would serve the purpose of improving the background evenness. This calibration was achieved by taking an average of all the pixel values over 50 frames and adding or subtracting an integer from each pixel to make it equal the grand average for the entire frame. This calibration file could then be stored in the measurement algorithm as a camera setting file to calibrate all images.

4.1.4 Conveyor Uniformity

The woven polyester belt that was originally used for fiber transportation was very inconsistent and hairy along its length. This hairiness caused computational errors as the

software scanned an image in search of fibers to analyze. The processing algorithm scans the image 10 pixels from the belt edge in search of a fiber; consequently, if the belt contains protrusions that extend more than the allotted 10 pixels, they will be analyzed as fibers. Therefore, it was determined that a more uniform belt should be used for fiber conveying purposes.

The thickness of a replacement belt needed to be as close as possible to the polyester belt that Stroupe used to assure that the focus on the fibers is maintained. In addition, the belt needed to be constructed of an insulating material that would allow the fibers to exhibit the same behavior that was previously observed. The belt was also required to be opaque to prevent the emitting LED light from passing through it. If the belt were transparent or translucent, the belt stripper would not function properly because belt identification difficulties.

After an exhaustive search, a synthetic flat belt made of urethane was chosen to provide improved belt uniformity and image quality. The selected belt had a width of 0.625" and a thickness of 0.055", which is slightly thicker than the polyester conveyor. Due to its urethane construction, the belt was thought to exhibit the insulating properties that were desired of it. Once the belt was obtained and placed in the system, the fiber behavior and image quality was observed.

4.1.5. System Vibration

A great deal of vibration was present in the system due to the oscillation of the comber roll friction drive assembly. This vibration produced minor movements in the camera, which hindered the effectiveness of the background calibration and caused the loss of focus. Therefore, a new frame and mount were constructed to allow for isolation of the

camera from the vibration of the comber roll. This isolation served to secure the proper calibration and focus so that superior image quality could be obtained.

4.2. Resolution Calibration

In order to obtain accurate fiber length measurements from the acquired images, a means of system calibration was needed. This was accomplished by obtaining a resolution value for the fiber length algorithm, which converts perimeter pixel counts into actual fiber lengths. This resolution value was gotten by presenting a thin and opaque line of known length to the camera for analysis. This analysis then incorporated the known length into Equation 4.1 to obtain the desired resolution value, where length is the known length, and e and o are the even and odd pixel counts respectively. After calculation, the resolution value is reported as microns per image pixel and is updated in the length processing code.

Resolution Value = (length * 2000) / (.948e + 1.343o) **Equation 4.1**

In order for the backlighting to cast an image of the opaque line to the camera, the line needed to be present on a transparent background, which would allow the lighting to pass through. Therefore, a thin line was drawn on a microscope slide, precisely measured using digital calipers and a magnifying glass, and was presented to the camera for analysis and the acquisition of a resolution value. An example of this calibration slide is shown in Figure 4.3. The software was set to obtain 50 resolution values from the known length and to record the average. This averaging method allowed for a more precise estimate of the value.

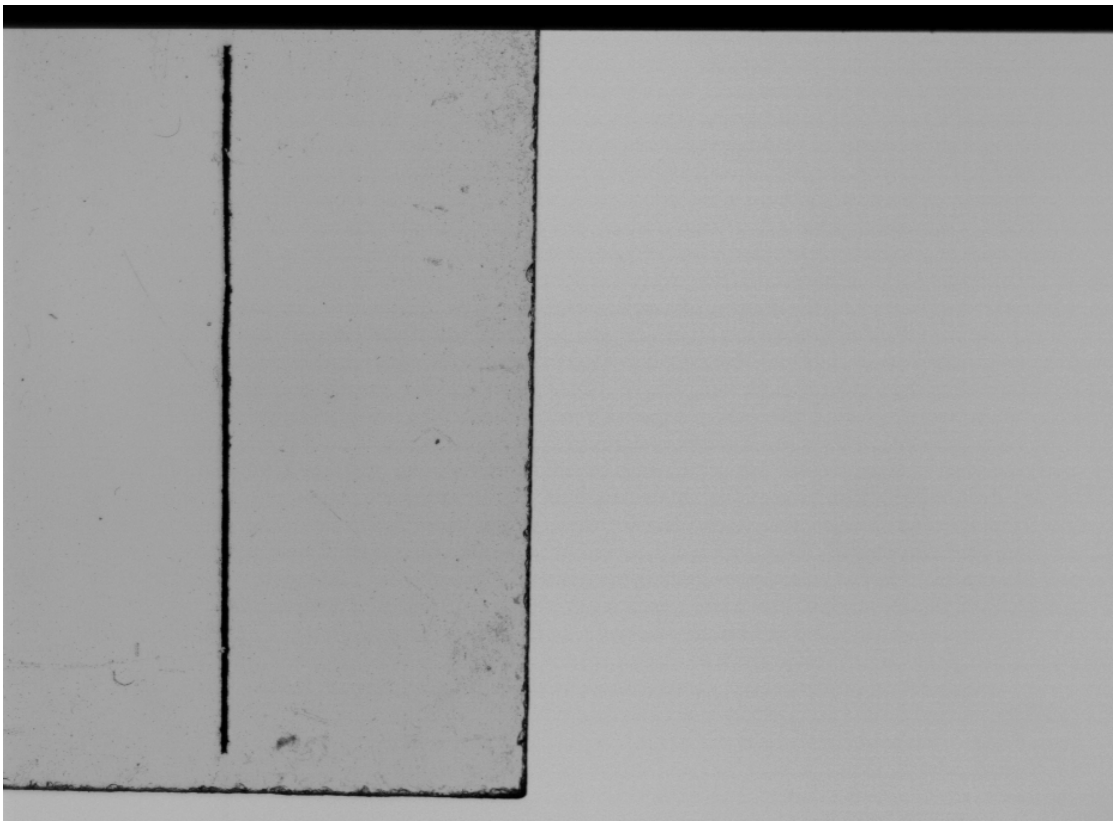

Figure 4.3: Resolution Calibration Slide

It can be seen that the edges of the microscope slide are dark enough to be detected by the thresholding algorithm. By positioning the bottom slide edge such that it extends beyond the field of view, the side and bottom edges are not analyzed in the resolution calibration, because they are seen as one continuous fiber extending beyond the field of view. The code has an incorporated function that halts the measurement of any fiber that touches the edge of an image. Therefore, only the calibration line is analyzed and an accurate resolution value can be obtained from the processed image without any interference from the slide itself. The threshold for obtaining the resolution is set at a high value of approximately 130 to prevent the detection of trash particles on the slide during calibration.

4.3 Fiber Individualization

Although calibration secured the accuracy of measurement for individual fibers, fiber crossing and entanglement hinders the ability of the algorithms to provide accurate and precise fiber length measurements. Crossed and entangled fibers present major time and functional challenges to the measurement algorithm; therefore, it was important to significantly reduce the frequency of these occurrences and ensure that a high percentage of individual fibers are presented to the camera for measurement. A number of mechanical and statistical methods were utilized in an effort to do so.

4.3.1 Fiber Characterization

To gain a more complete understanding of the types of fiber orientations in the system, many images of non-individualized fibers were observed and the orientations noted. Four primary types of improper fiber orientations have been identified. The U-away orientation is defined as a U-shaped fiber that has the bottom portion of its "U" directed away from the belt with an additional fiber crossing over it. Another orientation is labeled as a straight crossover, which describes two straight fibers that are in such close proximity on the belt that their protruding ends are allowed to cross. A hook is a fiber with one end hooked around another fiber, and is recognized as a third orientation. The final fiber type is defined as an entanglement, which is identified as multiple fibers that are crossed and knotted with one another. Examples of each of these orientations are represented in Figure 4.4.

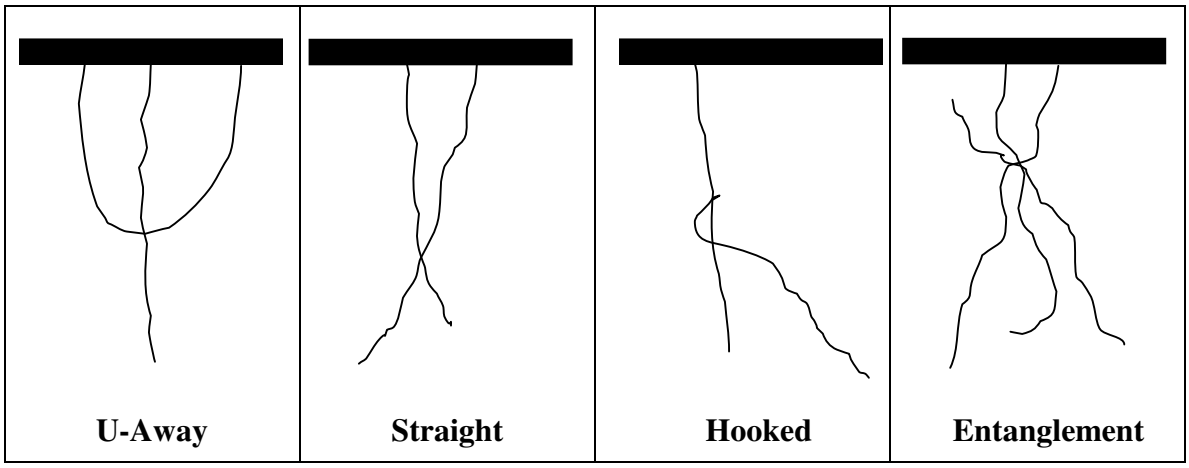

Figure 4.4: Improper Fiber Orientations

4.3.2 Mechanical Modifications

In order to determine the methods by which inter-fiber contact was likely to occur, the fiber behavior was closely observed and studied. These observations and studies revealed that mechanical modifications could perhaps be made to improve the delivery of individual fibers to the camera.

One of the primary methods of fiber crossing and entanglement was the interaction of fibers on the conveyor with fibers on the opposite (positive) electrode plate. This interaction caused many of the individualized fibers on the belt to become entangled with opposing fibers. It is believed that this fiber contact is a major source of all fiber orientations seen previously in Figure 4.4. A mechanical means of eliminating this interaction was sought.

A miniaturized version of the existing machine setup was modified and used as a model to observe the effect of the changes. The modification consisted of cutting a 1/4" wide by 1/8" deep slot down a portion of the center of the plate opposing the conveyor. The purpose of the slot was to provide a vertical spacing between the fibers residing on the plate and the fibers on the belt, as shown in Figure 4.5.

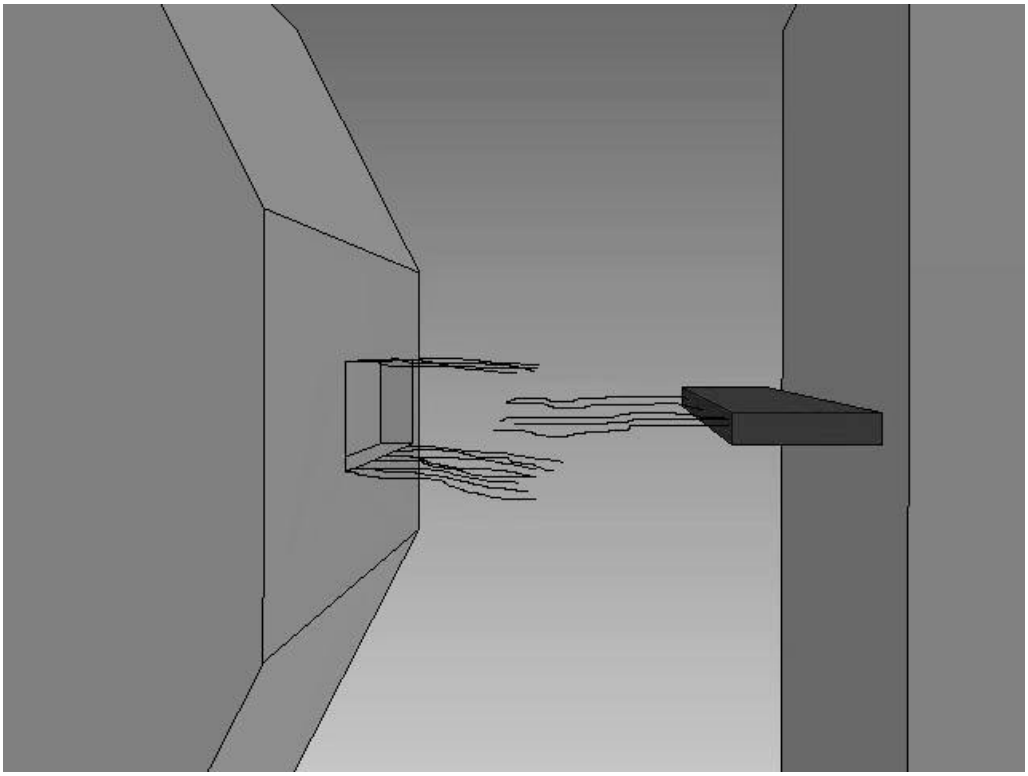

Figure 4.5: Fiber Orientation with Milled Slot

The beginning of the slot was cut approximately 8 inches down from the fiber delivery area in order to maintain the strong electrostatic field strength near the belt in the fiber entry zone. Outside of this zone, any fibers that have not settled onto the belt are pulled toward the top and bottom edges of the slot where the electrostatic field is the strongest. This effect prevents fibers from sticking to the middle portion of the slot, across from which the conveyor traverses. Therefore, it greatly reduces the number of fibers on the belt that come into contact with fibers on the opposing electrode. Tests performed on the smaller model showed that the desired effects were achieved, and the slot was implemented in the larger system.

Another method of reduced fiber individualization was the inability of fibers to move rapidly downward from their top entry point on the electrodes, to the transport zone of the

conveyor. This slow movement of fibers to the conveyor contributed directly to an increase in fiber density between the electrodes. Naturally, as the fiber density increased, the probability of fiber crossovers and entanglements also increased. Therefore, it was necessary to increase the rate at which fibers moved to the conveyor.

It was known that significantly reducing the fiber delivery rate to below 0.10 Hz would allow the fibers more time to travel to the conveyor, which would keep the fiber density between the plates to a minimum. However, slowing the feed motor to these speeds results in such great fiber spacing that processing times become significantly increased. Hence, an alternate method of increased fiber removal was needed.

The electrostatic field strength between the electrodes is inversely proportional to the distance between them, as shown in Equation 4.2.

$$E = V/d \qquad \textbf{Equation 4.2}$$

To reduce the amount of time taken for fibers to migrate to the conveyor, it is desirable to have a concentrated area of amplified field strength near the conveyor that rapidly decreases as the vertical displacement from the conveyor increases. An electrostatic field that is strong and concentrated near the belt was believed to provide a force that would pull the fibers more quickly toward it. Therefore, the electrodes were redesigned as in Figure 4.6 to provide the desired electrostatic field map.

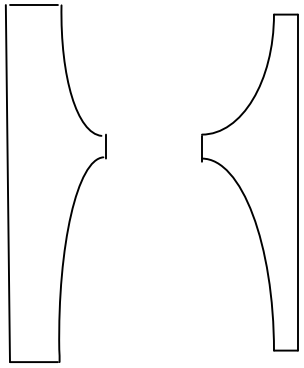

Figure 4.6: Modified Electrodes

As seen in Equation 4.2, the electrostatic field strength can also be modified not only by changing the distance between the electrodes, but also by altering the voltage level between them. Increasing the voltage was thought to also improve the rate at which fibers migrated to the vicinity of the conveyor. Therefore, the voltage on the positive terminal was increased from +10 kV to +25 kV by using a DX250 high voltage supply for electrostatic generation, which is produced by Emco High Voltage. This voltage increase provides superior electrostatic field strength, while also allowing for greater spacing between the electrodes, which can further reduce fiber to fiber interaction.

In initial tests of fiber separation and alignment on the belt, it was also observed that fibers were sticking excessively to the charged plates instead of bounding between them, as theory would suggest. Fibers that remained adhered to the electrodes in this manner blocked the influx of fibers into the electrostatic field and created entanglements with them as they entered. It was presumed that either the coating applied to the electrodes after production or that the surface roughness may have been a cause of this unexpected fiber behavior. In an effort to eliminate this potential cause, the plates were removed and mechanically polished to

a mirror finish to assure that the surfaces were smooth and absent of any coatings. These efforts had no effect on improving the fiber behavior.

4.3.3 Sample Conditioning

In order for the electrostatic field to have the desired effect, it was thought that the moisture content of the fibers needed also to be maintained at a minimum level. It was known that cotton fibers are not naturally conductive and that moisture is the key component of the fibers that allows them to attain some level of electrical conductivity. Without moisture, the electrostatic field would have very little effect in catching, straightening, and transporting the fibers to the conveyor.

The observations that were made in an unconditioned laboratory, where the machine and sliver samples were originally stored, revealed that the fiber behavior in the system was less than desirable. As noted previously, the fibers appeared to stick to the plates and displayed little mobility, which was detrimental to fiber transport and individualization. Since the plate surfaces had been ruled out as a possible cause, it was hypothesized that low moisture content in the fibers was a reason for this behavior. Therefore, relative humidity measurements were taken in the laboratory environment using a digital hygrometer to test the possibility that the fibers were moisture deprived. The hygrometer readings revealed that the relative humidity in the lab was merely 28%. It has been shown that the moisture regain of cotton fibers at this percentage is only around 4 percent [24]. Therefore, it was decided to moisten a sample of fibers to determine if increasing the moisture in the sample had an effect on the fiber behavior. Immediately after moistening the sample, the bounding motion of the fibers increased in velocity and frequency. It was also apparent that the fibers were being

captured and straightened more effectively by the electrostatic field. These observations coincide with the results of the study by Kim and Lewis [19].

In order to increase the moisture level in the fiber samples, they and the system were moved to the physical testing laboratory, where standard conditions are maintained. The standard conditions for the lab are a temperature of 78°F ±2 and a relative humidity of 68% ±2. At these conditions, it has been shown that the moisture regain of cotton is 8.5 percent [24], which is more than twice the moisture present in the fibers previously. As was shown previously in Figure 2.12, the resistance of cotton fibers decreases dramatically with the absorption of moisture. Therefore, a definite change in fiber behavior in the electrostatic field at these conditions would be expected as well.

4.3.4 Experimental Design

In searching for possible modes of the various fiber configurations, it became clear that some crossovers were caused by the contact of two fibers that had attached in very close proximity on the conveyor. It was known that belt speed and the fiber feed rate into the system could be controlled to alter the spacing of the fibers on the belt. Therefore, these factors were included in a designed factorial experiment in an effort to determine the machine settings that would minimize the occurrence of crossovers without significantly increasing the time required to measure a given number of fiber lengths. Electrode plate spacing and moisture content were included as factors in the experiment as well.

In order to meet the prescribed objective a $2^{\wedge 4-1}$ fractional factorial screening experiment, with two replications, was designed for analysis. The four factors varied for this study were fiber feed rate, belt speed, plate spacing (measured from the top of the plates), and fiber conditioning. With two levels for each factor and two replications, there were a

total of 16 runs. Each of the runs was completed at standard conditions in the physical-testing laboratory at NCSU. This experiment, which is shown in Table A.1, was both designed and randomized using Minitab statistical software.

It was known from experience that a sliver feed rate of less than 0.15 Hz at any practical conveyor speed would cause an unacceptable increase in processing time. Hence, 0.20 Hz was set as the low level of the factor feed rate. The high level for feed rate was chosen to be 0.40 Hz because higher frequencies were known to cause excessive fiber densities between the electrodes at any belt speed. The low (0.19 m/s) and high (0.22 m/s) values of belt speed were selected to represent the range over which the belt had been previously varied during trials. The low level of plate spacing was set at 2.6 inches and the high level was set at 3.2 inches, where the distances were measured from the top of the plates. The low level (2.6 inches) represents the minimum distance necessary for the straightening of long fibers, while 3.2 inches is the maximum separation allowed by adjusting system components. For moisture content levels, unconditioned (low) and conditioned (high) fiber samples were used.

After completing the experimental runs and saving the images from each trial, the images were subsequently analyzed and the proportion of properly individualized pixel blocks was calculated for each run. A total of 400 fibers were observed for each trial and the number of properly individualized and crossed-over pixel blocks were noted for calculation of the response. .

4.4 Conveyor Overlap

While completing the trial runs and examining the fiber length data and images, it also became clear that, in addition to fiber individualization issues, many fibers were not

being presented to the camera in their entirety. In some cases, less than half of a fiber's length was being analyzed and measured. This is similar to the HVI measurement system, where unknown portions of fibers are hidden inside of the clamp. Obviously, this manner of presentation of fibers to the camera had a profound effect on the fiber length results that were obtained.

The reason for this lack of full fiber presentation to the camera was identified as overlapping of fibers onto the conveyor. Since backlighting was being used to cast an image of the fiber to the camera, and because the conveyor was opaque, there was no contrast present between the belt and overlapping portions of fibers. Therefore, the fiber measurement software was unable to distinguish between the two, and only the fiber segment protruding beyond the belt edge could be measured. Because the square urethane belting had a width of 5/8", there was 15.9 mm of width available on top for straight fibers and more than 31.8 mm for "U"-shaped fibers to overlap. This led to severe inaccuracies in the length data, such as reduced mean lengths and inflated short fiber contents.

In an effort to reduce the severity of fiber overlapping, a thinner conveyor was sought to minimize the area available for fibers to attach. By reducing the area on top of the belt, it was hypothesized that the amount fiber overlap onto the conveyor could be decreased and that the measurements would increase in accuracy. Many potential conveyors of different shapes, sizes, and materials were obtained and are summarized in Table 4.1. Each of these conveyors was subjected to numerous runs, and notes on their effects were made after observing fiber images and behavior.

Table 4.1: Conveyor Materials and Shapes

Material	X-Section	Dimensions
Urethane	Round	Diameter: 0.063”
Viton®	Round	Diameter: 0.125”
Nylon Mono.	Round	Diameter: 0.008”
Wire (Kynar Insul.)	Round	Diameter: 0.018”
Ribbon (Met./PET)	Rectangle	W: 0.125” H: 0.031”

4.5 Sample Selection

In addition to accurately and precisely measuring the fibers that are presented to the camera, it is also very important in cotton fiber testing to determine whether any bias is inherent in the system for the selection of fiber samples. Naturally, 100% of the fibers exiting the comber roll opening of our device did not proceed to the camera for measurement. Therefore, it was important to determine whether long and short fibers were being lost selectively. Any disproportionate loss of any fiber length can cause bias in the length results.

The testing for selection bias consisted of collecting fiber samples from the feed chute and from the conveyor (post-measurement) by way of air suction. After collection of the fiber samples, they were subsequently measured with the HVI by a trained technician. The results of the HVI data were then analyzed to conclude whether a biased selection of fibers had occurred.

Prior to conducting this experiment, some mechanical modifications had been made to reduce the number of fibers lost to the surroundings. Initially, to increase the velocity of the fibers exiting the chute, a narrower tube of 0.38-inch internal diameter acrylic was used to replace the existing 1.00-inch I.D. tube. This replacement served to increase the air velocity inside of the chute and, thus, the exiting fiber velocity. The increased fiber velocity aided the fibers in being blown to a precise point on the electrode plates.

By using the 0.38-inch internal diameter tube for fiber delivery, it was not possible to cover the entire opening of the comber roll exit. Therefore, a device for funneling the fibers into the smaller tube was constructed. The funnel was made of polycarbonate and was initially tapered at an angle of approximately 75 degrees from horizontal. However, upon testing, it was determined that a 75-degree angle did not prevent fibers from clogging the funnel opening. The funnel was then modified to have a larger opening with less of an angle to the horizontal. Also, the irregular shape of the comber roll exit prevented the funnel from sealing the opening; therefore, a gasket was made to fit atop the funnel and seal off the exit to prevent fiber loss. After these modifications, testing showed that the wider opening allowed the fibers to pass more easily through the funnel and into the 0.38-inch internal diameter delivery tube; however, slight clogging was noticed at long running times and high fiber feed rates. Therefore, a tube suction device was needed to prevent the clogging during the startup and purging processes. During these processes, the feed roll speed is increased by 100 times to ensure that the sliver is inserted fully into the system on startup, and to clear any remaining sliver while purging. The device was also needed to remove any fiber clogging that may occur during normal running conditions. The design of the suction device was to be such that it would not interfere with the flow of fibers through the tube. The tube suction was designed and constructed to fit onto the end of the delivery chute, as seen in figure 4.7.

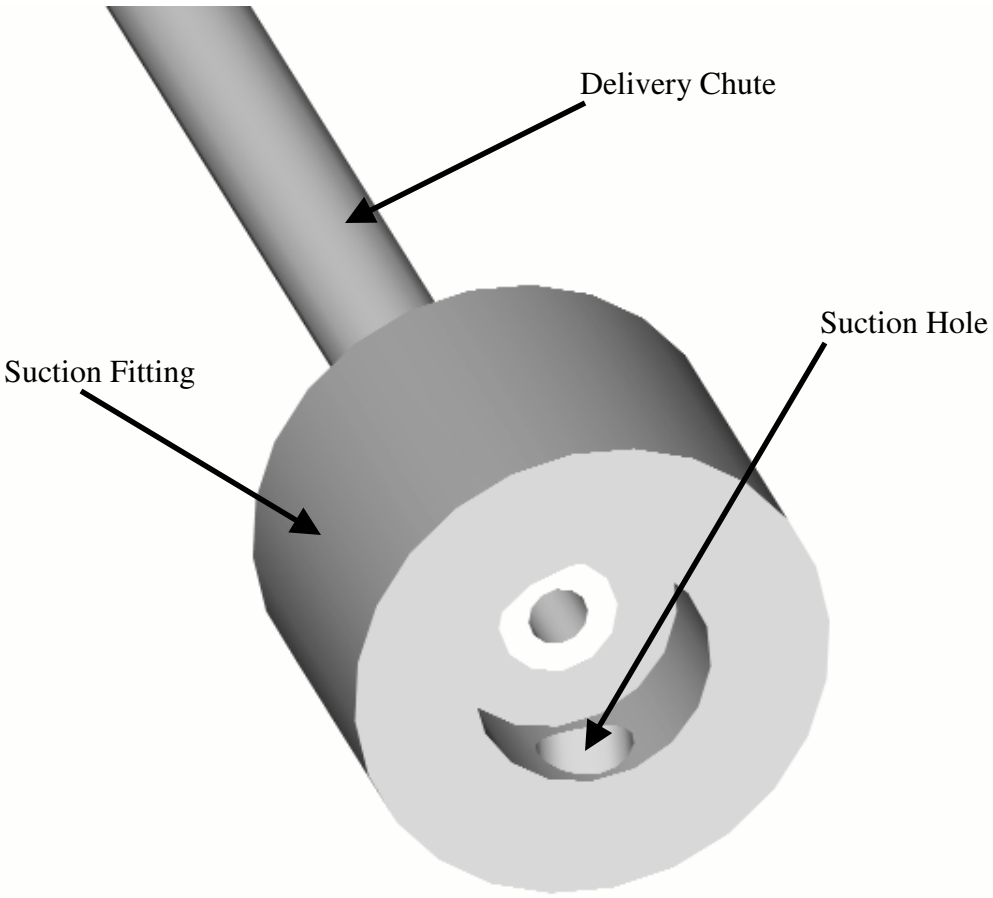

Figure 4.7: Suction Device for Delivery Chute

A suction device was inserted into the suction hole, and the fibers were removed successfully during the startup and purging processes. Fiber clogs inside of the delivery chute were also dislodged effectively by the apparatus. Note that the suction hole was offset from the chute opening to prevent it from interfering with the fibers as they exited.

To further increase the fiber velocity and improve the precision of fiber delivery to the electrodes, the diameter of the friction drive wheel was increased to provide a greater ratio between the drive wheel and comber roll shaft. The original drive wheel for the comber roll had a diameter of 2 inches. This diameter, combined with the 1-inch diameter shaft of the comber roll provided a 2:1 comber roll to drive wheel ratio. By combining this ratio and

the maximum speed of the drive motor, the comber roll reached theoretical speeds of 3600 rpm. A 3.5:1 comber roll to drive wheel ratio was achieved by replacing the 2-inch diameter drive wheel with a 3.5-inch diameter drive wheel. This change increased the comber roll speed to a theoretical value of 6300 rpm, which served to provide greater air and fiber velocities for precise fiber delivery. Additionally, it was hypothesized that these changes would improve the fiber individualization of the system.

4.6 Data Analysis

Sample data were collected with our machine prior to any changes for the purpose of HVI and AFIS comparisons, as well as post-modifications comparisons within our own system. Once the device was deemed to provide acceptably accurate data when compared to the results of other measurement systems, a designed experiment was conducted to determine the effects of various sample sizes on the repeatability of our measurements. Through such an experiment, our objectives were to determine the minimum sample size needed for excellent repeatability, and to block the effect of changing conditions from day to day in the laboratory environment. In addition, a second cotton sliver sample was included in the experiment to test the effectiveness of our system in distinguishing the lengths of two different fiber populations.

The experiment was designed using Minitab statistical software and included the three factors listed above. For the factor sample size, 4 levels were chosen for use. These levels were 125, 250, 500, and 1000 fibers. The old sliver and a new sliver were used as the two levels of cotton fiber samples. A full factorial experiment was designed with 8 replicates of each combination, and the replicates were randomized within four blocks, which represented the four days in which the runs were to be completed. This design resulted in a total of 64

runs that would be completed in blocks of 16 runs across four different days. The mean length, upper quartile length, short fiber content, and 2.5% span length were recorded as responses for each run. Prior to each experimental trial, the system was purged of any residual fibers to prevent fiber contamination. In addition, exact startup and shutdown procedures were utilized for each run.

To further test the accuracy of our measurements, it became necessary to introduce fibers of a known length into the system. Because the true length parameters of our cotton samples were not known, it was difficult to determine just how accurate the results were. However, the introduction of known fiber lengths improved our ability to access the measurement accuracy.

At the time of our study, there was no means by which to obtain cotton fibers of known lengths. Therefore, alternate synthetic fiber possibilities were explored. Initially, a small sample of nylon fibers was obtained to test its behavior in the system. Due to the low moisture regain of nylon, charging of the fibers was insufficient for their capture and straightening in the electrostatic field. Hence, nylon was ruled out as a potential fiber for use in the accuracy determination of our system.

After further research in fiber moisture regain and electrical conductivity, the graph that was previously discussed in Figure 2.12 of the literature review was discovered. As was shown in the figure, the electrical conductivity of cotton and rayon are very similar at varying levels of relative humidity. It was also known that rayon has very high moisture regain, which is beneficial for its use in our system. Therefore, a sample of rayon fiber was obtained for observation of its behavior in our device. It was concluded that the behavior of the rayon fibers in the electrostatic field was almost identical to that of cotton. Subsequently, rayon

samples of 0.25, 0.50, and 1.50 inches were acquired for use. The 0.25 and 0.50-inch fibers had linear density of 1.5 denier, while the 1.50-inch fibers were determined to be approximately 3.0 denier.

Once the samples were received, we opened the fibers by hand and allowed them to condition overnight. The following day, fibers were weighed very precisely and a mixture of 80% long fibers by weight and 10% each of the short fibers by weight was made. This mixture was straightened manually and carefully formed into a sliver for insertion in the system. Under the assumption that the fibers were mixed very thoroughly, we could test for any remaining bias that may be present in fiber selection, in addition to measurement accuracy. Besides the mixture of short and long fibers, the half-inch and quarter-inch fibers were introduced separately into the device for further accuracy assessment.

4.7 Statistical Methods

Descriptive statistics were used to investigate the various parameters for conveyor overlap and fiber presentation. Design and Analysis of Experiment (DOE) techniques were utilized in an effort to minimize fiber crossovers and determine the effects of various machine and environmental parameters. ANOVA techniques were also employed to investigate statistical differences between fiber samples, as well as to determine significant improvements in fiber individualization.

5. Results and Discussion

5.1 Initial Data Review

The completion of the system setup and software programming allowed for the acquisition of the first images and fiber length data. The graphs and statistics shown in Figure 5.1 are representative of the many data samples that were obtained prior to any system modifications. At the time of this data collection, only the thresholding and outlining algorithms were in use, with no method of crossover separation. We do not expect to measure any fibers longer than 1.50 inches; therefore, measurements exceeding this length (due to crossovers and entanglements) are removed from the fiber length arrays. In addition, fibers less than 2.0 mm are neglected.

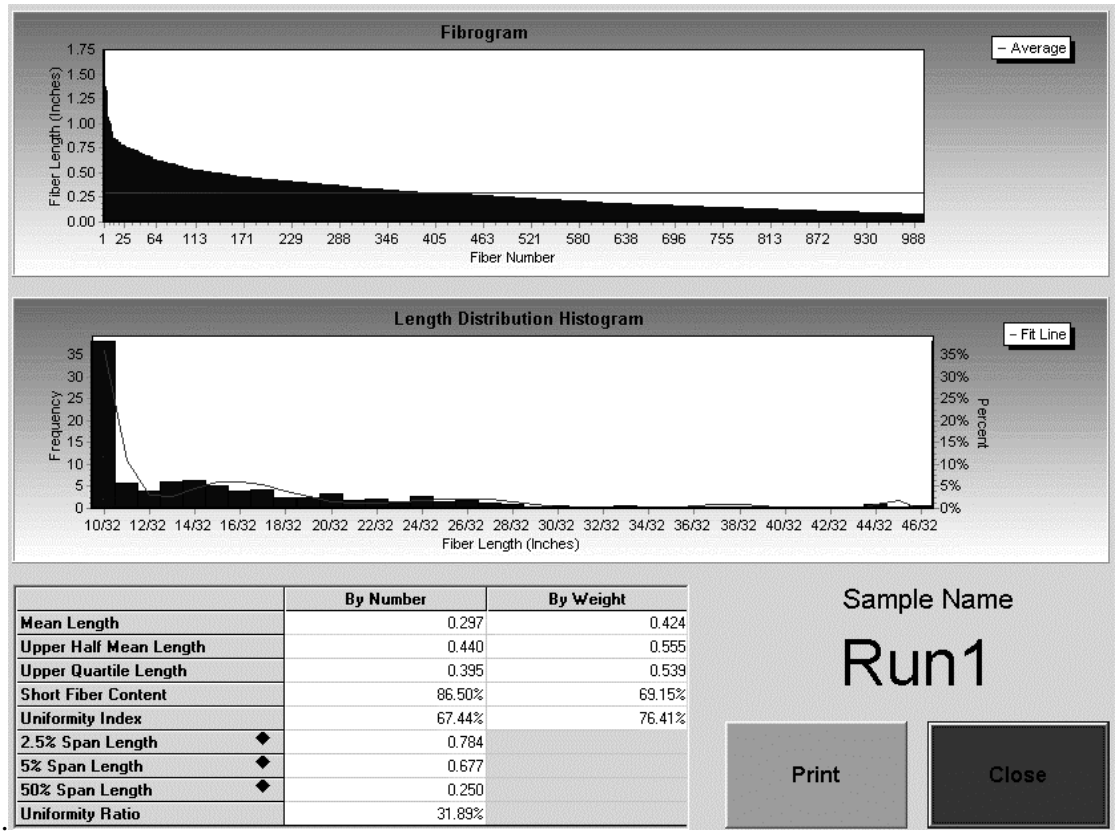

Figure 5.1: Initial Sample Data

At first glance, it is obvious that the information in Figure 5.1 is not representative of the length distribution of the fibers in the sample. With a reported 0.42-inch mean length by weight and 69.2% SFC by weight, our initial data showed no similarities to the 0.89-inch mean length and 14.7% SFC that were obtained on AFIS using the same sliver sample. Additionally, the upper quartile lengths and span lengths of our measurements are significantly lower than the AFIS results. Image quality, biased sample selection, and flawed fiber presentation were identified and investigated as the primary sources of error in our length measurement statistics.

5.2 Image Quality

Due to the foundation and basis of our system, superior image quality was identified as the first and most important source of error to confront. Prior to installation of the pulsing power supply and the inclusion of the camera calibration routine, the processed image in Figure 5.2 was obtained. The image was taken while the pulsing power supply was in place with a 1/1000-sec. shutter speed and a threshold value of 8. The implementation of a uniform backlighting source by Stroupe permitted the use of a more effective global thresholding technique, as opposed to the local thresholding method used by Ikiz. This allowed for a threshold comparison of each pixel to the overall average of the image, which makes the program faster and simpler.

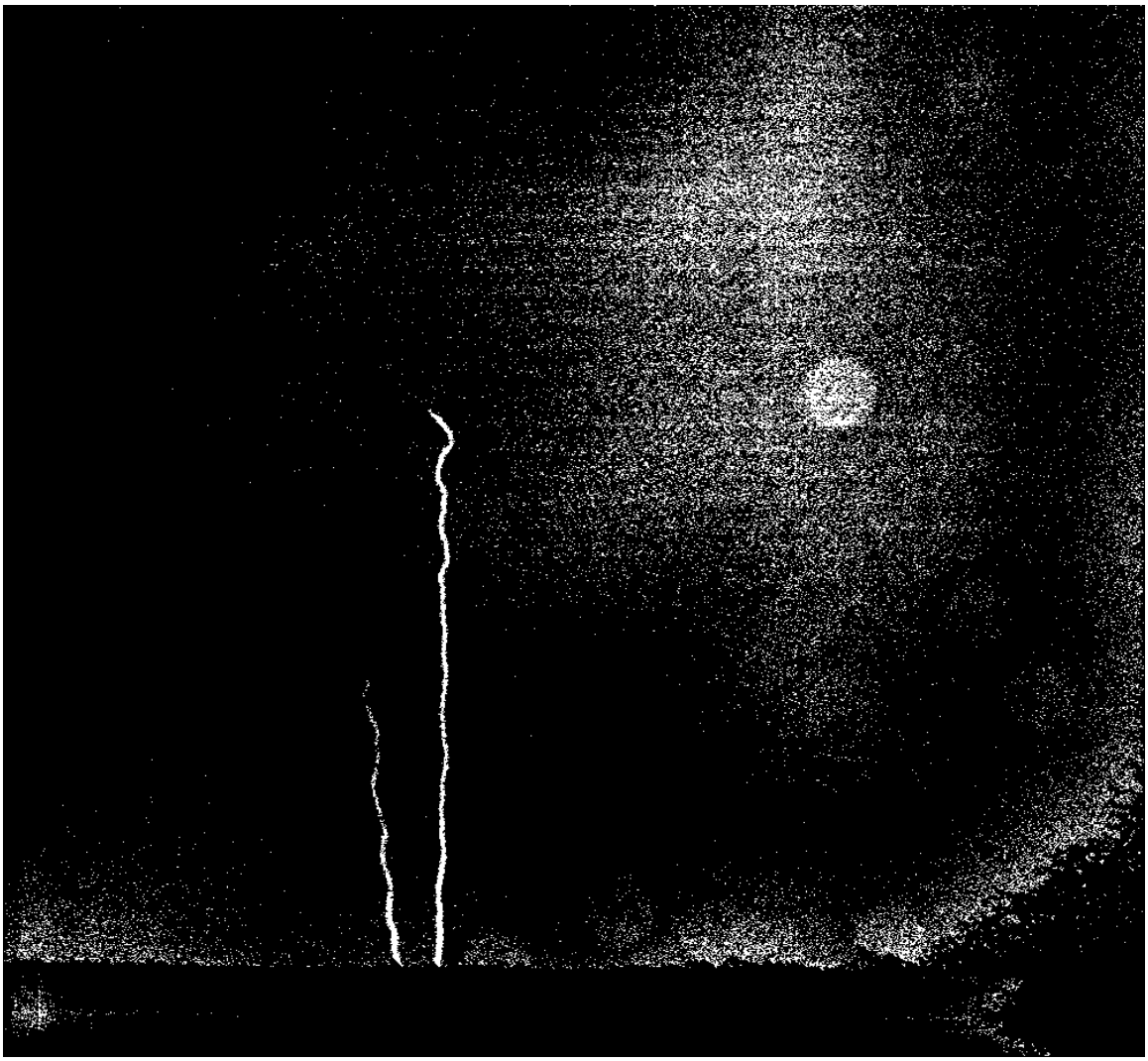

Figure 5.2: Processed Fiber Image with Continuous Lighting at 1/1000 sec. Shutter

At a 1/1000-sec. shutter speed with the continuous LED lighting, the noise-level in the image is extremely high. The noise is a result of insufficient uniformity in the background gray-levels. The variation in the background pixels is greater in many areas than the assigned threshold value. Increasing the threshold would have reduced the amount of such noise; however, even at the threshold value of 8 the fibers still contain broken skeletons. Increasing this value would only serve to further increase the number of fiber breaks by making the detection of fibers more difficult. It should be noted that the more uniform

urethane belt had been implemented when Figure 5.2 was taken, and that the fiber protrusions that were previously an issue are no longer present.

After implementing the pulsing power supply, the pre-processed images from PDV show frame grabber were observed and an example image is shown in Figure 5.3. The image was taken with the proper shutter speed and LED timing setup.

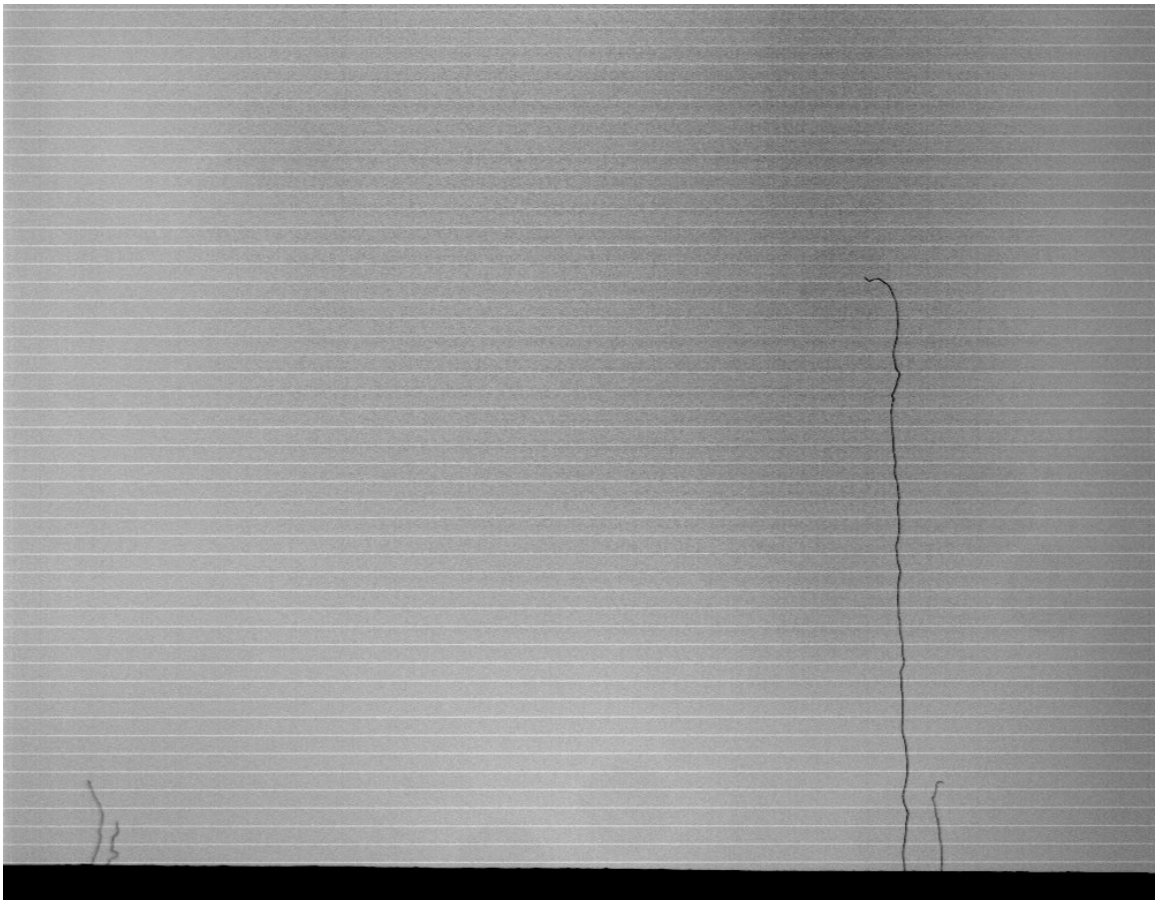

Figure 5.3: Original Image with the Pulsing LED

By visually inspecting the images, it appeared that there was better contrast between the background and fibers. This was confirmed after examining the pixel values and the contrast levels of the image. However, the "banding effect" (scan lines with higher pixel

values) caused the fibers to lose contrast with the background in the areas where the lines passed. These bands produced broken skeletons after thresholding and, as a result, led to inaccurate length measurements.

Later, it was observed that by presenting an opaque object across the top rows of the image, the banding was eliminated. Therefore, the camera was rotated 180 degrees to allow the belt to be at the top of the image, which provided the few dark rows that were needed to eliminate the bands. After this rearrangement, six pre-processed images were obtained for analysis, an example of which is shown in Figure 5.4.

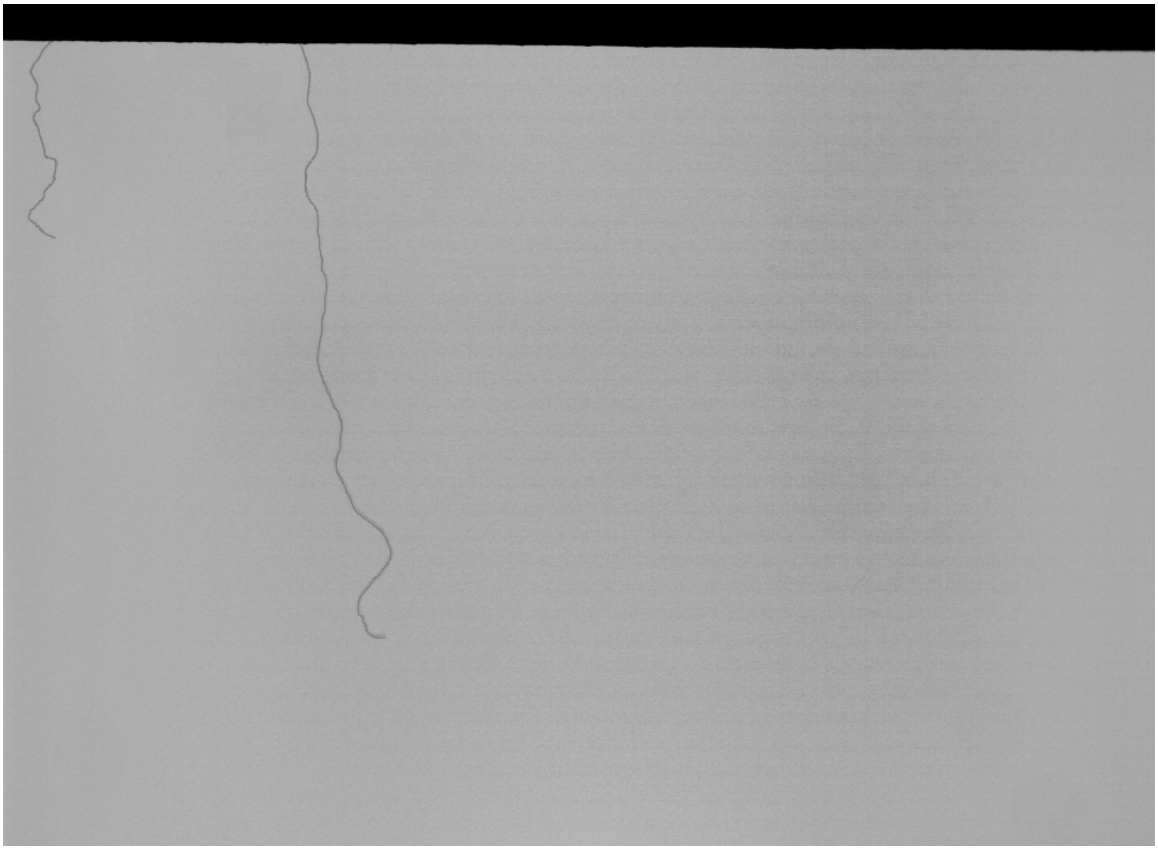

Figure 5.4: Original Image with Pulsing LED after Re-Arrangement

By placing the belt in the top of the image as seen in Figure 5.4, the "banding" in the background has been smoothed and the fiber has excellent contrast over its entire length. The diameter and contrast levels were determined for each of the 6 preprocessed images using the same procedures that Stroupe employed. The shutter speed was again set with the timing diagram for pulsing power supply in place and the results are shown in Tables 5.1 and 5.2.

Table 5.1: Apparent Fiber Diameter Statistics

Position	Fiber 1	Fiber 2	Fiber 3	Fiber 4	Fiber 5	Fiber 6	Overall
200	3	3	4	3	3	2	
300	4	3	3	4	3	3	
400	2	3	3	3	3	2	
500	3	2	3	3	2	3	
Average	3.0	2.8	3.3	3.3	2.8	2.5	3.0

From looking at Table 5.1 and comparing these results to Stroupe's, it is evident that the fiber diameters have been reduced by using the pulsing power supply. At the 1/1000-sec. shutter speed, Stroupe reported an average fiber diameter of 5 pixels. At only a 65 µs faster shutter speed, the pulsing power supply provides images with pixel diameters that average only 3 pixels. This width reduction is a result of the very short (10µs) light pulse that is produced by the new LED power supply and increased contrast.

Table 5.2: Fiber Contrast Level Statistics

Position	Fiber 1	Fiber 2	Fiber 3	Fiber 4	Fiber 5	Fiber 6	Overall
200 L	38	31	35	26	38	30	
200 R	37	30	32	24	44	33	
300 L	35	47	33	25	30	32	
300 R	25	37	31	21	28	24	
400 L	42	37	36	26	53	33	
400 R	41	31	36	23	51	26	
500 L	49	41	30	20	36	33	
500 R	50	40	31	16	39	31	
Average	40	37	33	23	40	30	34

The data in Table 5.2 show improved contrast levels over the contrast data obtained by Stroupe. In fact, the contrast levels in the images are more than two times his calculated contrast average of 14, which was shown previously in Table 2.6. This dramatic improvement in the contrast between the fibers and the background significantly reduced the number of broken skeletons and resulted in more accurate individual fiber length measurements. Once the implementation of the pulsing power supply and calibration routine were in place, the processed image in Figure 5.5 was acquired, again using a threshold value of 8.

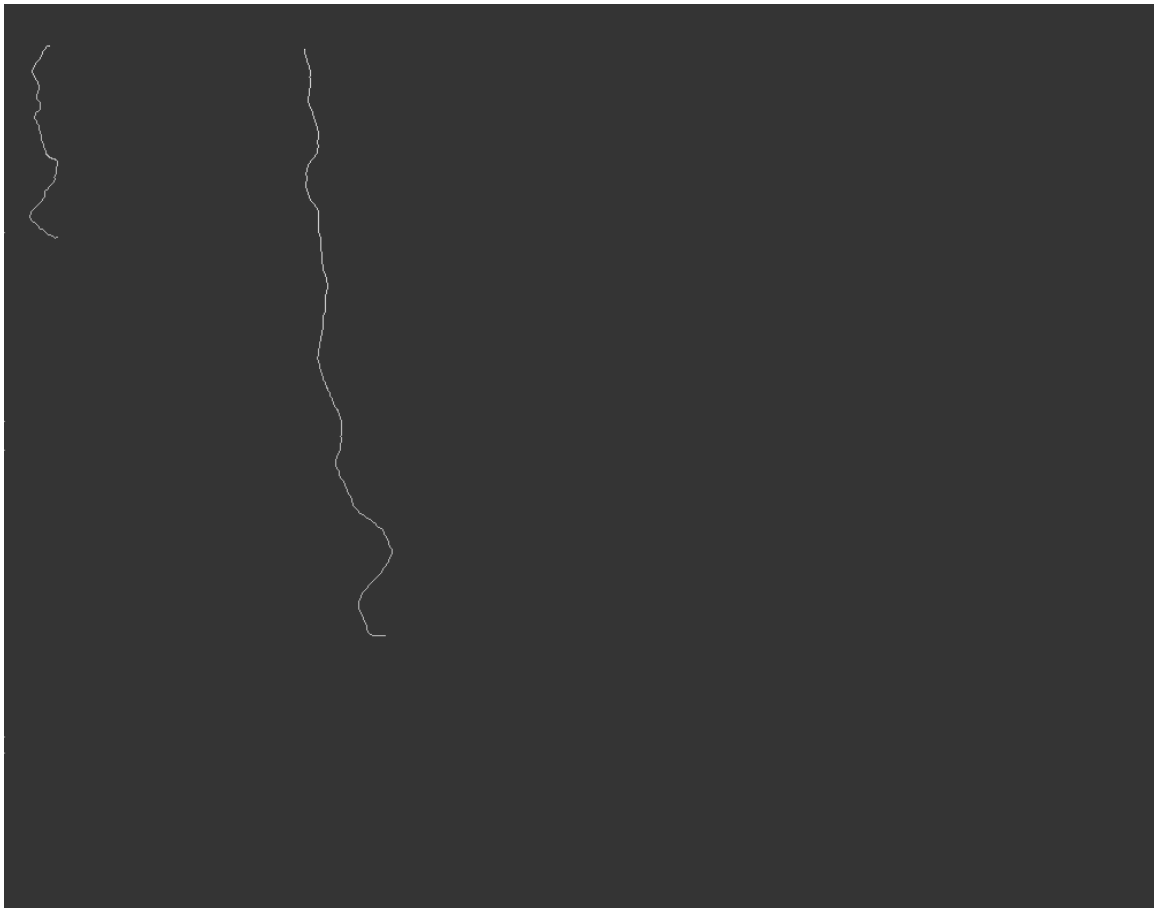

Figure 5.5: Processed Image after All Modifications

By comparing the image in Figure 5.5 to the original image in Figure 5.2, it can be seen that the inclusion of the background calibration routine has resulted in an elimination of all background noise. In addition, the protruding portions of the fibers have been detected without the presence of broken skeletons, which is allowed by the use of a pulsing power supply. It should be noted that some broken skeletons still exist in images where the fibers move drastically in or out of the camera's plane of view. Although the image in Figure 5.5 is merely one example of the improvement in image quality, this scene was repeated for a vast majority of the images that were obtained following the lighting and imaging changes.

5.3 Sample Selection

This improvement in image quality turned the focus of the research to the sample selection process. The data in Table 5.3 show the HVI and AFIS results for the upper half mean (UHM) and the short fiber content (SFC) for three samples of 10,000 fibers, taken from both the delivery chute and the belt. It appears from the data that the UHM decreases and the SFC increases for these subsequent steps of the fiber individualization and delivery process. In order to determine if the difference in the UHM and SFC of each section was statistically significant, an Analysis of Variance (ANOVA) was performed. The results of the ANOVA, which are shown in Appendix B with their supporting graphics, indicate that the UHM decrease and the SFC increase is significant at these successive machine sections.

Table 5.3: HVI Data from Chute Samples

Sample	UHM	SFC
1	0.87	24.3
2	0.85	24.9
3	0.87	22.6
Average	0.86	23.9

Table 5.4: HVI Data from Belt Samples

Sample	UHM	SFC
1	0.83	31.5
2	0.81	35.1
3	0.82	31.3
Average	0.82	32.6

The force of the air exiting the delivery tube likely caused the decrease in the UHM from the delivery tube to the belt suction. This force exerted by the air stream had the consequence of blowing longer fibers, which have a larger surface area, through the electrode plates and into the surroundings. Therefore, the fibers being delivered to the camera for

measurement have a lower UHM and a higher SFC than the fiber sample taken from the delivery tube.

In an effort to retain longer fibers, the rotational velocity of the comber roll was reduced and visual observations of the effects were made. After reducing the comber roll to approximately 2000-rpm, it was seen that longer fibers were retained for measurement. The images and the length measurement data confirmed this visual observation. The slower comber roll inhibited the fiber's ability to be directed at a precise point onto the electrode plates; however, the accompanying reduction in air velocity prevented longer fibers from being blown through the electrostatic field.

This change in comber roll velocity also had its effects on the delivery chute. Because the force of the air though the chute had been reduced, fibers were more susceptible to being caught inside of the tube and clogging became much more frequent. Therefore, we removed the chute and funnel assembly and readjusted the comber roll position so that exiting fibers were aimed toward the positive electrode. Observations revealed that, without the presence of the chute, there was no means by which fibers could be guided toward the plates. Once they exited the comber roll, the fibers were scattered and drifted slowly toward the electrodes, with a majority of the fibers escaping the electrostatic field. To reduce the number of fibers lost to scattering, the comber roll assembly and exit were moved closer to the electrodes. Through trial and error, the vertical position of the comber roll was set at approximately 7 inches from the top of the electrodes. This height represents the minimum distance between the comber roll exit and the electrode plates at which the force of the air flow does not, once again, begin to blow the longer fibers through the electrostatic field. Also at this height, the electrostatic field strength between the comber assembly and the

plates is small enough to prevent fibers from bounding upwards toward the comber exit. With this new configuration in place, observations were made. It was concluded that moving the comber roll closer to the electrode plates had indeed reduced loss of fibers to the surroundings, while retaining longer specimens for measurement.

On the basis of these results, it was concluded that the mechanical changes made prior to the collection of the fiber samples for the ANOVA were not effective in providing a system with unbiased fiber selection. Although the smaller diameter delivery tube and higher comber roll speeds did improve the precision of the fiber delivery, the increased fiber and air velocities served only to add to selection bias by forcing the longer fibers through the electrostatic field. It is concluded here, therefore, that either no fiber delivery chute should be used, or that the usage of any chute to inhibit fiber scattering, should have a large enough diameter to produce small air velocities and eliminate the possibility of clogging. The threat of clogging is reduced with larger diameter tubes because of reduced friction between fibers and the chute walls. This revised method of fiber delivery is also supported by the fiber individualization results that are discussed in Section 5.5.

The previous reduction in comber roll speed and subsequent removal of the fiber delivery chute, allowed for the retention of a greater number of fibers between the electrode plates. Therefore, the 0.44 Hz specification by Stroupe [28] for the feed roll speed is no longer valid. Visual inspections of fiber individualization and spacing on the conveyor resulted in the reduction of the feed roll speed to 0.20 Hz as the optimum fiber input rate.

5.4 Static Fiber Repeatability

Although measurement accuracy is essential, perhaps the most important aspect of fiber length measurement is the ability to obtain precise estimates of the length parameters. Any inaccuracies in the data can be accounted for by adding a correction factor that is specific to each condition; however, it is not possible to make such corrections for the measurement precision. The following experiment was conducted in an effort to determine the repeatability of our system.

The test was conducted by obtaining repeated measurements on a single stationary fiber. The fiber was placed in its entirety under the camera with a resolution of 38 microns, and 100 measurements of its length were acquired. The thinning algorithm, which was reported by Ikiz as providing the most precise results, was not being used at the time of the test. The new pulsing LED power supply had been implemented, however. The results, which can be found in Table C.1, showed the standard deviation of the sample to be 0.042 mm (0.002 in). By constructing a normal quantile plot, it was determined that the sample data was not significantly different from normal. Therefore, it is expected that 95% of the measurements for a static fiber will be within ± two standard deviations of the mean value, which results in a measurement precision of ± 0.08 mm (± 0.003 in). The anticipation is that precision will be further improved with an implementation of the thinning algorithm.

The results of this experiment have shown that fibers can be measured with excellent precision if they are presented individually and in their entirety to the imaging device, which is the subject of the following section.

5.5 Fiber Presentation

The significant advances that were made in image quality and sample selection shifted the project focus to improving fiber presentation to the camera. The quality of fiber presentation was defined in terms of improved individualization, reduced conveyor overlap, and the identification of additional errors in fiber display.

5.5.1 Individualization

Before any modifications to the electrodes had been made, data was collected on the percentage of crossovers and entanglements in order to get an idea as to the extent of such occurrences. Three samples of fiber images were examined, resulting in a total of 1,302 fibers, and the proportion of crossed and entangled fibers was calculated. In evaluating each of the images, a given pixel block was labeled as "individual" or as "not individual", where the latter designation refers to a pixel block that contains either crossed or entangled fibers. The proportion of "not individual" counts was calculated for each sample, along with a confidence interval for the binomial experiment. The results of this data collection, which are shown in Table D.1, estimated the combined percentage of "not individual" fibers at 21.0%, with a 95% confidence interval on the percentage of [18.9%, 23.4%]. That is, we would expect 95% of our samples to have a combined crossover and entanglement percentage of at least 18.9%, or at most 23.4%. Clearly, this level of fiber crossing and entanglement is unacceptable.

To test whether the reduction in the comber roll speed (as discussed in section 5.3) had any effect on fiber individualization, the above data were compared with the individualization data for the slower comber and feed roll speeds. The resulting proportions and their 95% confidence intervals, displayed in Table D.2, show that the two proportions are

not significantly different. Therefore, it cannot be concluded that slowing the comber roll speed from 6300 rpm to 2000 rpm has a major effect on fiber individualization. Based on these results and the retention of longer fibers, the comber roll was set at the low speed. In addition to preventing the loss of longer fibers, the slower comber roll speed is also expected to help reduce fiber damage during the individualization process.

Additional crossover and entanglement data was collected to determine the effect of removing the fiber delivery chute and readjusting the opening assembly. Two samples of fiber images were obtained, resulting in a total of 986 fibers, and the combined percentage of crossovers and entanglements was estimated at 12.3%, with a 95% confidence interval on the percentage of [10.3%, 14.5%]. These results, shown in Table D.3, indicate that the crossover and entanglement percentage has been reduced by nearly one-half of the percentages calculated in the initial assessment. A two-proportion test comparing this data to the original crossover data estimated an 8.7% decrease in the number of crossovers and entanglements, with a 95% confidence interval on the change of [-5.8%, -11.8%]. That is, we are nearly 95% confident that the percentage of crossovers and entanglements has been reduced by as little as 5.8% or as much as 11.8%, which for a sample of size of 1000 fibers represents anywhere from 58 to 118 fewer crossovers and entanglements. The results of this test are shown in Table D.4.

It is concluded here that the removal of the fiber delivery tube had a major effect on improving fiber individualization. However, it should be noted that these samples were collected on separate days in an uncontrolled environment. Therefore, it is quite possible that there may have been a difference in the moisture level of the fibers (or in some other environmental factor) on the two days that made the largest contribution to the crossover

reduction. Although additional post-modification observations, made in different conditions, resulted in approximately the same percentages, a well-designed experiment will be necessary to separate the effects of these factors. It is suspected, however, that many of the crossovers were occurring by way of fiber interaction inside of the chute, with fibers sitting momentarily on the duct wall and colliding with one another. In addition, many of the entanglements may have been caused by turbulence, which was a result of the high air velocity that exited the chute and was directed between the plates.

After cutting the slot into the positive electrode plate, increasing the voltage to +25 kV, enlarging the electrode spacing to 2 inches, and cutting curvature into the electrodes, further individualization data were collected. The estimated percentage of crossovers and entanglements showed no significant differences after any of these mechanical changes. It is concluded, therefore, that the modifications to the electrodes did not have a significant effect on the crossover percentage; however, their effects were highly beneficial in the areas of conveyor overlap and the rate of fiber removal.

Of the estimated remaining 12.3% improperly individualized fibers, approximately 85% of those are expected to be crossovers with only 15% entanglements. Through end detection, it can be determined whether a pixel block is a crossover or an entanglement. Pixel blocks with four ends consist of two crossed fibers, and fibers with more than four ends are considered entanglements. By incorporating an algorithm to accurately separate the lengths of the crossed fibers, anywhere from 96-98% of the fiber lengths can be accurately determined, which leaves only 2-4% that cannot be. To compensate for the remaining percentage, each fiber end in an entanglement (ends > 4) is located. The total number of ends is then divided by two, to represent the number of fibers in the entanglement. If the

number of detected ends is odd, then the resulting fraction is rounded up to the nearest integer. For example, if the algorithm detects 5 fiber ends, then it is determined that there are three fibers in the entanglement. We then truncate the "x" shortest fibers from the array, where "x" is the total number of entangled fibers in the sample. One weight mean length is added back for each truncated fiber, which serves to minimize the induced error. We decided to truncate the shortest fibers from the array because short fibers have the smallest impact on the by weight parameters.

Currently, we have no algorithm for accurately separating fiber crossovers. As a temporary solution, the entire length of the crossover is divided by a factor of two, so that each fiber gets half of the length. Since the expectation is to have anywhere between 80 to 120 crossovers in a sample of 1000 fibers, we realize that this solution is inadequate. Therefore, a more robust method of crossover separation is desired.

5.5.1.1. Designed Experiment

Analysis of the designed experiment did not render significant results. Of the four factors and interactions, only feed rate was marginally significant in determining the proportion of properly individualized fibers, with a p-value of 0.055. Many transformation attempts were made to improve the model fit; however, an R-squared value of 0.530 was the best fit obtained. It is concluded, therefore, that the factors or range of factors in the experiment may not have been adequate to describe the fiber individualization of system. It is also quite possible that the error or noise component was too large to allow for detection of the signal component.

5.5.2 Conveyor Overlap

After making significant improvements in fiber individualization, the reduction of fiber overlap onto the belt became a major point of emphasis. Upon securing the conveyor materials that were listed previously in Table 4.1 and completing visual observations of the runs, the results were summarized, and are discussed in the following paragraphs. In addition to a discussion of their effects on fiber overlap and orientation on the belt, the effect on the fiber behavior is also noted for each material.

Round Urethane

The round urethane belting, which had a diameter of 1/16", helped to reduce the amount of fiber overlap. In addition, its effect on fiber behavior was very minimal. Fibers appeared to be attracted to, and would stick fairly readily on this conveyor. During the trails, the belt was allowed to be in contact with the negatively charged plate surface to prevent fibers from wrapping around it. Therefore, only about half of the 1/16" diameter (1/32") of the belt was available for overlapping by the fibers. Although this belt provided improvement in fiber overlap when compared to the original urethane belting, it still allowed for approximately 0.8 mm of overlap for a straight fiber, which is greater than the 0.5 mm precision that was set by Ikiz. For a U-shaped fiber, the amount of available overlap for this belt is more than doubled to 1.6 mm. It was also observed that, despite allowing the belt to be in contact of with the negatively charged plate, some of the fibers still managed to wrap around the belt perimeter. A situation such as this increased the amount of fiber overlap to more than two times the diameter of the belt, which equates to approximately 3.2 mm.

Viton®

The round Viton® belt, which is a fluoropolymer made by DuPont, had a diameter that was two times larger than the round urethane belting. Therefore, the available area for fiber overlapping was 1.6 mm for straight fibers and 3.2 mm for U-shaped fibers. Fibers also tended to wrap around the perimeter of this conveyor, which led to 6.4 mm of fiber overlap. The only advantage of this conveyor over the others was that fibers adhered more readily to its surface. Once the fibers came into contact with the Viton®, very few of them transferred charge and jumped from the belt. This has obvious advantages in area of fiber individualization. However, the extent of the overlap for this conveyor imparted too much error into the measurements to overcome.

After testing the round urethane belting and the Viton® belting, it became apparent that both belts were adequate in the attraction and holding of individual fibers for transport to the camera. However, the diameter of each belt was large enough to create significant measurement error for any overlapping fibers. It was necessary, therefore, to search for other possible conveying materials with much smaller cross-sectional dimensions. A nylon monofilament fishing line was chosen for this purpose.

Nylon Monofilament

The nylon monofilament used was that of fishing line, and it had a diameter of 0.008 inches. This small diameter allowed for approximately 0.1 mm of overlap for straight fibers, 0.2 mm for "U"-shaped fibers, and 0.4 mm for fibers that wrap entirely around the line. So, even for the maximum overlap of 0.4 mm with this belt, the precision is less than to the 0.5-mm precision that Ikiz stated. However, upon testing the monofilament line for adequate fiber transport, it was observed that the line was not very attractive to the fibers. Very few

fibers adhered to the nylon surface and, thus, a small number of fibers were transported to the camera's viewing area for measurement.

It was unclear at the time as to why the fibers were not conveyed very well by the nylon monofilament. Two possibilities for the cause of this result were suggested. It was known that the moisture regain of nylon is about 4.0 percent. Therefore, one possibility was that the moisture in the material allowed charges between the fibers and the belt to transfer more readily than in the previous materials, preventing the adherence of fibers to the surface. The other possibility, of course, was that the small diameter of the monofilament forced the fibers to jump to impossibly precise locations in order to attach.

Wire

The next step was to make trial runs using a Kynar®-insulated copper wire. This material was chosen because it had a small diameter (0.018") and a fluoropolymer insulator, which was similar to Viton® material that previously resulted in excellent fiber behavior. The outer insulating material (Kynar®) did not absorb moisture; therefore, the possible issue with moisture regain, as discussed with the nylon monofilament, was of no concern. The diameter of the wire allowed for approximately 0.23 mm of overlap for straight fibers, 0.46 mm for overlapping U-shaped fibers, and 0.92 mm for fibers that wrapped around. These numbers show that, by preventing the fibers from wrapping around the wire, a measurement precision close to 0.5 mm can be reached for each fiber, as long as no portion of the fiber stretches along the wire parallel to its length direction. When a portion of a fiber becomes stretched out parallel along the surface of the conveyor the camera cannot see it and the length is measured incorrectly.

Initial runs showed that the wire was attractive to the fibers and that the fibers tended to remain in a fixed position after coming into contact with its surface. Visual observations revealed that relatively few fibers stretched out parallel along the wire's length. At the time of the trials, however, there was no method to prevent fibers from wrapping entirely around the wire, so the desired precision could not be reached.

At this point, it became clear that the amount of fiber length lost in measurement due to overlap could be reduced significantly by shrinking the cross-sectional area of the conveyor. However, as a consequence of this reduction in cross-sectional area, fibers tended to wrap around the conveyor. To prevent fibers from doing so, a plate was constructed with a slot, as shown in Figure 5.6.

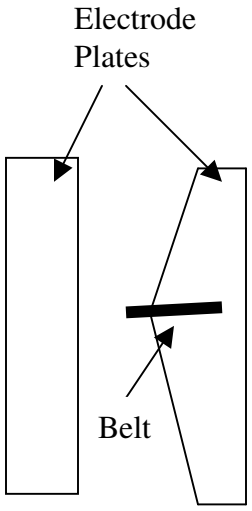

Figure 5.6: Plate Modification

The purpose of this design was to allow the flat urethane belt to traverse inside of the slot to eliminate the possibility of fibers wrapping around it. This setup also greatly reduced the area on top of the conveyor for fibers to attach. Therefore, any fiber that might attach to the conveyor and travel to the camera for analysis would have, at most, only a few pixels of

overlap. A slight protrusion of the belt was allowed so that it would be closer to the opposing plate than the electrode in which it was contained and, therefore, could be more attractive to the fibers. The plate containing the slot was tapered in order to provide an area of increased electrostatic field strength near the belt, which served to attract the fibers to this region. Once the modifications were complete, observations of fiber behavior and the resulting length statistics were made.

It appeared initially, that the new slot design performed its intended function well. Fibers were not allowed to wrap around and had very little overlap onto the protruding portion of the conveyor. The length results showed increases in the mean length statistics and a reduction in the short fiber content percentages, meaning that more of each individual fiber was being presented. However, further observations revealed that fibers were not being removed from the system as readily as before. Therefore, the density of the fibers between the plates was increased and entanglements became more prominent. The suspected reason for this reduction in fiber removal was that the belt did not protrude far enough beyond the plates. The electrodes were constructed of aluminum and charges can move easily through them. Charges cannot move easily inside of the non-conductive urethane belting. Therefore, the hypothesis was that the grounded electrode had a stronger induced charge than the belt, and because the grounded electrode and the belt were practically equidistant from the positive electrode, the fibers preferred to bound between the plates rather than attach to the belt.

Two possible methods of increasing the attraction of the fibers to the belt were devised. The first was to obtain a semi-metallic conveyor that would allow charges to flow more freely and generate stronger induced charges, while still maintaining some degree of

insulation to prevent the detachment of fibers. For this purpose, a 60% metallic by 40% polyester spool of ribbon was acquired. The ribbon had a width of 0.125 inches and could be cut to length. The depth of the electrode slot had previously been cut for the width and thickness of the flat urethane belting; hence, we were unable to use the slot for this conveying material. Instead, the pulley system was rearranged so that the conveyor could be turned 90 degrees and traversed as seen in Figure 5.7. This configuration provided very little area for fiber overlap on top of the conveyor.

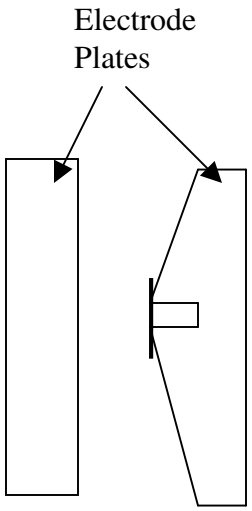

Figure 5.7: Belt Turned 90 Degrees

Trial observations led to the conclusion that fibers were indeed attracted to the semi-metallic ribbon. It is unclear whether this attraction was because of stronger induced charges in the metallic component of the ribbon, or due to an increase in available surface area of the conveyor by turning it 90 degrees. This configuration was eventually ruled out as a potential solution because of the ribbon's surface roughness, which prevented the fibers from being removed by the belt suction device. Also, this setup provided no means of preventing fibers from wrapping around and behind the conveyor.

The second method of increasing the attractiveness of the fibers to the belt was to redesign the electrode plates once again. After investigating a few possibilities, the electrodes were modified as seen in Figure 5.8.

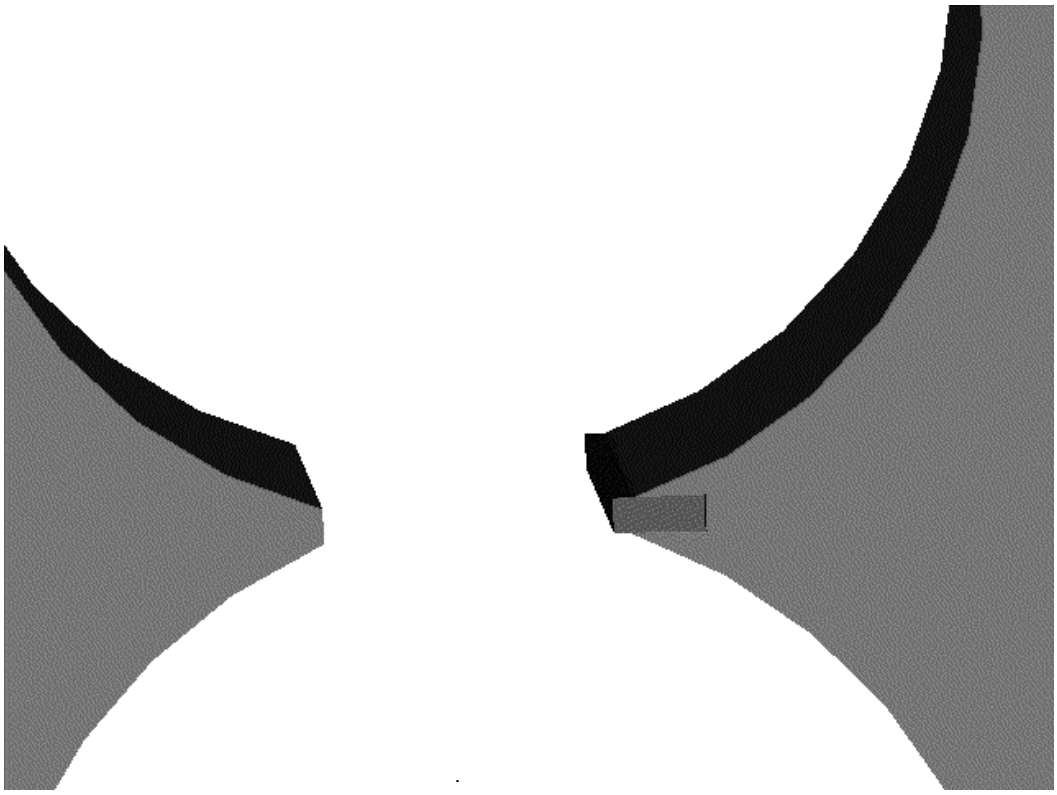

Figure 5.8: Curved Plate Surfaces

We believed that this configuration would minimize the attraction of the fibers to plate and maximize their desirability for the belt. By cutting a curved surface into the electrodes, the electrostatic field decreases sharply with an increasing vertical displacement from the edges of the belt. This assures that the electrostatic field strength is absolutely the strongest in the area surrounding the belt. It also sharply reduces the strength of the induced charge on the negative plate with a move in the vertical direction from the belt, which allows

the induced charges on the belt to have the greatest attractiveness to the fibers. The only exception to this would be at the points of the slot that are just above and below the conveyor. It is expected that the induced charge is the greatest at these corners. However, the areas of these corners are so small in comparison to the belt that any acceleration of the fibers in their direction would likely result in the fibers coming into contact with the conveyor. Again, a slight protrusion of the urethane belt of approximately 2-mm was allowed so that the belt would be closer to the positive electrode than the plate in which it was contained. Without this protrusion, fibers tended to bound between the plates rather than attach to the belt.

It was concluded that the plate design in Figure 5.8, combined with increased moisture content in the fibers did, in fact, improve the ability of cotton fibers to seek out and adhere to the conveyor. Therefore, this new configuration allowed for fiber overlap reduction without decreasing the rate of fiber removal from the system or harming fiber individualization.

To determine the extent of fiber overlap after implementing the changes, data was collected and used to estimate the number of overlapping pixels. This was accomplished by setting up two halogen lamps in a manner consistent with the frontlighting technique described by Ikiz [15]. This technique was used to reflect light from the overlapping portion of fibers in such a manner that the number of pixels on top of the conveyor could be counted. Four samples of 30 fibers were examined and the overlapping pixels were counted for each overlapping fiber. These results, which are shown in Table E.1, revealed that there were 27.2 pixels of overlap on average for the four samples, which equates to approximately 1.03 mm. The 95% confidence interval for the average overlapping pixels was found to be from [15,

40] pixels, or [0.57 to 1.52] mm, which is very small when compared to the hidden portion of fibers inside of the sampler for HVI. Another important conclusion from the data was that 62% of the viewed fibers had virtually no overlapping pixels.

5.5.3 U-Shaped Fibers

Other inaccuracies in the reported length statistics were caused by fibers that formed a U-shape at the contact point with the conveyor, an example of which is shown in Figure 5.9. In this position, the software recognizes a single fiber as two individual fibers, and the length calculations and fiber counts are made as though two separate fibers exist. This situation contributes to obvious statistical errors.

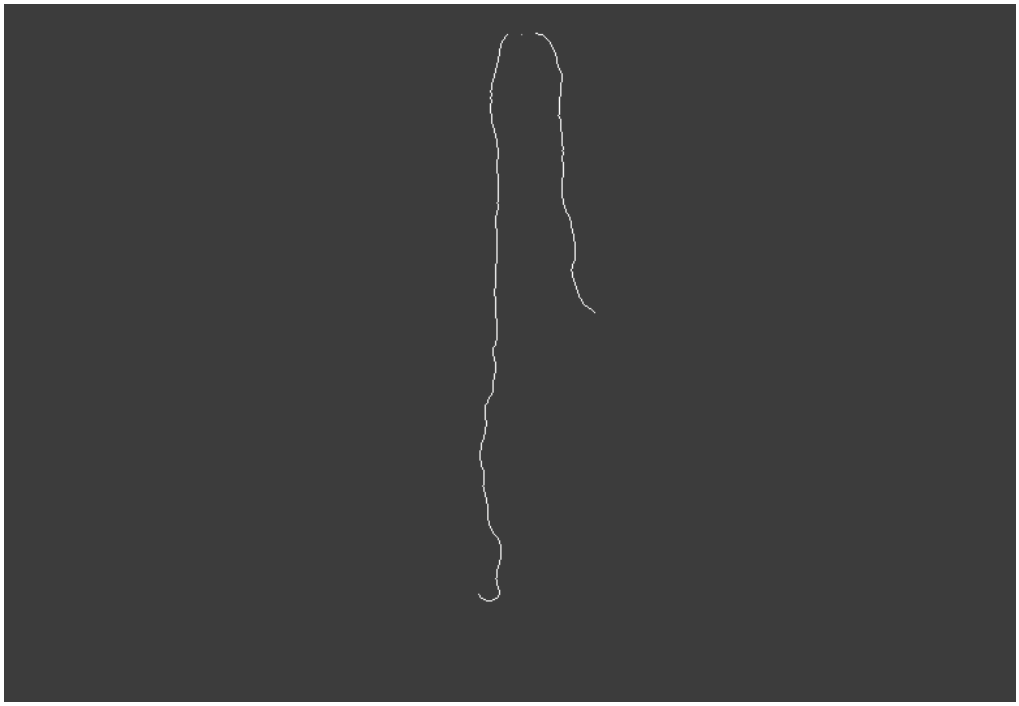

Figure 5.9: Example of a U-Shaped Fiber

To minimize the number of such occurrences, the fiber analysis code was modified to utilize the function for fiber end detection. The pixel distances between the fiber ends closest

to the conveyor are calculated and compared to some set value. This value was determined by examining fiber images and counting the distance between the broken ends of U-shaped fibers. The cumulative density function, shown in Table E.2, was calculated for these data and the control value was set at 63 pixels. This is the pixel value below which nearly 96% of the distances between the u-shapes are expected to fall. If the pixel distance between the ends is determined to be less than or equal to the control value, then the two ends are assumed to be part of a single fiber. The two length segments are then summed together, along with the distance between them, and the fiber count is reduced by one. Of course, this method introduces the possibility of connecting two fibers that are actually separate; however, the exact probability is fairly small and is dependent upon the spacing of fibers on the conveyor.

5.6 Final Data Analysis

5.6.1 Sample Data

Once the improvements to image quality, sample selection, and fiber presentation were implemented, further fiber length data was collected and analyzed for the same sliver sample that was used previously. Figure 5.10 shows the results for a measurement of 1000 cotton fibers with our apparatus after the modifications. These results were chosen to represent a typical data set, as judged informally, and are displayed for the sole purpose of drawing comparisons with previously shown data. Comparisons to HVI and AFIS results are made in a following section.

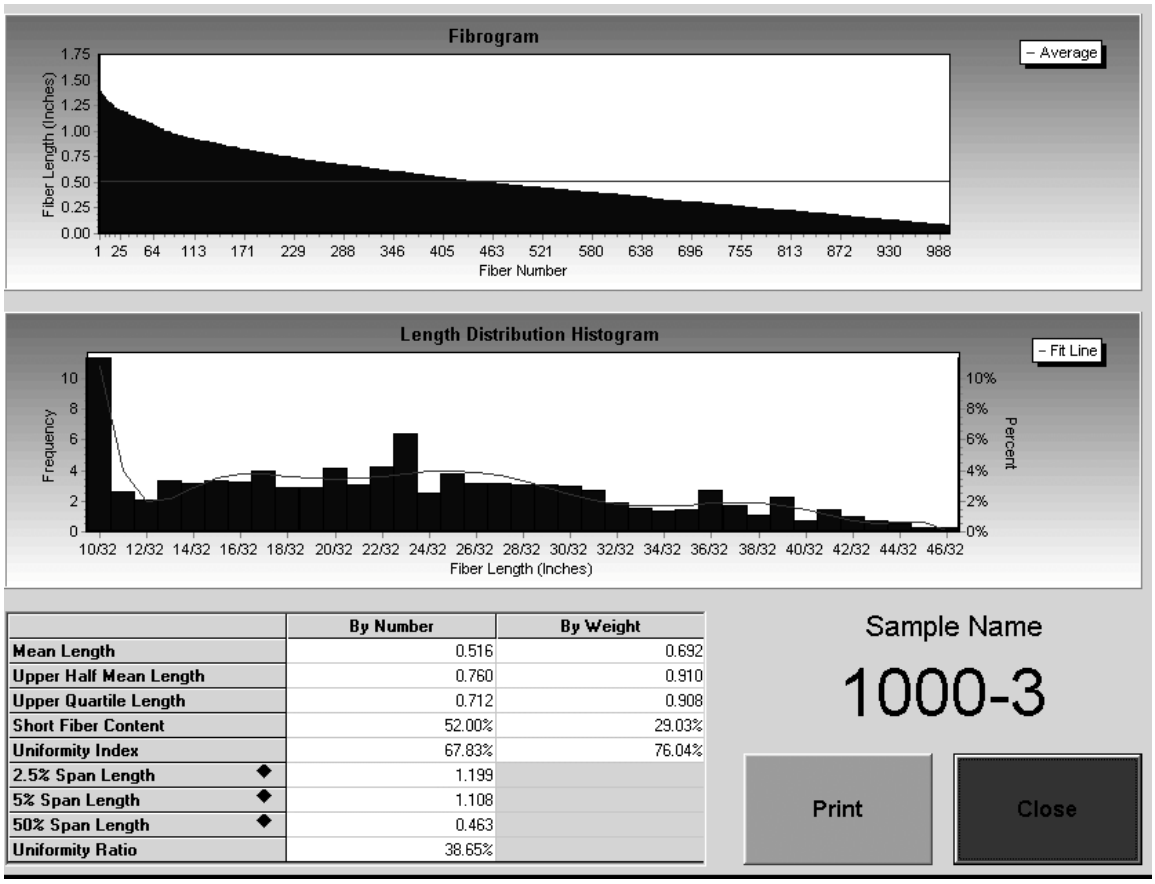

Figure 5.10: Post-Modification Data

By comparing Figure 5.10 to that of the initial data in Figure 5.1, it can be seen that there have been significant improvements in the accuracy of the length statistics and graphics. The mean length and upper quartile length have shown drastic increases in magnitude, which are much closer to the levels that would be expected for a sample of cotton fibers. Also, the short fiber content has shown a marked decrease to more reasonable values. This improvement in the data is a result of fewer broken skeletons, the retention of longer fibers in sample selection, connected U-shapes, and reduced fiber overlap.

5.6.2 Results of Designed Experiment

The results of the designed experiment revealed that the day and sample size were significant factors in determining the magnitude of all the recorded responses. Specifically,

the M(w) showed significantly higher values, and the SFC(w) had significantly lower values for both sliver samples on day three than on other days. A graphical display of these results can be seen in Figure 5.11. Measurements of the laboratory temperature and relative humidity were recorded prior to conducting trials on each day. On day three, the relative humidity was recorded as being 66.0%, which was approximately 4% higher than on the other days. Therefore, it is likely that this increased relative humidity was a major factor in the acquisition of significantly different results on the third day.

In addition to the One-Way ANOVA, a regression analysis was also performed on the M(w) data from this experiment, with sample size and relative humidity included in the model as covariates. These results, which are displayed in Appendix G, show that the factors sliver, relative humidity, and sample size were highly significant; with sliver and relative humidity having the largest effects on the model.

It is not clear at the present time exactly what effects the increased relative humidity had, although several hypotheses have been developed. First, it is possible that the higher moisture content of the fibers allowed them to be straightened more effectively, therefore, reducing the number of broken skeletons on day three. An examination of the saved images for the trials did not provide enough evidence to confirm or deny this hypothesis.

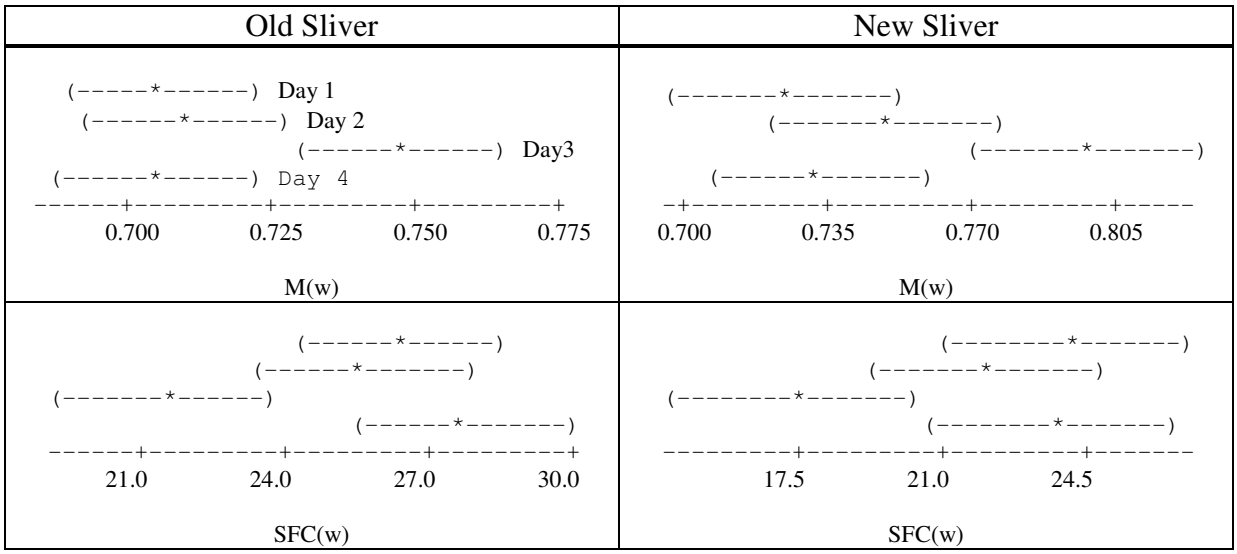

Figure 5.11: Individual 95% CIs for Day Effect Based on Pooled StDev

It is also feasible that the increased humidity contributed to a biased selection of fibers. On days with higher humidity, the fibers become more active, and the bounding motions increase in velocity and frequency. This increase in activity could allow shorter fibers to elude the electrostatic field and escape measurement. Since fiber density on the belt and time required for obtaining a given number of fibers are directly related, the increased trial times on day three indicates a lower fiber density, and makes the loss of shorter fibers the most likely scenario of the two.

Other factors not related to relative humidity could have also been responsible for the measurement differences on day three. The camera calibration and focus may have been slightly different, which would have a major effect on the results. Also, the voltage level on the plates may not have been constant from day to day, which could affect the selection of fibers. Additional experimentation will be necessary to determine the exact cause of the differences measured on day three.

Also as a result of the experiment, the sample size was found to have a significant effect on the magnitude of the response parameters. Specifically, the M(w), UQL(w), and 2.5% Span Lengths were often significantly higher for a sample size of 125 than for the other sample sizes, while the SFC(w) results were significantly lower. A graphical display of these results can be seen in Figure 5.12. It appears that incremental increases in sample size show a trend toward decreasing length and increasing short fiber content. The only exception to this trend can be seen in the results for the 2.5% span length for the old sliver. The figure shows sample sizes of 125 to have a lower estimated mean for the 2.5% span length than the larger sample sizes. An examination of the data revealed that there was one extremely low value that greatly reduced the estimated mean and caused this inconsistency. These results indicate that, as the sample size increases, there is a build-up of dust and short fiber particles on the plates and surrounding areas that negatively affect the measured fiber length parameters. To compensate for this, small fiber samples should be collected and combined into larger data sets. Between the collection of each small sample, the system should be purged of any dust and fiber particles. This method will reduce the effects of fiber build-up and serve to provide more reliable fiber length results.

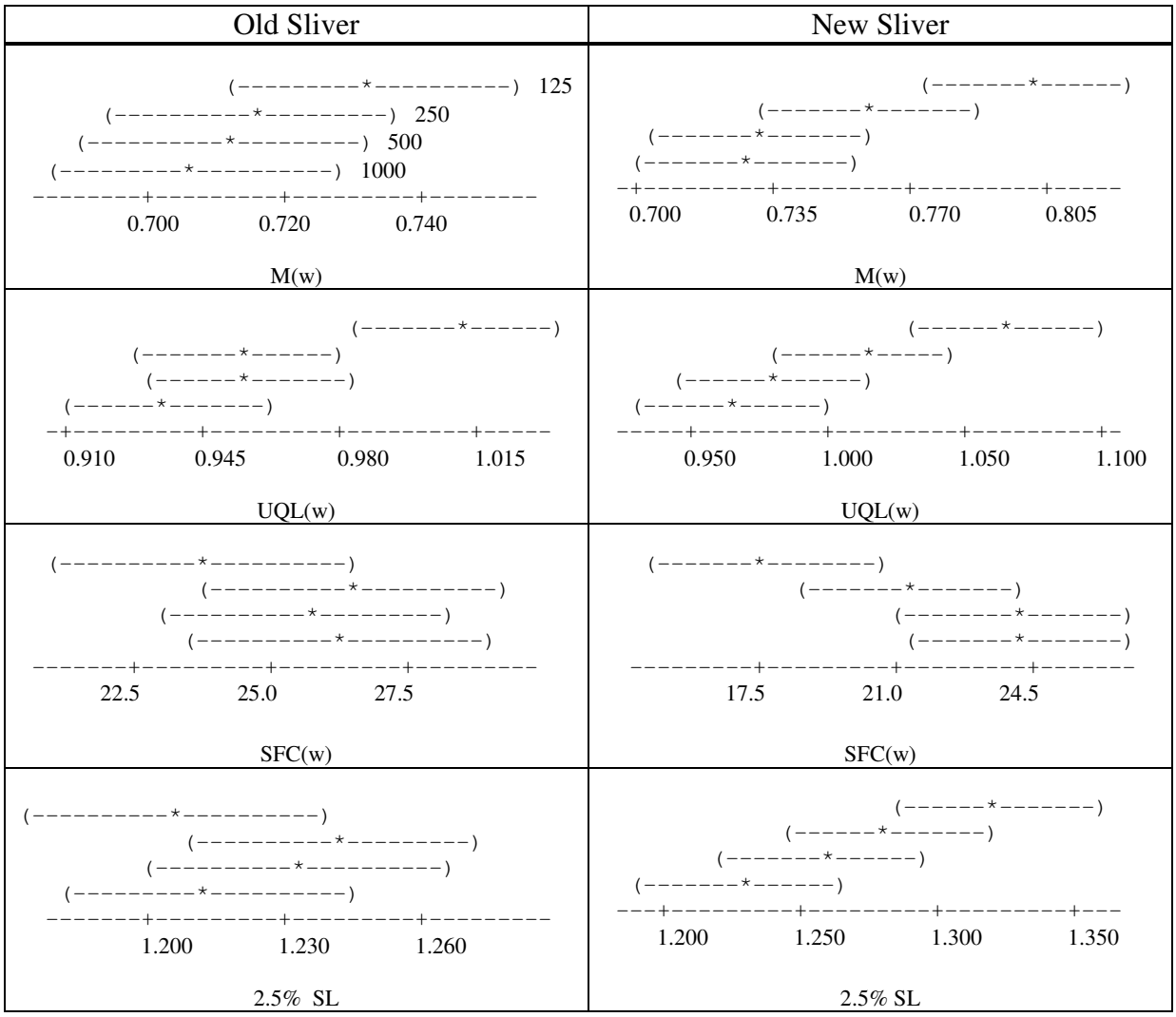

Figure 5.12: Individual 95% CIs for Sample Size Effect Based on Pooled StDev

Another objective of the experiment was to determine our system's ability to distinguish between the lengths of two different fiber populations. An ANOVA was performed to test for any difference between the two sliver samples. The results of this analysis are shown in Table 5.5. The analysis was conducted by using all 15,000 fiber measurements from each sliver. It was determined by the measurements with our system, that the two sliver samples did, in fact, have significantly different values of the parameters observed. Specifically, the new sliver sample was found to have a higher M(w), UQL(w),

and 2.5% Span Length, in addition to a lower SFC(w). A test for equal variances showed that the standard deviations for the M(w) were not equal for the two sliver samples. Therefore, a test allowing variances not being equal was conducted for this parameter to allow for the differences in the variances. This test also found a significant difference between the mean lengths of the slivers, with the new sliver sample containing the longer fibers.

Table 5.5: Test for Difference between the Old and New Sliver

Parameter	Estimate of (New – Old)	95% Lower	95% Upper
M(w)	0.034 in.	0.017 in.	0.051 in.
UQL(w)	0.036 in.	0.015 in.	0.057
SFC(w)	-3.569%	-1.816%	-5.323%
5% Span	0.033 in.	0.009 in.	0.057 in.

By observing the interaction plot in Figure 5.13, it can be seen that the difference in the recorded M(w) values for the two sliver samples becomes less significant with increasing sample size; especially for sample sizes of 500 and 1000. This indicates that the effect of dust build-up on the plates and in the air has a greater effect on the newly acquired sliver sample. It is hypothesized that the longer fiber length distribution and lower short fiber content of the new sliver, allows the build-up of lint and dust to have a greater effect on its measured statistics over time. Again, combining smaller sub-samples into a larger sample can minimize or eliminate this effect.

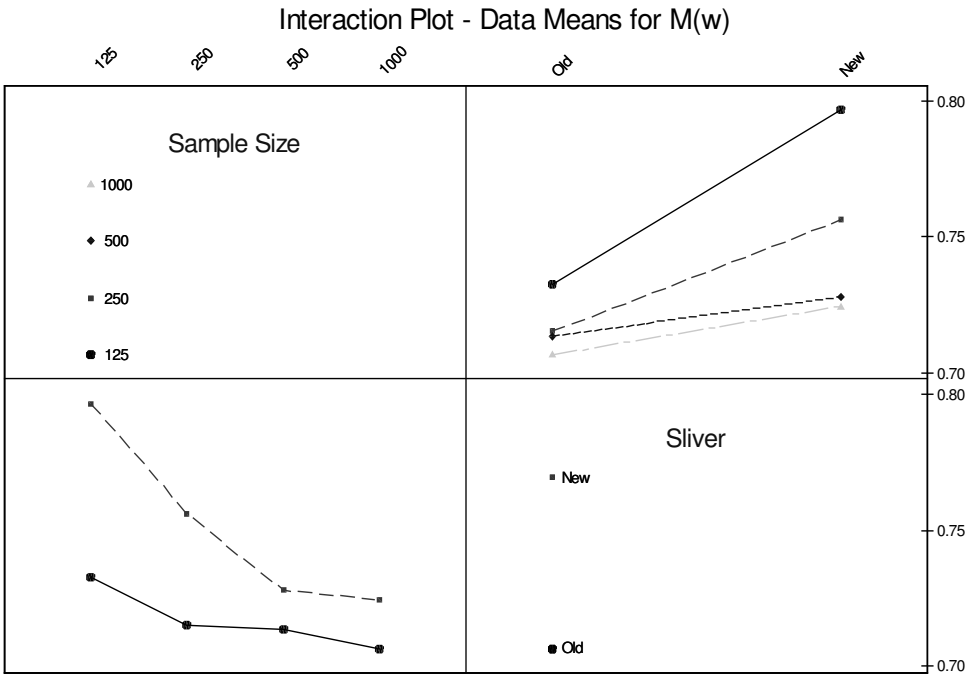

Figure 5.13: Interaction Plots for M(w)

Tests for equal variances were also conducted in order to determine which sample sizes, if any, give parameter variances that are different from one another. These results are shown in Appendix G. It was concluded that none of the sample sizes resulted in parameter variances that are significantly different. For example, the standard deviation on the M(w) for samples of 125 fibers, are not significantly different than the standard deviation on the M(w) for samples containing 1000 fibers. Statistically speaking, we would not expect this to be the case. In fact, we would expect the standard deviation to decrease by the square root of the sample size. However, the use of this theoretical concept assumes that the population from which the sample is being taken does not change. Because no significant difference in the parameter variances occurred when increasing the sample size from 125 to 1000 fibers, it is suspected that the sliver population varies along its length, resulting in sampling variation. A larger sample is more likely to experience a change in its population during a trial than a

small sample. In addition, it is most likely that the larger sample sizes introduce other error sources into the data that are not as prevalent in smaller samples, such as fiber contamination, build-up of short fibers, loss of focus, and calibration shift. Each of these can cause a change in the population with increasing sample size. By taking small samples from various sections of the sliver, these sources of variance can be reduced and more precise estimates of the length parameters may be obtained.

5.6.3 Data Comparisons with HVI and AFIS

The old and new sliver samples that were used in the previous experiment were subsequently tested using AFIS in order to make comparisons with our results. The AFIS measurements agreed with ours; showing significant results, indicating that the new sliver consisted of slightly longer lengths and less short fiber content than the old. An ANOVA that was conducted using the AFIS results estimated the parameter differences shown in Table 5.6.

Table 5.6: Test of Differences between Old and New Sliver Based on AFIS Results

Parameter	Estimate of (New – Old)	95% Lower	95% Upper
M(w)	0.017 in.	0.007 in.	0.026 in.
UQL(w)	0.017 in.	0.007 in.	0.026 in.
SFC(w)	-1.567%	-0.939%	-2.194%
5% Span	0.023 in.	0.010 in.	0.364 in.

By comparing the differences estimated by the AFIS with those of our system, it can be seen that our method results in higher estimates of the difference. It is interesting to note that our results were obtained by using 15,000 fiber measurements from each sliver, whereas the AFIS method generally requires 30,000 fibers from each sample. However, we were still

able to detect this small difference in the parameters with far less measurements. In fact, when analyzing just 1000 fibers (8 samples of 125) for each sliver, our machine was able to detect a significant difference in the two slivers for each of the parameters with the exception of the UQL(w), which had a p-value of 0.075.

The previous experiment also provided many data sets that could be used to compare the accuracy of our parameter measurements with HVI and AFIS measurements. HVI measurements were made on a sample of fibers taken from the delivery chute, while additional AFIS measurements came directly from old the sliver sample. Our measurements were all taken using the same sliver from which the HVI and AFIS samples originated. The results summary table shown in Table 5.7 will be the basis of the following discussion.

By first comparing the HVI and AFIS data, it can be seen that the AFIS reported a mean length by weight (0.89 inches), which was greater than the upper half mean length reported by HVI (0.86 inches). Because the HVI samples had been introduced to our comber roll assembly, it is evident that significant fiber breakage occurred during the individualization process. The comber roll speed has since been slowed, however, and it is likely that fiber breakage is not currently as severe.

When comparing our overall statistics to those of the HVI, many similarities are evident. Our overall SFC(w) of 24.97% and UI(w) of 75.67% are very close to the HVI SFC(w) of 23.93% and UI(w) of 76.10%. The UHM does not compare as well, however, with our system reporting a UHM(w) of 0.947 inches and HVI reporting 0.860 inches. Without broken skeletons and fiber overlap, it is obvious that our UHM(w) would have been even higher and our SFC(w) lower when compared to HVI. This result would have been expected, however, because the comber roll speed was nearly three times faster when the

chute samples were collected. Therefore, it is expected that fiber breakage is now less than it was previously, and that the UHM(w) is, in effect, longer; and the SFC(w) is, in effect, less. This conclusion makes comparisons to the AFIS data much more reasonable.

After making this comparison, it can be seen that the M(n), M(w), and UQL(w) results from our system are much lower in magnitude than the AFIS measurements. Additionally, our short fiber content measurements are much higher than those of AFIS. This result is not unexpected, however, because of the remaining broken skeletons and overlapping fibers that are present with our system. More in depth comparisons show that the smaller sample sizes and the conditions of day three produce results that are closest in magnitude to the AFIS measurements.

Table 5.7: Results Summary Tables for System Comparisons

HVI Results			
	UHM	**SFC**	**UI**
	0.860	23.93	76.10

AFIS Results							
	M(n)	**M(w)**	**UQL(w)**	**SFC(n)**	**SFC(w)**	**2.5 SL**	**5 SL**
	0.670	0.890	1.130	36.83	14.07	1.38	1.290

	Our Results												
	Sample Size	**M(n)**	**M(w)**	**UHM(n)**	**UHM(w)**	**UQL(n)**	**UQL(w)**	**SFC(n)**	**SFC(w)**	**UI(n)**	**UI(w)**	**2.5 SL**	**5 SL**
Day 1	125	0.523	0.721	0.784	0.968	0.753	1.009	39.20	21.72	66.74	74.52	1.180	1.137
	250	0.508	0.703	0.758	0.941	0.709	0.965	55.00	30.85	66.98	74.73	1.226	1.111
	500	0.52	0.713	0.713	0.946	0.722	0.970	45.30	24.86	67.05	75.37	1.239	1.128
	1000	0.496	0.688	0.743	0.916	0.689	0.920	49.80	28.07	66.79	75.15	1.220	1.112
	Day Average	**0.512**	**0.706**	**0.750**	**0.943**	**0.718**	**0.966**	**47.325**	**26.38**	**66.89**	**74.94**	**1.216**	**1.122**
Day 2	125	0.521	0.704	0.768	0.927	0.705	0.970	47.60	26.66	67.81	75.93	1.869	1.138
	250	0.550	0.736	0.815	0.962	0.772	0.948	42.80	22.47	67.55	76.57	1.304	1.144
	500	0.513	0.695	0.695	0.922	0.696	0.948	49.50	27.41	67.39	75.39	1.210	1.116
	1000	0.520	0.703	0.772	0.928	0.718	0.935	47.35	26.00	67.39	75.72	1.212	1.123
	Day Average	**0.526**	**0.710**	**0.763**	**0.935**	**0.723**	**0.950**	**46.813**	**25.64**	**67.54**	**75.90**	**1.399**	**1.130**
Day 3	125	0.590	0.776	0.865	1.012	0.864	1.028	38.00	19.10	68.18	76.63	1.299	1.192
	250	0.561	0.730	0.814	0.953	0.77	0.974	40.00	22.20	68.95	76.57	1.226	1.149
	500	0.573	0.751	0.751	0.983	0.794	0.982	40.60	22.08	68.72	76.36	1.255	1.178
	1000	0.563	0.737	0.818	0.955	0.774	0.956	43.35	22.84	68.74	77.12	1.240	1.148
	Day Average	**0.572**	**0.749**	**0.812**	**0.976**	**0.801**	**0.985**	**40.488**	**21.56**	**68.65**	**76.67**	**1.255**	**1.167**
Day 4	125	0.522	0.731	0.784	0.979	0.732	1.007	48.80	22.55	66.49	74.68	1.260	1.187
	250	0.508	0.692	0.758	0.925	0.735	0.930	52.40	29.57	67.02	74.85	1.209	1.112
	500	0.517	0.696	0.696	0.919	0.715	0.927	47.80	27.27	67.86	75.75	1.230	1.138
	1000	0.508	0.699	0.754	0.915	0.71	0.934	48.10	27.26	67.38	75.36	1.181	1.102
	Day Average	**0.514**	**0.705**	**0.748**	**0.935**	**0.723**	**0.950**	**49.28**	**26.66**	**67.19**	**75.16**	**1.220**	**1.135**
	Overall	**0.531**	**0.718**	**0.768**	**0.947**	**0.741**	**0.963**	**45.98**	**24.97**	**67.57**	**75.67**	**1.275**	**1.138**

5.6.4 Cut-Length Analysis

The 80/10/10 by weight mixture of rayon fibers was formed into a sliver and placed into our system for measurement. A graphical representation of the results is shown in Figure 5.14.

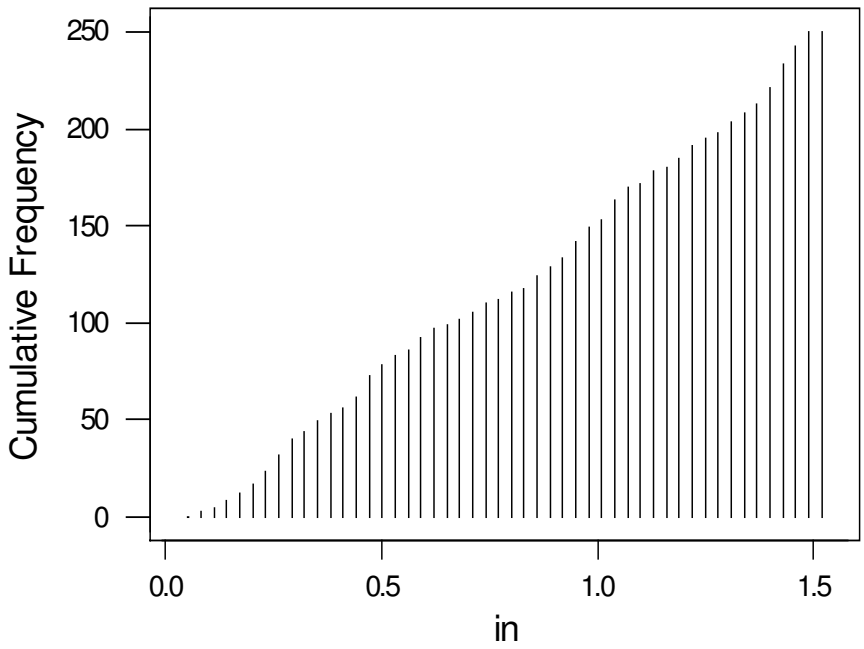

Figure 5.14: Results from Rayon Mixture

It was expected that the cumulative frequency histogram would contain three distinct increases near 0.25, 0.50, and 1.50 inches. However, by observing Figure 5.14, it can be seen that the actual results are far different from what was anticipated. Although small jumps may be noticed near each of the lengths, they are not very pronounced. The most obvious conclusion that one can make is that most of the 1.50-inch fibers were broken. These broken fibers were caused by a combination of the opening, mixing, and comber roll individualization processes. It is uncertain as to which of these processes had the greater impact on fiber breakage.

Another conclusion that may be drawn from the figure is that there is a bias toward the selection of longer fibers. Out of the sample of 250 fibers, we would have expected to obtain approximately 77 long fibers, 58 half-inch fibers, and 115 quarter-inch fibers if no bias were present. This means that at approximately the half-inch mark on the length axis, the cumulative frequency was expected to be around 173 fibers. It can be seen that the cumulative count in Figure 5.14 does not reach 173 until well past the one-inch mark. It appears that our device did not measure most of the quarter-inch fibers because they contribute a much lower percentage than anticipated. The expected frequencies were calculated under the assumption that perfect mixing was present in the sliver sample, however. We believe that this assumption is a very bad one in our case. Therefore, from the results of this experiment, it is not entirely conclusive as to whether any sampling bias remains in our system, although there is an indication toward the loss of shorter fibers.

Histograms of the cut quarter and half-inch fiber measurements, which were measured independently, are shown in Figure 5.15. After examining the images, it became clear that some long fiber contamination was present during the trials. Measurements of fibers contaminating the system were removed from the data sets, along with measurements of broken skeletons.

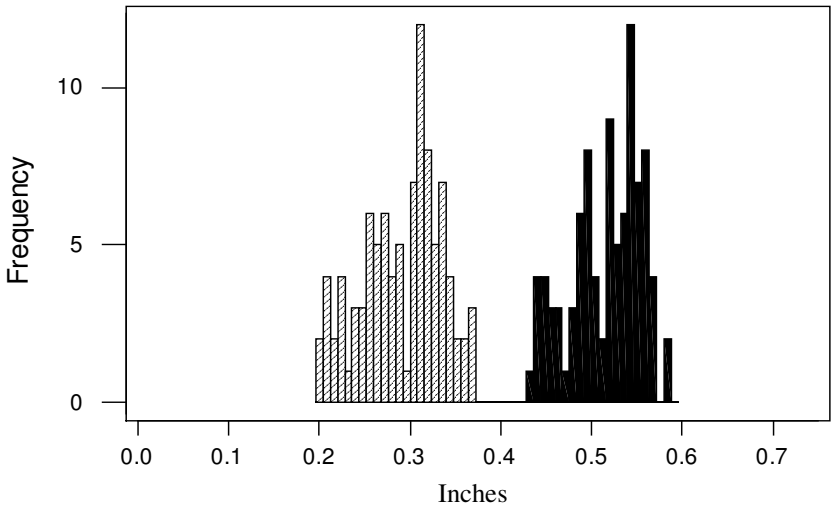

Figure 5.15: Histograms of 0.25-inch and 0.50-inch Cut Length Measurements

By examining Figure 5.15, it can be seen that there are two distinct fiber populations. However, the average lengths for both populations were measured to be higher than their specified cut-lengths. Hand measurements revealed that, in fact, the rayon fibers were cut slightly longer than the advertised length. Hand measurements showed the length of the advertised 0.25-inch fibers to actually be around 0.31 inches, while the 0.50-inch were hand measured to be approximately 0.55 inches. Therefore, it was concluded that our machine is fairly capable of accurately measuring the mean length of cut fibers if no broken skeletons or fiber contamination is present.

By further examining Figure 5.15, it can be seen that the length measurement histograms are skewed toward lower values. It is concluded that a portion of this effect was caused by fiber breakage and/or short fiber contamination. However, the majority of the lower tail is a result of varying levels of fiber overlap, which has a significant presence for an estimated 40% of the fibers. If the measurement accuracy and precision is to be improved upon, a means of further overlap reduction will be necessary.

6. Conclusions

The initial system configuration was not adequate for providing reliable and accurate cotton fiber length measurements. Errors in image quality, bias in sample selection, and flawed fiber presentation resulted in statistics with highly inaccurate length and short fiber content measurements. Multiple modifications resulted in significant improvements in each of the stated areas, which helped enhance the validity of the fiber length data.

Image quality was greatly improved with the implementation of a pulsing LED power supply. The short pulse time of this device served to lower the apparent fiber diameters in the images and double the contrast between the fibers and background. Such improvements significantly decreased the number of broken fiber skeletons. The camera calibration routine also improved image quality by smoothing the images and reducing the noise levels, which helped make the detection of fibers simpler.

A resolution value calibration method was developed by using a microscope slide with an opaque line of known length drawn on its surface. The processing algorithms accurately detected the outlined the perimeter of the calibration line. The edges of the slide were appropriately removed from the calibration function, and an accurate and precise resolution value was returned for use.

An Analysis of Variance showed that a bias existed initially in the fiber selection. The results revealed that the UHML was higher and the SFC was lower for samples in the delivery chute when compared to fibers on the conveyor. Therefore, it was concluded that our sample selection process had a bias toward shorter fiber lengths. Slowing the rotational velocity of the comber roll from 6300 rpm to 2000 rpm reduced the air drag on the fibers and improved the system's ability to retain longer lengths. A cut-length analysis revealed that the

system might now actually have a bias toward longer fibers, although these results are not entirely conclusive.

It was determined that the slower comber roll speed did not harm fiber individualization, but that clogging of the fiber delivery chute and funnel assembly did become more frequent. This frequency necessitated the removal of the funnel and chute from the comber roll opening. A subsequent proportions test showed that the removal of the delivery assembly had reduced the proportion of fiber crossovers and entanglements by 8.7% on average, which meant that the number of crossovers and entanglements had been reduced by nearly one half of their original numbers.

A repeatability study showed that a single static fiber can be measured within a range of 0.160 mm (0.006 in) 95 percent of the time if it is presented individually and in its entirety to the imaging device. The entirety of presentation was improved by cutting a slot into the electrode plates, whereby the conveyor could traverse. By allowing only a slight protrusion of the conveyor from the electrode, the amount of fiber overlap onto the conveyor was greatly reduced and found to be 1.03 mm on average, with 62% of the observed fibers having virtually no overlap at all. Milling a curved surface into the plates assured that the electrostatic field was strongest near the center, and improved the affinity of fibers for the protruding edge of the conveyor.

It was found that, in addition to overlapping the conveyor, fibers with U-shaped orientations toward the belt were often broken into two fiber segments by the processing algorithms. Collected data revealed that an estimated 95% of these fibers could be corrected by connecting the two segment ends closest to the belt if they were no more than 63 pixels apart. This correction was included successfully in the processing code.

The importance of fiber moisture levels was also revealed through these studies. At low levels of relative humidity (< 55%), the fibers do not have enough moisture for sufficient straightening or transfer of charge for rapid transport to the conveyor. At higher moisture levels (> 70%) the fibers show improvements in straightening and tremendous increases in velocity and frequency of motion. It is suspected that the optimum fiber conditioning for best performance lies somewhere in the 60-70% relative humidity range.

A designed experiment revealed that the sample size and day have a significant effect on the magnitude of the fiber length parameters. In effect, the M(w) decreases and the SFC(w) increases with increasing sample size. We believe that this change in parameters occurs with larger sample sizes because of increasing dust and short fiber particle contamination. Larger sample sizes of 1000 fibers did not produce a significantly different level of parameter variances than sample sizes of 125 fibers. This unexpected result can likely be attributed to sampling variance. It is not known exactly what caused the day to provide significantly different levels of length parameters; however, voltage level, relative humidity, and camera calibration are all possibilities.

The system also proved to be very effective at detecting differences between sliver samples that have slightly different length populations. AFIS results agreed that the new sliver sample contained longer fibers with less short fiber content; however, the estimated differences were greater with our system.

It was also determined that the system is fairly accurate in measuring the mean length of a given sample of fiber cut-lengths. The measurements were skewed toward the lower values, however. Varying levels of fiber overlap onto the conveyor predominantly caused

this skew in the data. The measurement precision could be greatly improved by further reducing or eliminating fiber overlap.

Each of the modifications that were made was crucial in advancing the system to become a commercially viable product that provides accurate and reliable fiber length results. The final data review showed that the results of our system have been greatly improved and that they are now more comparable to the results of the HVI, which is the current industry method by which every bale of cotton in the United States is measured.

7. Recommendations for Further Research

The current research resulted in significant improvements to the newly developed fiber length measurement system. However, the results have also shown that further research and improvements are needed for the system to achieve its desired performance. The following is a discussion of the areas in which further work should be concentrated.

Perhaps the most important region for additional research is in the area of the machine components and their interactions with one another, and with the environment. A determination of what, specifically, causes the magnitudes of the statistics to change significantly from day to day must be made. An experiment to investigate the causes should include fiber samples with different levels of moisture content, various voltage levels on the electrode plates, and camera focus settings. The fiber length parameters should be recorded as the responses for such an experiment.

A more precise evaluation of whether a sample selection bias exists should also be completed. The results of this work indicate that there may be a bias toward selecting longer fibers. However, our sample bias experimentation was not entirely conclusive. During such an evaluation, it would also be beneficial to record how the machine parameters and environmental conditions change or alter the selection of fibers. Therefore, a selection bias experiment may be completed in conjunction with the experiment discussed in the previous paragraph.

The results of this work indicate that a significant amount of fiber breakage occurs in the comber roll opening assembly. An experiment to determine the extent of fiber breakage, as well as the conditions under which fiber breakage is minimized would be beneficial. Also based on experimental results, it seems necessary that the amount of fiber overlap should be

further reduced or eliminated. With varying levels of fiber overlap present, it is currently difficult to get truly accurate length measurements of all individual fibers. This situation biases the mean length results downward and the short fiber contents upward. Because the mean lengths and upper quartile length are based on averages, it is possible to correct this bias by adding the mean overlap to the statistics once they have been calculated, which is the recommendation of this work. The short fiber content and span lengths are calculated on an individual fiber basis, however. The only truly accurate correction would be to add the appropriate overlapping length to each fiber. Therefore, a method of determining the amount of fiber overlap for each individual fiber is necessary if the overlap is not completely eliminated.

Broken skeletons, half of which are caused by fibers that exit the camera's focus range, also contribute greatly to the biased fiber length parameters. Although the occurrence of broken skeletons has been greatly reduced to approximately 5%, the acquisition of a new camera that is designed specifically for our purpose, and a lens with a greater depth of focus, could serve to virtually eliminate all cases of focus-based breaks. The remaining broken skeletons occur because of a flaw in the "nub-cleaning" algorithm, which removes excess pixels that occur as a result of thinning. This "nub-removal" function should be examined carefully to diagnose and correct the flaw.

Other programming concerns have also evolved through the course of this research. Currently, the time required to measure a given number of fibers is much larger than anticipated. Nearly two minutes are required to complete a sample of 125 fiber measurements. A function timing analysis has shown that the thinning algorithm is responsible for approximately 90 percent of this time. Therefore, a more efficient thinning

algorithm may be required for the measurement process time to be significantly reduced. However, with the increasing CPU processor speeds, time may soon fall as a major issue. Processors that are two times faster than the 1.9 GHz processor that we are using, now exist. Before any major effort is put into developing a new thinning algorithm, it is recommended that a faster CPU be installed and the effects on processing time observed.

Another programming feature that should be carefully considered is the crossover algorithm. A means to accurately separate the lengths of fiber crossovers is needed. Because crossovers are still relatively frequent in their occurrence, the current method of dividing the entire length of the crossover by two is insufficient to provide entirely accurate length parameters.

Occasionally, programming errors occur that cause the fiber measurement software to crash. There are two circumstances under which these failures occur. The first method of software failure happens when a fiber nep is presented to the camera for measurement. An investigation into the reason for nep program crashes should be made and corrected. Another method of software failure occurs when the camera produces flawed images. These flaws occur when the images are spit into two halves, and the fiber measurement algorithm does not know how to handle such occurrences. The cause of such image flaws should also be investigated and corrected.

A final programming change is recommended for the data collection, storage, and calculation procedures. In its current state, the program acquires the allotted number of fiber measurements, stores them into a data file, calculates the length statistics, and purges the system. This research has shown that the program cycle should be altered slightly. It is recommended that the program be altered to obtain fiber lengths in small groups of 100-125

fibers. After each group is collected, the program should prompt a system purge and promptly call for the collection of another group of fiber lengths. This cycle should continue until the given number of fibers has been collected. All of these fiber lengths should be stored into a single array from which all length parameters can be calculated.

On the mechanical side of the system, a couple of recommendations are also in order. At this time, the best purging method has been to run the system for 15 seconds with all suction activated, and then a vacuum is used to remove the remaining loose fiber from the system. If the above programming cycle change is to be enacted, a new system for purging loose fiber from the system may be required.

In regard to fiber behavior, it is recommended that the plates be reconstructed so that the mounting screws do not offer any interference. Presently, the screws attach the electrodes to the mounting assembly on the inner faces. This design allows the screws to inhibit fiber motion and often results in fiber entanglements.

It is also important to develop a means of preparing and inserting fiber into the system that is not in sliver form. Such preparation and insertion devices are not currently available for the system, but they will be vital for the length measurement of cotton bale samples.

8. References

1. ASTM Definitions, A Compilation of ASTM Standard Definitions, 8th Edition, ASTM, Philadelphia, PA, 1994.

2. ASTM Standard D 1440-90, Standard Test Method for Length and Length Distribution of Cotton Fibers (Array Method), Annual Book of ASTM Standards, Vol. 07.01, 1994.

3. ASTM Standard D 5867-95, Standard Test Methods for Measurement of Physical Properties of Cotton Fibers by High Volume Instruments, Annual Book of ASTM Standards, Vol. 07.01, 1994.

4. ASTM Standard D 5866-95, Standard Test Methods for Neps in Cotton Fibers (AFIS-N Instrument), Annual Book of ASTM Standards, Vol. 07.01, 2002.

5. Balasubramanian, N., Influence of Cotton Quality, The Indian Textile Journal, 48-51, November 1995.

6. Bragg, C. K. and F. M. Shofner, A Rapid, Direct Measurement of Short Fiber Content, Textile Research Journal, **63**, 171-176 (1993).

7. Brown, H. M., A pneumatic Method of Measuring Cotton Fiber Staple Length, Textile Research Journal, **28**, 516-520 (1958).

8. Cheng, K. P. S., and Y. S. J. Cheng, Cotton Testing, Traditional vs. Advanced, Textile Asia, **33**, 44-45 (2002).

9. Cotton Incorporated, Classification of Upland Cotton, http://www.cottoninc.com/CottonClassification/homepage.cfm.

10. Cotton Incorporated, Cotton Quality - U.S. Cotton Fiber Chart for 2001, http://www.cottoninc.com/TextileWorldMap2001/homepage.cfm.

11. Cui, X., and T. A. Calamari, Short Fiber Content of Cotton and Its Measurement, Proceedings Beltwide Cotton Conferences, 718 (1999).

12. Cui, X., T. A. Calamari, and M. W. Suh, Theoretical and Practical Aspects of Fiber Length Comparisons of Various Cottons, Textile Research Journal, **68**, 467-472 (1998).

13. Duckett, K. E., Z. Zhou, R. S. Krowicki, and P. E. Sasser, Cotton Fiber Fineness Distributions and Their Effects on the Tenacities of Randomly Sampled HVI Tapered Beards: Linear Density Effects, Textile Research Journal, **63,** 737-744 (1993).

14. Gibson, L., HVI Short Fiber Content Measurement, Proceedings Beltwide Cotton Conferences, 1406-1407 (1999).

15. Ikiz, Y., Fiber Length Measurement by Image Processing, PhD Dissertation, North Carolina State University (2000).

16. Ikiz, Y., J.P. Rust, W.J. Jasper, and H.J. Trussel, Fiber Length Measurement by Image Processing, Textile Research Journal, **71**, 905-910 (2001).

17. India Agronet Agriculture Resource Center, Uniformity Ratio Classifications, http://www.indiaagronet.com/cotton/Resources/11/11center.htm.

18. Kessler, L., and W. K. Fisher, A Study of the Electrostatic Behavior of Carpets Containing Conductive Yarns, Journal of Electrostatics, **39**, 253-275 (1997).

19. Kim, Y. K., and Lewis, A. F., Scientific Study of Flock Materials and the Flocking Process, National Textile Center Annual Report: November 1998, 177-187.

20. Kim, Y. K., and Lewis, A. F., Scientific Study of Flock Materials and the Flocking Process, National Textile Center Annual Report: November 1999, 9 pages.

21. Knowlton, J. L., HVI Short Fiber Content, EFS System Conference Presentations (1999).

22. Krowicki, R. S., J. P. Hemstreet, D. P. Thibodeaux, and K. E. Duckett, Problems in Determining Length Parameters on the HVI, Proceedings of the Sixth Annual EFS Research Forum, 14-30 (1993).

23. Mogahzy, Y. E., and R. M. Broughton, Regressional Observations of HVI Fiber Properties, Yarn Quality, and Processing Performance of Medium Staple Cotton, Textile Research Journal, **62**, 218-226 (1992).

24. Morton, W. E., and J. W. S. Hearle, Physical Properties of Textile Fibers, The Textile Institute, Machchester, UK 1993.

25. PTU-3012 Pulsing Power Supply Operations Manual, CCS Inc., Waltham, MA (2002)

26. Shofner, F. M., M. G. Townes, and G. F. Williams, US Patent Number 5,491,876 (1996).

27. Solution 2000, Enlightened Through Experience, Catalogue for CCS Inc, Waltham, MA (2000).

28. Stroupe, S. P., Method for Preparation and Delivery of Cotton Fibers for Digital Imaging, Master's Thesis, North Carolina State University (2002).

29. Swicofil AG Textile Services, Understanding the Flocking Process, http://www.swicofil.com/flock.html.

30. TM-1020-15 Digital Camera Operations Manual, Pulnix America, Inc., Sunnyvale CA. (2001).

31. Zeidman, M. I., S. K. Batra, and P. E. Sasser, Determining Short Fiber Content in Cotton, Textile Research Journal **61**, 21-30 (1991)

APPENDICES

Appendix A

Table A.1: Designed Experiment for Crossovers

Spacing	Feed	Belt	Moisture	Proper Proportion	Run Order	StdOrder	Blocks	CenterPt
2.58	0.2	0.19	-1	0.881	5	1	1	1
2.58	0.2	0.19	-1	0.894	16	2	1	1
2.58	0.2	0.22	1	0.878	4	3	1	1
2.58	0.2	0.22	1	0.864	10	4	1	1
2.58	0.4	0.19	1	0.856	6	5	1	1
2.58	0.4	0.19	1	0.841	11	6	1	1
2.58	0.4	0.22	-1	0.898	2	7	1	1
2.58	0.4	0.22	-1	0.863	12	8	1	1
3.19	0.2	0.19	1	-	3	9	1	1
3.19	0.2	0.19	1	0.892	15	10	1	1
3.19	0.2	0.22	-1	0.895	13	11	1	1
3.19	0.2	0.22	-1	0.884	14	12	1	1
3.19	0.4	0.19	-1	0.869	7	13	1	1
3.19	0.4	0.19	-1	0.876	9	14	1	1
3.19	0.4	0.22	1	0.846	1	15	1	1
3.19	0.4	0.22	1	0.892	8	16	1	1

Appendix B

Table B.1: Two Sample Test of UHM for Chute (section 1) and Belt Suction (section 2)

Two-Sample T-Test and CI: UHM, Section

```
Two-sample T for UHM

Section     N      Mean     StDev   SE Mean
1           3    0.8633    0.0115    0.0067
2           3    0.8200    0.0100    0.0058

Difference = mu (1) - mu (2)
Estimate for difference:  0.04333
95% CI for difference: (0.01885, 0.06782)
T-Test of difference = 0 (vs not =): T-Value = 4.91  P-Value = 0.008  DF =
4
Both use Pooled StDev = 0.0108
```

Table B.2: Two Sample Test of SFC for Chute (section 1) and Belt Suction (section 2)

Two-Sample T-Test and CI: SFC, Section

```
Two-sample T for SFC

Section     N      Mean     StDev   SE Mean
1           3     23.93      1.19      0.69
2           3     32.63      2.14       1.2

Difference = mu (1) - mu (2)
Estimate for difference:  -8.70
95% CI for difference: (-12.63, -4.77)
T-Test of difference = 0 (vs not =): T-Value = -6.15  P-Value = 0.004  DF
= 4
Both use Pooled StDev = 1.73
```

Appendix C

Table C.1: Description Statistics for 100 Single Fiber Measurements

Descriptive Statistics: Length (mm)

Variable	N	Mean	Median	TrMean	StDev	SE Mean
Length	100	22.402	22.405	22.403	0.042	0.004

Variable	Minimum	Maximum	Q1	Q3
Length	22.298	22.494	22.376	22.430

Appendix D

Table D.1: Initial Crossover Percentage

CI for One Proportion – Initial Crossover Assessment

Sample	X	N	Sample p	95.0% CI
Initial Data	274	1302	0.210445	(0.188594, 0.233613)

Table D.2: Crossover Test for Difference between Fast and Slow Comber Roll

Test and CI for Two Proportions – Slow Comber vs. Fast Comber

Sample	X	N	Sample p
Fast Comber	274	1302	0.210445
Slower Comber	295	1332	0.221471

Estimate for p(1) - p(2): -0.0110260
95% CI for p(1) - p(2): (-0.0424505, 0.0203985)
Test for p(1) - p(2) = 0 (vs not = 0): Z = -0.69 P-Value = 0.492

Table D.3: Crossover Percentage after Tube Removal

CI for One Proportion – After Tube Removal

Sample	X	N	Sample p	95.0% CI
Tube Removed	121	986	0.122718	(0.102881, 0.144838)

Table D.4: Crossover Test for Difference between Initial and Tube Removed Data

Test and CI for Two Proportions – Initial Data vs. After Tube Removal

Sample	X	N	Sample p
Initial Data	274	1302	0.210445
Tube Removed	121	986	0.122718

Estimate for p(1) - p(2): 0.0877274
95% CI for p(1) - p(2): (0.0575666, 0.117888)
Test for p(1) - p(2) = 0 (vs not = 0): Z = 5.70 P-Value = 0.000

Appendix E

Table E.1: Basic Statistics for Overlapping Fiber Pixels

One-Sample T: Sample Average

Variable	N	Mean	StDev	SE Mean
Sample Avera	4	27.23	7.78	3.89

Variable	95.0% CI
Sample Avera	(14.86, 39.61)Pixels

Appendix F

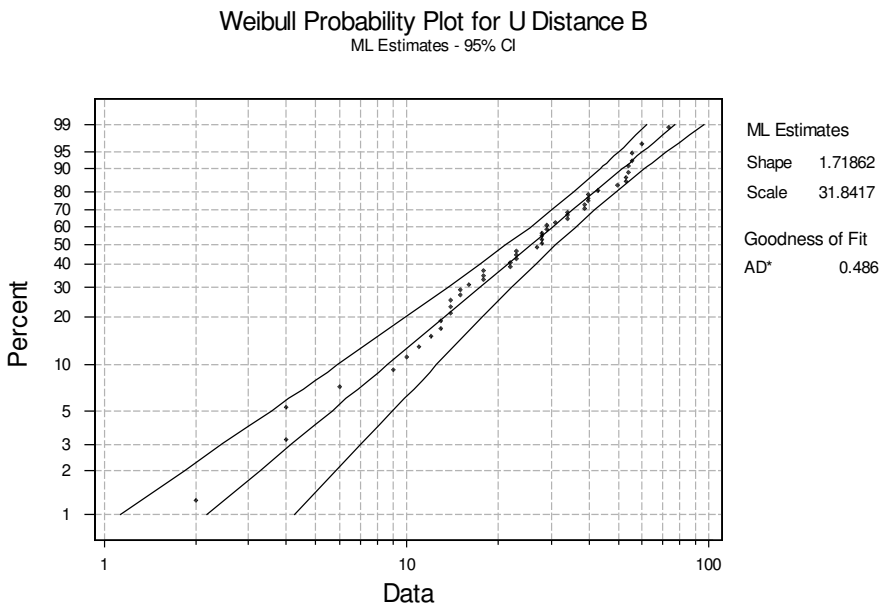

Cumulative Distribution Function

Weibull with first shape parameter = 1.71862 and second = 31.8417

x	P(X <= x)
21.0000	0.3868
22.0000	0.4112
23.0000	0.4355
24.0000	0.4594
25.0000	0.4831
26.0000	0.5063
27.0000	0.5291
28.0000	0.5515
29.0000	0.5733
30.0000	0.5945
31.0000	0.6152
32.0000	0.6353
33.0000	0.6547
34.0000	0.6735
35.0000	0.6916
36.0000	0.7091
37.0000	0.7259
38.0000	0.7421
39.0000	0.7575
40.0000	0.7724
41.0000	0.7865
42.0000	0.8000
43.0000	0.8128
44.0000	0.8251
45.0000	0.8367
46.0000	0.8477
47.0000	0.8581
48.0000	0.8680
49.0000	0.8773
50.0000	0.8860
51.0000	0.8943
52.0000	0.9020
53.0000	0.9093
54.0000	0.9162
55.0000	0.9226
56.0000	0.9285
57.0000	0.9341
58.0000	0.9394
59.0000	0.9442
60.0000	0.9487
61.0000	0.9529
62.0000	0.9569
63.0000	0.9605
64.0000	0.9638
65.0000	0.9669
66.0000	0.9698
67.0000	0.9724
68.0000	0.9749
69.0000	0.9771
70.0000	0.9792
71.0000	0.9811
72.0000	0.9828
73.0	0.9844
74.0	0.9859

Appendix G

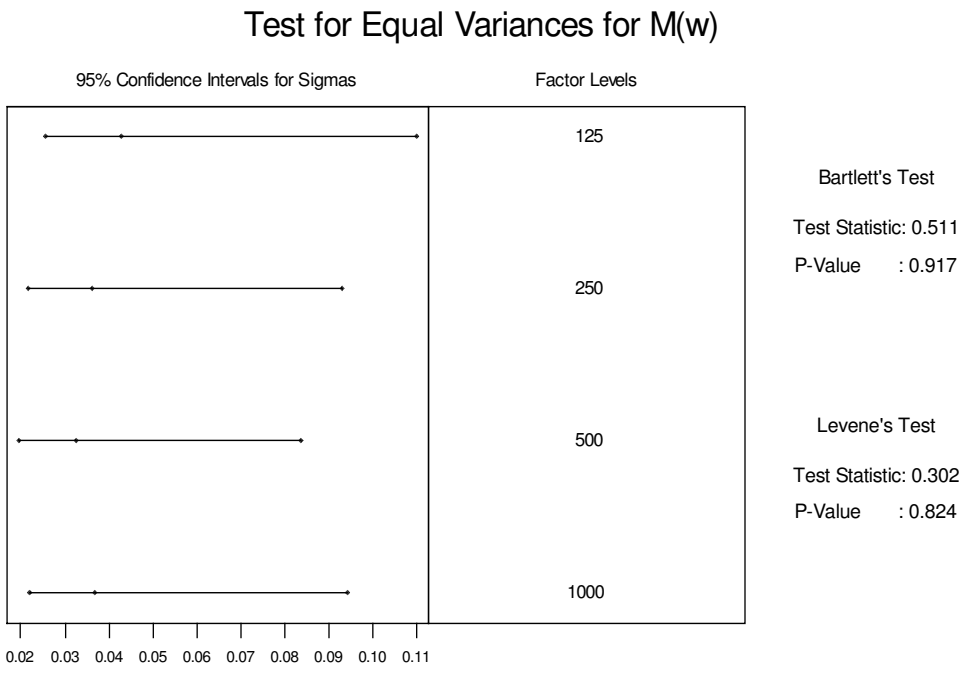

Figure G.1: Test for Equal Variances of M(w) for New Sliver

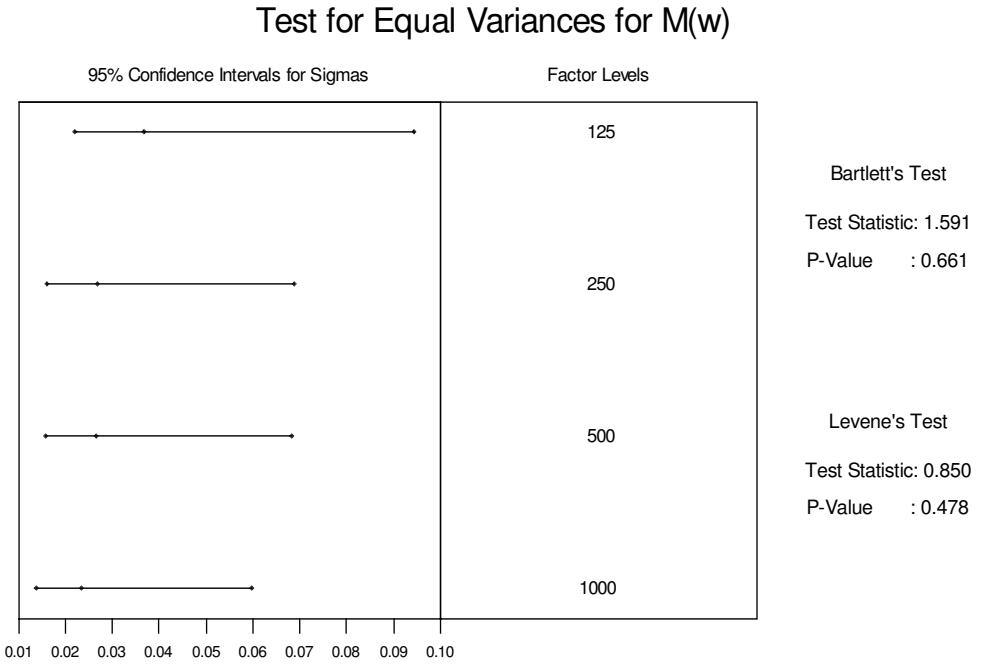

Figure G.2: Test for Equal Variances of M(w) for New Sliver

Covariate Regression

Response M(w)

Summary of Fit

RSquare	0.839852
RSquare Adj	0.770698
Root Mean Square Error	0.020089
Mean of Response	0.734109
Observations (or Sum Wgts)	64

Analysis of Variance

Source	DF	Sum of Squares	Mean Square	F Ratio
Model	19	0.09311967	0.004901	12.1446
Error	44	0.01775656	0.000404	Prob > F
C. Total	63	0.11087623		<.0001

Lack Of Fit

Source	DF	Sum of Squares	Mean Square	F Ratio
Lack Of Fit	12	0.00300706	0.000251	0.5437
Pure Error	32	0.01474950	0.000461	Prob > F
Total Error	44	0.01775656		0.8692
				Max RSq
				0.8670

Parameter Estimates

Term	Estimate	Std Error	t Ratio	Prob>|t|
Intercept	0.744	0.010044	74.07	<.0001
sample size[250-125]	-0.03025	0.014205	-2.13	0.0388
sample size[500-250]	0.00325	0.014205	0.23	0.8201
sample size[1000-500]	-0.03	0.014205	-2.11	0.0404
Sliver[New]	0.032	0.005022	6.37	<.0001
RH[61-59]	-0.0105	0.014205	-0.74	0.4637
RH[62-61]	0.02825	0.014205	1.99	0.0530
RH[64-62]	0.0575	0.014205	4.05	0.0002
sample size[250-125]*Sliver[New]	-0.011438	0.007102	-1.61	0.1145
sample size[500-250]*Sliver[New]	-0.013375	0.007102	-1.88	0.0663
sample size[1000-500]*Sliver[New]	0.00175	0.007102	0.25	0.8065
sample size[250-125]*RH[61-59]	0.05575	0.020089	2.78	0.0081
sample size[250-125]*RH[62-61]	-0.07775	0.020089	-3.87	0.0004
sample size[250-125]*RH[64-62]	-0.0065	0.020089	-0.32	0.7478
sample size[500-250]*RH[61-59]	-0.0515	0.020089	-2.56	0.0139
sample size[500-250]*RH[62-61]	0.03675	0.020089	1.83	0.0741
sample size[500-250]*RH[64-62]	0.008	0.020089	0.40	0.6924
sample size[1000-500]*RH[61-59]	0.034	0.020089	1.69	0.0976
sample size[1000-500]*RH[62-61]	0.00325	0.020089	0.16	0.8722
sample size[1000-500]*RH[64-62]	-0.0095	0.020089	-0.47	0.6386

Effect Tests

Source	Nparm	DF	Sum of Squares	F Ratio	Prob > F
sample size	3	3	0.00651919	5.3848	0.0030
Sliver	1	1	0.01638400	40.5988	<.0001
RH	3	3	0.01754525	14.4921	<.0001
sample size*Sliver	3	3	0.00638180	5.2713	0.0034
sample size*RH	9	9	0.01066752	2.9371	0.0081